Aus dem Walter-Brendel-Zentrum für Experimentelle Medizin (WBex)

Institut der Ludwig-Maximilians-Universität München

Direktor: Prof. Dr. Daphne Merkus

Relevance of Lymphocytes in Collateral Artery Growth (Arteriogenesis)

Dissertation
zum Erwerb des Doktorgrades der Dr. rer. nat.
an der Medizinischen Fakultät
der Ludwig-Maximilians-Universität München

vorgelegt von
Konda Kumaraswami
aus Naspur, Indien

im Jahr

2022

Mit Genehmigung der Medizinischen Fakultät

der Ludwig-Maximilians-Universität München

Berichterstatter: Prof. Dr. Elisabeth Deindl

Zweitgutacher: Prof. Dr. Alexander Bartelt

Dekan: Prof. Dr. med. Thomas Gudermann

Tag der mündlichen Prüfung: 27. Juli 2022

AFFIDAVIT

I hereby declare that the submitted thesis entitled **Relevance of Lymphocytes in Collateral Artery Growth (Arteriogenesis)** is my own work. I have only used the sources indicated and have not made unauthorized use of services of a third party. Where the work of others has been quoted or reproduced, the source is always given.

I further declare that the submitted thesis or parts thereof have not been presented as part of an examination degree to any other university.

Munich, 27.07.2022 Konda Kumaraswami

Meghana Aslesha

TABLE OF CONTENTS

LIST OF FIGURES

ABBREVIATIONS

WT	wild type
KO	Knockout
aFAL	after femoral artery ligation
CLPs	common lymphoid progenitors
CFI	Collateral flow index
APC	antigen-presenting cells
aNT	Annealing temperature
LDL	Low-density lipoproteins (LDL)
ox-LDL	oxidized LDL
CVD	Cardiovascular diseases
PAD	Peripheral arterial diseases
TCR	T cell receptor
BCR	B cell receptor
FACS	fluorescence-activated cell sorting
DAPI	4', 6-diamidin-2-phenylindole
FCS	Fetal calf serum
EDTA	Ethylenediaminetetraacetic acid
PBS	Phosphate-buffered saline
HCL	Hydrochloric acid
PCR	Polymerase chain reaction
BrdU	Bromodeoxyuridine

i.p.	Intraperitoneal
i.v.	Intra venous
IFN	Interferons
γδ	Gamma delta
αβ	Alpha beta
MZB	Marginal Zone B cells
NK	Natural killer cells
NKT	Natural killer T cells
DCs	Dendritic cells
MRC1	Mannose receptor C-type 1
CD	Cluster of differentiation
WBC	White blood cells
RBC	Red blood cells
DAMP	Damage-associated molecular patterns
MHC	Major histocompatibility complex
ELISA	Enzyme-linked immunosorbent assay
LDI	Laser Doppler Instrument
ROI	Region of Interest
MFI	Mean fluorescence intensity
LTBR	Lymphotoxin beta receptor
IL-17A	Interleukin-17A
IL-4	Interleukin-4

IL-6	Interleukin-6
IL-10	Interleukin-10
LPS	Lipopolysaccharide
GM-CSF	Granulocyte-macrophage colony-stimulating factor
TGF	Transforming growth factor
PDGFβ	Platelet-derived growth factor beta
PDGFβ-R	Platelet-derived growth factor beta receptor
S.D.	Standard Deviation
S.E.M.	Stand Error of Mean

1. ZUSAMMENFASSUNG

Arteriogenese beschreibt den Wachstumsprozess natürlicher Bypässe von präexistenten Arteriolen zu vollfunktionsfähigen Arterien, welcher den Blutfluss nach Okklusion einer Arterie wiederherstellen und so Ischämieschaden und Nekrose verhindern kann. Die Auswanderung von Neutrophilen aus den Kollateralen und Mastzelldegranulation sind hierbei zeitlich früh ablaufende Prozesse. Die Rolle von B-Zellen in der Arteriogenese noch nie untersucht worden und weiterhin gibt es konträre Aussagen über die Funktion CD4- und CD8-positiver T-Zellen in der Arteriogenese. Daher zielte meine Studie darauf ab, die Rolle der Lymphozyten in der Arteriogenese näher zu beleuchten. So zeigten Rag1 knock-out (KO) Mäuse, bei denen die B- als auch die T-Zellen-Populationen fehlen, eine eingeschränkte Arteriogenese. Die Analyse der Makrophagen-Phänotypen im perivaskulären Raum zeigte, dass der Rag1 Knock-out mit einer erhöhten Anzahl an inflammatorischen Makrophagen ($CD68^+/MRC1^-$) und einer erniedrigten Anzahl an regenerativen Makrophagen ($CD68^+/MRC1^+$) einherging. Dies lässt darauf schließen, dass das adaptive Immunsystem die Arteriogenese beeinflussen könnte, indem es die Polarisation der Makrophagen beeinflusst. Des Weiteren zeigten Wildtyp-Mäuse (WT) nach CD20 vermittelter B-Zell-Depletion eine verringerte Arteriogenese und verminderte Akkumulation regenerativer Makrophagen. Allerdings wurden neben B-Zellen auch T-Zellen sowie eosinophile Granulozyten durch die CD20 Depletion erfasst: Mittels Durchflusszytometrie konnte ich zeigen, dass die Expression von CD20 nicht auf B-Zellen beschränkt war, sondern auch andere Zelltypen, wie $CD4^+$ T-Zellen, $CD8^+$ T-Zellen, γδ T-Zellen und eosinophile Granulozyten CD20 exprimieren können. Mittels bildgestützter Zytometrie und unter Verwendung zweier unterschiedlicher CD20 Antikörper konnte ich diese Beobachtung bestätigen. Dies erklärt warum eine CD20-Depletion auch T-Zellen, γδ T-Zellen und eosinophile Granulozyten betraf. Mit diesen Ergebnissen lässt sich eine vorläufige Schlussfolgerung über die Rolle der B-Zellen in der Arteriogenese ziehen.

Zur Untersuchung der alleinigen Rolle von B-Zellen im Rahmen der Arteriogenese stellen B-Zell defiziente (JHT KO) Mäuse eine bessere Alternative dar. Im Vergleich zu WT-Mäusen zeigten B-Zell defiziente Mäuse verminderte Arteriogenese, wobei sich jedoch die lokale Akkumulation von inflammatorischen ($CD68^+MRC1^-$) und regenerativen ($CD68^+MRC1^+$) Makrophagen zwischen beiden Gruppen nicht unterschied. Histologische immunfluoreszenz-

Analysen zeigten das Vorhandensein von $CD20^+$ Zellen in B-Zell defizienten Mäusen und führten zu der Vermutung, dass die Präsenz von $CD20^+$ Zellen in B-Zell defizienten Mäusen möglicherweise verantwortlich für diese unveränderte Makrophagen Akkumulation sei. Die Depletion von CD20 in B-Zell defizienten Mäusen führte hierbei zur einer stark verschlechterten Arteriogenese und eine einhergehende vermehrte Anzahl an inflammatorischen ($CD68^+/MRC1^-$) und einer verringerten Anzahl an regenerativen ($CD68^+/MRC1^+$) Makrophagen.

Darüber hinaus offenbarten Analysen von TCRα KO-Mäusen, dass diese eine unveränderte Arteriogenese aufwiesen und eine vermehrte Akkumulation an regenerativen Makrophagen zeigten. Trotzdem wirkte sich, überraschenderweise, die Depletion von γδ T-Zellen negativ auf die Arteriogenese sowohl bei TCRα KO-Mäusen als auch bei WT-Mäusen aus. Außerdem reduzierte die γδ T-Zell Depletion die lokale Ansammlung von regenerativen ($CD68^+/MRC1^+$) Makrophagen. Somit konnte ich im Rahmen meiner Untersuchungen zum ersten Mal die Beteiligung von γδ T-Zellen bei Prozessen der Arteriogenese zeigen. γδ T-Zellen exprimieren IFN-γ im Zuge der Arteriogenese. Analysen zum Aktivierungsstatus von Makrophagen zeigten, dass das Vorhandensein von γδ T-Zellen eine Vermehrung der Expression von CD169 (Siglec-1) zur Folge hatte. CD169 Makrophagen offenbarten eine fördernde Wirkung auf die Gefäßproliferation durch vermehrte Expression von IL-10 und PDGFβ. Zusammenfassend konnten meine Studien überzeugende Hinweise auf die Involvierung von B-Zellen und γδ T-Zellen in die Prozesse des Wachstums natürlicher Bypässe (Arteriogenese) liefern.

SUMMARY (English)

Arteriogensis is a natural bypass growth of preexisting arteriole to fully functioning arteries that rescue organs from ischemic damage and necrosis. Neutrophil extravasation and mast cell degranulation are the early cellular events in this process. The Role of B cells in arteriogenesis has never been studied. There is contradictory evidence of $CD4^+$ and $CD8^+$ T cells role in arteriogenesis. My study aims to identify the role of lymphocytes in arteriogenesis. Using Rag1 KO mice, I found lack of B and T cells Rag1 KO mice showed impaired arteriogenesis. Macrophage phenotype analysis in perivascular space revealed that impaired arteriogenic response in Rag1 KO mice was associated with increased number of inflammatory ($CD68^+MRC1^-$) macrophages and reduced number of regenerative ($CD68^+MRC1^+$) macrophages indicating the role of adaptive immune system in resolving the inflammation and facilitate the collateral artery growth. Next, in WT mice, CD20 mediated B cell depletion resulted in impaired arteriogenesis associated with the reduced regenerative macrophage accumulation. Not only B cells, but fraction of $CD20^+$ T cells and eosinophils were also depleted by CD20 depletion. Flow cytometry analysis showed that CD20 expression was not limited to B cells but also other cell types, i.e., CD4 T cells, CD8 T cells, γδ T cells, and eosinophils. Imaging cytometry using two clones of CD20 antibodies confirms this observation and explains why CD20 depletion affected CD4 T cells, γδ T cells, and eosinophils. These results draw a tentative conclusion on the role of B cells in arteriogenesis. B cell-deficient (JHT KO) mice provide a better alternative to study the role of B cells in arteriogenesis. B cell-deficient mice showed reduced arteriogenesis; however, inflammatory ($CD68^+MRC1^-$) and regenerative ($CD68^+MRC1^+$) macrophage accumulation were not affected by B cells absence. Histology immunofluorescence analysis showed the presence of $CD20^+$ cells in B cell-deficient mice, and these cells might be the reason why B cell-deficient mice have similar macrophages compared to WT mice. CD20 depletion in B cell-deficient mice showed a strong negative effect on arteriogenesis, associated with an increased number of inflammatory ($CD68^+MRC1^-$) macrophages and decreased regenerative ($CD68^+MRC1^+$) macrophages. Next, analysis from TCRα KO mice showed me that lack of CD4 and CD8 T cells does not impact arteriogenesis and favored regenerative ($CD68^+MRC1^+$) macrophage accumulation. Nevertheless, surprisingly, γδ T cell depletion negatively affected arteriogenesis in TCRα KO mice and WT mice. Furthermore, γδ T cell depletion also reduced the regenerative ($CD68^+MRC1^+$) macrophage

accumulation. My study, for the first time, identified the involvement of γδ T cell in arteriogenesis. γδ T cells expressing IFN-γ in arteriogenesis. Macrophage activation status analysis showed that CD169 (Siglec-1) expression decreased in γδ T cell depleted mice. CD169 macrophages showed vascular growth-promoting properties as analyzed by expression of IL-10 and PDGFβ. In conclusion, my study provides convincing evidence of the contribution of B cells and γδ T cells in collateral artery growth (arteriogenesis).

2. INTRODUCTION

2.1 Immune system-an overview

The immune system is a diverse system evolved into a well-organized defense to protect multicellular organisms from pathogens. The diversity in functionality is the co-ordination and involvement of many organs, cells, and pathways. The complexity in defense response execution is highly fascinating to study. Rapid response is seen immediately after the system encounters the pathogens; however, a precise recognition and destruction mechanism is time-consuming. Based on the same criteria, the immune system can be explained in two classes (Kuby Immunology, 7th edition).

2.1.1 Innate immunity

Innate immunity is classified as a non-specific fast responding defense system. It uses built-in molecular and cellular barriers to protect against infections or common invaders. The barriers include physiological such as skin, and chemical barriers, such as damaged associated molecular patterns (DAMPs), which leads to blocking entry, rapid identification, and phagocytic destruction (Beutler B et al., 2004), (Land WG et al., 2015). In addition, the complement system holds a special role in the innate immune system (Rus H et al., 2005).

2.1.2 Adaptive immunity

Adaptive immunity is different from innate immunity because it needs a longer time to react; however, it is highly specific and effective in tackling pathogens (Kuby Immunology, 7th edition). The primary cells that control the adaptive immunity rely on B and T lymphocytes which take time to get into action because it needs innate immunity support to present antigens to the receptors to activate (Danilova N et al., 2012). In the following step, lymphocytes program the strategies to eliminate the invaders effectively. However, once the strategy is ready by selecting specific types-called clonal selection, adaptive immunity makes sure that the invaders cannot escape. More precisely, the destruction strategy is memorized and prepared for the rapid response for the subsequent encounter. This is a unique feature of the adaptive immune system (Kuby Immunology, 7th edition).

Figure 1

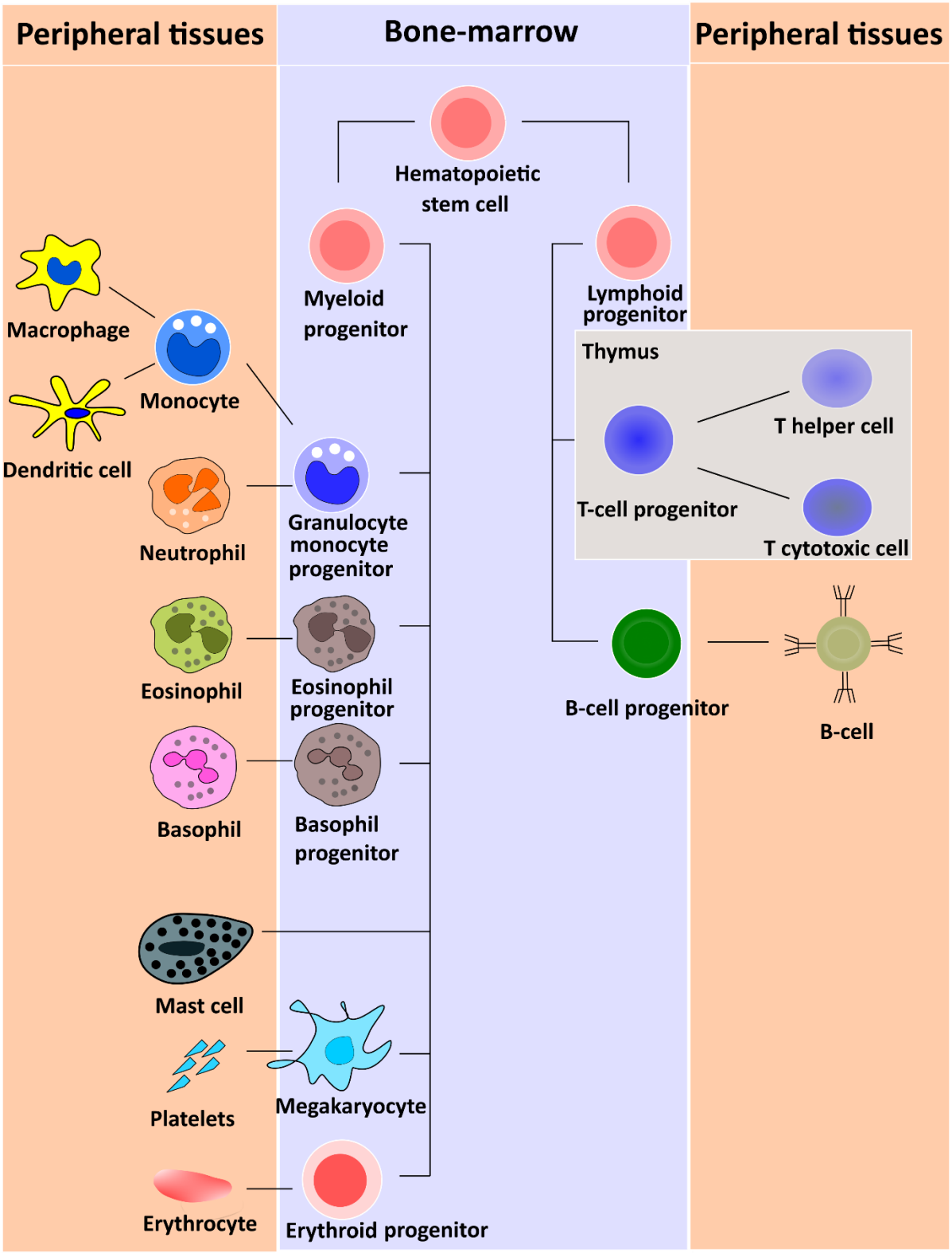

Figure 1. Hematopoiesis schema showing myeloid cells raise from the common myeloid progenitor. T and B lymphocytes rise from lymphoid progenitor cells. (Figure is adopted from Kuby Immunology, 7th edition)

2.1.3 Cells of Immune system

Under the steady-state condition, the common myeloid progenitor cells generate granulocytes, monocytes, and macrophages, whereas the common lymphoid progenitor cells generate B lymphocytes and T lymphocytes (Fig. 1).

Myeloid cells are first responding to the pathogens and communicate with lymphoid cells. They include neutrophils, basophils, mast cells, eosinophils, monocytes, macrophages, and dendritic cells. Lymphocytes are the key players of adaptive immunity which include B lymphocytes, T lymphocytes, and NK cells. After it encounters with antigen-presenting cells, B cells get activated and ultimately differentiate into plasma cells, which produces antibodies. T lymphocytes are majorly subdivided into two types. T helper cells and T cytotoxic cells. Natural killer cells do not express antigen-specific receptors. They are considered innate immune cells. NKT cells type of lymphocytes shares features of T cells and NKT cells (Kuby Immunology, 7th edition).

2.1.4 B lymphocytes

Hematopoietic stem cells undergo different development stages and generate common lymphoid progenitors (CLPs) in the bone marrow. CLPs which remained in bone marrow further rose to B cells (Duchosal MA et al., 1997). During the developmental process, they acquire different surface markers, making it easy to understand what type of cells they are.

B cells are majorly two types; B1-B cells and B2-B cells. B1-B cells are raised from the fetal liver and constitute a significant portion of B cells during the development, but they remain a minor fraction in adults. B1-B cells produce natural antibodies of IgM and IgA; hence, they are considered innate B cells that mediate humoral immune reactions (Kuby Immunology, 7th edition). B2-B cells are involved in adaptive immune reactions. During the development, CLPs cells generate pro-B and pre-B cells and finally immature B cells. After this development, immature B cells migrate to into blood circulation, and reach the spleen for further maturation. Group of B2-B cells reach the marginal sinus of the spleen (Marginal Zone B cells-MZB), interact with pathogens, and further mature to antibody-producing plasma cells. The

second type of B2-B cell-Follicular B cells are involved in antigen-specific long-lived antibody-producing plasma cells, memory cells with the co-ordination with dendritic cells and T cells.

2.1.5 T lymphocytes

T cells are generated in the thymus (Kumar BV et al., 2018). T cells are characterized by their cell surface receptor (TCR) (Kuby Immunology, 7th edition). T cells possibly can acquire two different receptors which decide their function, 1) αβTCR and 2) γδTCR. $\alpha\beta TCR^+$ T cells present in a large portion of lymphocytes (60-70%) whereas $\gamma\delta TCR^+$ T cells remains minor (0.5-5%). $\alpha\beta TCR^+$ T cells again subdivided into two major types based on co-expression of CD4 and CD8 surface protein. $CD4^+$ T cells, also called T helper cells, are activated by MHC class II from antigen-presenting cells (APC) and help B cells and macrophages for adaptive immune reactions (Luckheeram RV et al., 2012). Regulatory T cells from $CD4^+$ T cells further classified into two groups based on their FOXP3 transcription factor expression; $FOXP3^+CD4^+$ T cells and $FOXP3^-CD4^+$ T cells majorly involving in immune tolerance. CD8+ T cells are called as cytotoxic T cells and are responsible for killing function through binding with MHC class I molecules (Saigusa et al., 2020).

2.1.6 Monocytes/Macrophages-Sentinels of the Immune system

Monocytes are a highly heterogeneous cell population that makes up 5% to 10% of total white blood cells (WBC). They are raised from granulocyte monocyte progenitor in the bone marrow and mature after entering into peripheral tissue. Monocyte infiltrates into tissue and differentiates into macrophages. Tissue migrated macrophages play an essential role in repair and regeneration (Kuby Immunology, 7th edition). It's been reported that inflammatory monocytes, which are highly phagocytic in nature, can infiltrate into tissue more rapidly (Wynn & Vannella, 2016). Once infiltrated based on the tissue microenvironment, they can either proliferate or recruit more monocytes or be mixed cell populations at the lesion site (Gordon, 2003). Macrophages are also effective antigen-presenting cells and can activate T lymphocytes. Once activated, macrophages can participate in both innate and adaptive immune responses (Franken et al., 2016). Macrophage activation is typically carried out in two pathways; the classical and the alternative pathway. These activation pathways for which macrophage effector functions greatly depends on interaction with specific ligand take place.

The effector functions can be increased phagocytosis, pro-inflammatory and anti-inflammatory cytokine release and, vascular promoting growth factor expression (Gordon, 2003). The classical activation (M1 type macrophages) is more like an innate basis, which means the activation stimuli can be lipopolysaccharide (LPS) or interferon-gamma (IFN-γ) (Murray et al., 2014). The classically activated macrophages show typical features of inflammation promotion by releasing nitric oxide and IL-6, which are effective pathogen killers. In the other hand, macrophage interaction with T cells (T helper cells) can induce different macrophage phenotypes. The interaction can result in the release of IL-4/IL-13 can affect the different gene expressions in macrophages i.e. downregulation of inflammatory genes by IL-10 and TGF (Transforming growth factor) family cytokines. Macrophage activation by IL-4/IL-13 and together with IL-10 stimuli are considered as an alternative pathway. Alternatively activated (M2 type) macrophages possess anti-inflammatory features and majorly involve in tissue repair and regeneration (Gordon, 2003), (Murray et al., 2014). However, the activation stimuli are microenvironment specific and difficult to differentiate; for example, in chronic sterile inflammation conditions, macrophage acquire different metabolic signatures over mixed stimuli, which results in different effector functions though they express typical activation markers (Koelwyn et al., 2018). This information highlights the importance of studying the activation stimuli and activation status of the macrophages particularly in tissue microenvironment.

2.2 Cardiovascular diseases and global burden

Cardiovascular diseases include coronary artery diseases (CAD) and peripheral arterial diseases (PAD) are the vascular pathologies of blood vessels that are a burden for public health. World Health Organization has estimated 231.7 (crude death rate per 100,000 populations) deaths in 2019 that account for 32.7% of total deaths globally (WHO-2020-Geneva) indicating the serious concern about understanding the pathology of CAD in order to develop simple and effective therapeutic options is much demanded. The generalized risk factors for developing CAD are; unhealthy personal habits, including excessive alcohol consumption, which may lead to increased blood pressure, blood glucose levels, blood lipids and ultimately cause low-density lipoprotein deposits in arteries which form atherosclerosis plaque (WHO-2020-Geneva). This process is further extended by leukocyte infiltration and

activates the inflammatory responses. Such accumulation activates immune cells deposition and further extends the plaque formation and narrows the arterial lumen, which causes stenosis and myocardial infarction. 85% of CVD deaths are due to stroke. From the past decades, a piece of substantial knowledge has been achieved in CVDs research; however, many questions remained unanswered to understand the pathophysiology of cardiovascular diseases.

2.2.1 Immune-mediated Inflammation in Cardiovascular diseases

Low-density lipoproteins (LDL) are the initiating factors that trigger vascular inflammation. Deposited lipids activate endothelial cells and also macrophages. The coordination between endothelial cells and macrophages causes the release of adhesion molecules and chemokine to facilitate further immune cell extravasation (Hansson et al., 2006). Upon the infiltration of monocytes, local production of colony-stimulating factors converts monocytes to macrophages (Smith et al., 1995). Macrophages phagocyte oxidized LDL and present the related antigens. The residential dendritic cells (DCs) control the T cell activation; however, based on the danger signal, DCs can further activate adaptive immune responses (Niessner et al., 2006) (Niessner & Weyand, 2010). T cells and B cells activated by macrophage and DCs infiltrate to the lesion site in a similar mechanism by adhesion molecules and chemokines. Studies from human lesions and $Apoe^{-/-}$ mice showed evidence of the role of adaptive immunnity (Paulsson et al., 2000), (Liuzzo et al., 2000), (Schaheen et al., 2016). However, T cells and B cells subsets showed controversial evidence in CVDs (Tedgui & Mallat, 2006). $CD4^+$ T cells from the lesion site can express CD44 surface marker showed that the T cells were exposed to antigen before infiltrating the lesion. This observation indicates that rapid activation might occur in secondary lymphoid organs (Saigusa et al., 2020). Studies from CD4 knock-out mice or CD4 depletion in mice showed that $CD4^+$ T cells pro-atherosclerosis (Zhou et al., 2000) hence deficiency protected mice from atherosclerosis lesion development. In support of this observation, $CD4^+$ T cells from atherosclerosis-prone mice accelerated atherosclerosis in receipt mice (Zhou et al., 2000). However, T cells subtypes possess different roles, i.e. $CD4^+$ T regulatory cells showed anti-atherosclerotic in a mouse model (Ait-Oufella et al., 2006). $CD8^+$ T cell depletion showed also protected mice from atherosclerosis in atherosclerosis-prone mice. These $CD8^+$ T cells showed higher levels of IFN-γ compared to non-

atherosclerotic mice (Seijkens et al., 2019). However, opposite results were reported showing IFN-γ from $CD8^+$ T cells does not play any role in atherosclerosis (Kyaw et al., 2013). γδ T cells in other hand, has also been identified in atherosclerosis. Internalized cholesterol drives γδ T cells activation in atherosclerosis which leads to higher expression levels of IL-17. However, TCRγδ knockout does not show any difference (Chen H, et al. 2014).

2.3 Arteriogenesis-A natural bypass

Peri-collateral and pericardial vascular growth has been observed very often in patients suffering from arterial blocks. This alternative natural rescuing process at a certain level preserves the organs from ischemic damage and minimizes chronic events. When the arterial lumen narrowed due to plaques, blood will be re-directed to the small non-functional arteriole. Increased blood circulation in the arteriole applies fluid shear stress. This hemodynamic shear stress signal is transduced to molecular activation. This phenomenon was first-ever observed by Wolfgang Schaper and group (Van Royen et al., 2001). In 1995, they coined the word "Arteriogenesis" from the definition, the strength of natural bypassing mechanism in which naturally existed arteriole expand in their diameter (Fig. 2) (Limbourg et al., 2009) and start supplying oxygenated blood and rescue the tissue from ischemic damage (Carmeliet, 2000). Though the blood bypassing is rapid, expansion of arterioles is time-consuming process. Understanding the molecular mechanism involving the arteriogenesis possesses a tremendous therapeutic option for the patients whose surgical interventions to treat occlusions are unsuccessful or for whom the angioplasty is not feasible.

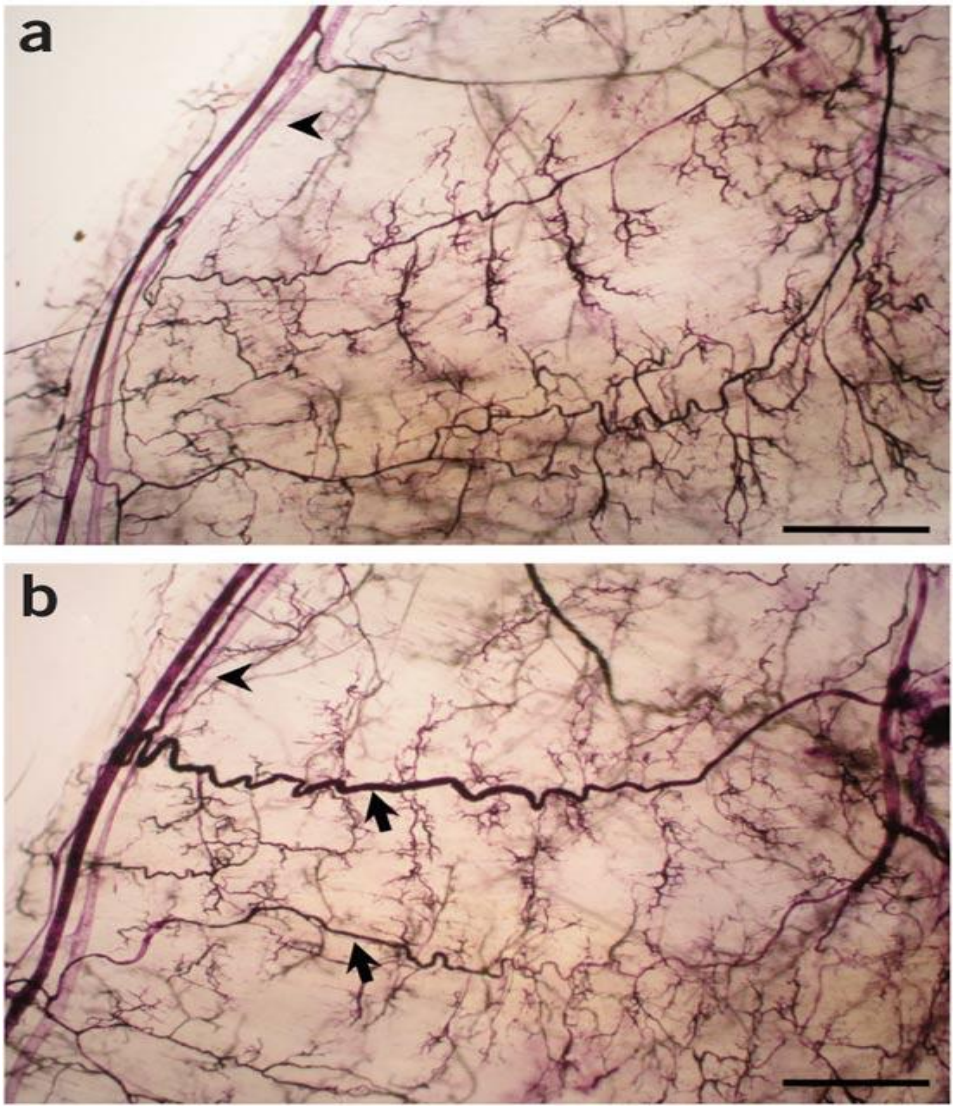

Figure 2. Images of growth of collateral arteries at 7 days after femoral artery ligation in mouse hind limb. **(a)** The femoral artery was sham-operated (non-ligated). **(b)** The femoral artery was ligated to induce arteriogenesis. Significant growth of collateral arteries was observed during arteriogenesis (arrows). The typical corkscrew formation of growing collaterals were seen. Veins are faintly stained (a, b, arrowhead) Scale bars, 1 mm (Limbourg et al., Nat Protocol 2009, reprinted with permission from the journal).

2.3.1 Arteriogenesis-Mechanism

Occlusion or stenosis in a major artery generates a pressure gradient between the pre-occlusive to post-occlusive regions. Re-directed blood flow applies shear stress on the vascular wall (Deindl & Schaper, 2005). This can activate endothelium to trigger inflammation and express adhesion molecules and chemokines to recruit leukocytes (Scholz et al., 2000). Arteriogenesis is greatly dependent on monocytes/macrophages; however, the involvement of T cells was reported earlier (Hellingman et al., 2012), (Van Weel et al., 2007), (Stabile et al., 2003). This mechanism is a similar way that atherosclerosis takes to progress. Monocyte pavement, macrophage conversion, lymphocyte recruitment are the sequential events in the progression of the lesion (Hansson et al., 2011). Analysis of the activation status showed that lymphocytes might expose to respective antigens more rapidly in secondary lymphoid organs before their infiltration to the lesion site. Based on the fact that studying the lymphatic environment could be interesting to deeply understand the innate and adaptive immunity in arteriogenesis.

2.3.2 Arteriogenesis-Therapeutic approach

Thrombus formation or stenosis in any major artery results in ischemic damage or necrosis of the tissue due to reduced oxygenated blood perfusion. Percutaneous angioplasty or bypass surgery is the current therapeutic options to treat such occlusive pathologies. Moreover, sometimes in-stent restenosis may be introduced at the intervention site which is again difficult to treat (van Royan, N. et al., 2009). However, arteriogenesis provides a natural alternative and rescues tissue from ischemic damage. Understating the factors which promote arteriogenesis thus attain interest to avoid invasive management of occlusive diseases.

Due to its complexity, arteriogenesis cannot be promoted with a single factor, as the growth of collateral arteries involves recruitment of leukocytes, which supply a multiple vascular growth-promoting factors and proliferation of endothelial, smooth muscle cells (Chillo et al., 2016). However, a few studies were attempted to induce arteriogenesis therapeutically.

Shear stress, which is a driving force of arteriogenesis, can be induced by physical exercise. Patients with stable CAD showed a hemodynamic improvement of collateral blood upon

prescribing 3 months of exercise training. A randomized, open-label, single-center trial-The impact of Intensive Exercise Training on Coronary Collateral Circulation in Patients with Stable Coronary Artery Disease (EXCITE) was conducted to study the impact of exercise on CAD outcome. Eligible patients were grouped into high-intensity training group vs moderate-intensity group and usual care group. Coronary collateral flow index (CFI) and Vo_2 peak response were significantly increased in the high-intensity group and moderate-intensity group but not the usual care group. However, EXCITE has few limitations; this study provides the clinical benefits of exercise in patients with stable CAD (Möbius-Winkler, S et al., 2016). Another approach, a double-blinded, randomized, placebo-controlled pilot study STimulation of ARTeriogenesis (START) was conducted on 40 patients with claudication treated with placebo or Granulocyte-macrophage colony-stimulating factor (GM-CSF) applied subcutaneously. GM-CSF has shown pro-arteriogenic properties in animal models (Buschmann, I. R, et al., 2001). However, there were no significant differences between the placebo and GM-CSF treated groups in the START trial. Small sample size and strong side effects were the limitations of the study. Hence the START trial does not recommend GM-CSF treatment to the patients with claudication (van Royan, N. et al., 2005).

2.4 Study motivation

Fluid shear stress is the physiological force behind the initiation of arteriogenesis. When an arterial occlusion occurred, the re-directed blood flow applies shear stress on arterioles endothelium results in inflammation. Shear stress-induced sterile inflammation attracts inflammatory cells includes mast cells, neutrophils, inflammatory monocytes, and lymphocytes. Soon after, neutrophils extravasation is regulated and mast cells disappear from the site. This regenerative phase is highly dependent on anti-inflammatory or regenerative macrophages. Recently, the mechanism behind mast cells, platelets, and neutrophils mediated inflammation in arteriogenesis was proposed (Lasch et al., 2019). The functional role of B and T lymphocytes, on the other hand, is still unknown.

The main aim of my study was to identify the relevance of lymphocytes in arteriogenesis. For this, firstly arteriogenesis was induced in mice lacking B and T cells (Rag1 KO). The role of B cells in arteriogenesis was evaluated using CD20 mediated B cell depleted mice and B cell-

deficient (JHT KO) mice. The role of T cells was evaluated using TCRα KO mice and mice treated with anti-TCRγδ antibody. These approaches were employed to identify specific lymphatic niche in arteriogenesis.

3. GENERAL MATERIAL

3.1 Materials

Table 1. Mouse strains

Strain	Background	Source
C57BL/6J	--	Charles River Laboratories, Deutschland
JHT KO mice	C57BL/6	Prof. Dr. Klaus Rajewsky, MDC, Berlin, Germany
TCRα KO mice	C57BL/6	Prof. Dr. Ludger Klein, LMU, Munich, Germany
Rag1 KO mice	C57BL/6	PD Dr. rer. nat. Reinhard Obst, LMU, Munich, Germany

Table 2. Medication

Name	Supplier
Fentanyl	CuraMED Pharma, Karlsruhe, Germany
Midazolam	Ratiopharm GmbH, Ulm, Germany
Medetomidine	Pfizer Pharma, Berlin, Germany
Buprenorphine	Reckitt Benckiser Healthcare, London, UK
Naloxone	Inresa Arzneimittel GmbH, Freiburg, Germany
Flumazenile	Inresa Arzneimittel GmbH, Freiburg, Germany
Atipamezole	Zoetis, Berlin, Germany

Table 3. Consumables

Name	Cat	Supplier
Student Fine Scissors	91460-11	FST, Germany
Olsen-Hegar Needle Holders with Suture Cutters	12002-12	FST, Germany

Student Dumont #7 Forceps	91197-00	FST, Germany
Dumont Forceps - Micro-Blunted Tips	11253-20	FST, Germany
Dumont Forceps - Micro-Blunted Tips	11253-25	FST, Germany
Student Dumont #5 Forceps	91150-20	FST, Germany
Student Vannas Spring Scissors	91500-09	FST, Germany
Student Fine Scissors	91460-11	FST, Germany
Olsen-Hegar Needle Holders with Suture Cutters	12002-12	FST, Germany
Student Dumont #7 Forceps	91197-00	FST, Germany
Dumont Forceps - Micro-Blunted Tips	11253-20	FST, Germany
Falcon tubes 15	10468502	Fisher Scientific GmbH, Schwerte, Germany
Falcon tubes 50	10788561	Fisher Scientific GmbH, Schwerte, Germany
96 well v bottom plate	3897	Costar, Schwerte, Germany
BD Microlance™ 3 24G	304100	Becton, Dickinson and Company, Ireland
BD Microlance™ 3 26G	303800	Becton, Dickinson and Company, Ireland
BD Microlance™ 30G		Becton, Dickinson and Company, Ireland
BD Plastipak™ 1	303172	Becton, Dickinson and Company, Ireland
Venofix® Safety	4056502-01	B. Braun Melsungen AG, Melsungen, Germany

Sterican® Kanuelen 30G	4656300	B. Braun Melsungen AG, Melsungen, Germany
ETHICON #3-0 SUTUPAK Sterile suture	EH6823	Johnson & Johnson International, Belgium
ETHICON 6-0 COATED VICRYL	V302	ETHICON, LLC, Cincinnati, USA
Probengefas 1.3 microtube EDTA coated	41.1395.005	SARSTEDT AG & Co. KG, Nümbrecht, Germany
Tissue-Tek Cryomold®	4566	Sakura Fineteck Europe B.V., Netherlands
Einbettkassetten	500/Grün	Engelbrecht Medizin-und Labortechnik GmbH, Edermünde, Deutschland
BD 2 Discardit II™ Syringe	300849	Becton, Dickinson and Company, Ireland

Table 4. Reagents

Table 4.1 General reagents

Reagent	**Cat**	**Supplier**
Phosphate buffered saline (PBS)	APO-ST009	Apotheke Klinikum der Universitat, Munich, Germany
Fetal bovine serum (FBS)	F7524	Sigma-Aldrich, Taufkirchen, Germany
Ethylenediaminetetraaceticacid (EDTA)	15575020	Invitrogen, Waltham, MA, USA
Collagenase IV	CLS4	Worthington, Freehold, NJ, USA
DNase I	11284932001	Roche, Penzberg, Germany
RPMI 1640 medium	31870-074	Gibco, Dubline, Ireland
Percoll®	17-0891-01	GE Healthcare, Chicago, IL, USA
Hank's Balanced Salt solution (HBSS)	H9394-500	Sigma-Aldrich, Taufkirchen, Germany,

4% paraformaldehyde (PFA)	1,176	Morphisto, Frankfurt am Main, Germany
Adenosine	A9251-25G	Sigma-Aldrich, Taufkirchen, Germany,
Tween® 20	A4974, 0500	AppliChem GmbH, Darmstadt, Germany
Potassium hydrogen carbonate	A0564, 1000	AppliChem GmbH, Darmstadt, Germany
Ammonium chloride	A-0171	Sigma-Aldrich, Taufkirchen, Germany,
Sucrose	A2211, 1000	AppliChem GmbH, Darmstadt, Germany
Adenosine	A9251-25G	Sigma-Aldrich, Taufkirchen, Germany,
Bovine Serum Albumin	A3059-50G	Sigma-Aldrich, Taufkirchen, Germany,
Tissue-Tek® O.C.T.	4583	Sakura Fineteck Europe B.V., Netherlands
ELISA MAX™ Standard Set Mouse IL-6	431301	BioLegend, Koblenz, Germany
ELISA MAX™ Standard Set Mouse IL-10	431411	BioLegend, Koblenz, Germany
4', 6-diamidin-2-phenylindole (DAPI)	D9542-5MG	Sigma-Aldrich, Taufkirchen, Germany

Table 4.2 Gradient Percoll solution

Percoll gradient	**For 100 ml**		**Color**
70 % Percoll	70 ml Percoll	30 ml HBSS	pink
37 % Percoll	37 ml Percoll	63 ml PBS	white
30 % Percoll	30 ml Percoll	70 ml HBSS	pink

Table 4.5 Buffers

Table 4.5.1 Red blood cell lysis buffer

Compound	Weight
Ammonium Chloride (NH4Cl)	8.26 g
Potassium bicarbonate (KHCO3)	1 g
EDTA	0.037 g
ddH2O	1 liter
pH	7.2

Table 4.5.2 Flow cytometry (FACS) buffer

Compound	Concentration
PBS	-
EDTA	2.5 mM
FCS	5%
Sodium azide	0.02%

Table 4.5.3 Fc-Blocking buffer

Name	Concentration
anti-CD16/32	1.6 µg / ml (in flow cytometry buffer)

Table 4.6 Antibodies

Table 4.6.1 Flow cytometry antibodies

Name	Clone	Cat	Supplier

Brilliant Violet 421 anti-mouse/human CD11b	M1/70	101235	BioLegend
Brilliant Violet 510 anti-mouse I-A/I-E (MHCII)	M5/114.15.2	107635	BioLegend
Brilliant Violet 605 anti-mouse Ly-6C	HK1.4	128035	BioLegend
Brilliant Violet 650 anti-mouse CD8a	53-6.7	100741	BioLegend
Brilliant Violet 711 anti-mouse TCR γδ	GL3	563994	BD Biosciences
Brilliant Violet 786 anti-mouse CD3	17A2	100231	BioLegend
FITC anti-mouse CD20	SA275A11	150408	BioLegend
PerCP/ Cyanine5.5 anti-mouse Ly-6G	1A8	127615	BioLegend
PE anti-mouse CD170 (Siglec F)	S17007L	155506	BioLegend
PE/Cy5 anti-mouse F4/80	BM8	123111	BioLegend
PE/Cy7 anti-mouse CD11C	N418	117318	BioLegend
APC anti-mouse CD19	1D3	17-0193-82	invitrogen
Alexa Fluor anti-mouse CD4	CD4	GK1.5	invitrogen
APC/Cyanine7 anti-mouse CD45	30-F11	103116	BioLegend
PE anti-mouse CD20	QCH6A7	12-0203-82	invitrogen
anti-mouse CD16/CD32	93	14-0161-82	invitrogen
Alexa Fluor 647 anti-mouse CD31	MEC13.3	102516	BioLegend
Alexa Fluor 647 anti-mouse CD169	3D6.112	142407	BioLegend
PE anti-mouse CD163	S15049I	155307	BioLegend
Alexa Fluor 647 anti-mouse CD31	MEC13.3	102516	BioLegend
Alexa Fluor 546 donkey anti-rabbit IgG (H+L)	--	A11081	invitrogen
Alexa Fluor 488 donkey anti-rabbit IgG (H+L)	--	A10040	invitrogen
Alexa Fluor 546 goat anti-rat IgG (H+L)	--	A21206	invitrogen

Table 4.6.2 Therapeutic antibodies

Name	Clone	Cat	Supplier
Ultra-LEAF™ Purified anti-mouse CD20 Antibody	SA271G2	152104	BioLegend
Ultra-LEAF™ Purified Rat IgG2b, κ Isotype control Antibody	RTK4530	400644	BioLegend
Ultra-LEAF™ Purified anti-mouse TCR γ/δ Antibody	UC7-13D5	107517	BioLegend
Ultra-LEAF™ Purified Armenian Hamster IgG Isotype control Antibody	HTK888	400959	BioLegend

Table 4.7 Real-time PCR primers

Target	Forward primer (5'-3')	anT	Cycles	Product (bp)
18S rRNA	For-GGACAGGATTGACAGATTGATAG	64	40	108
	Rev-CTCGTTCGTTATCGGAATTAAC			
CD20	For-TAAGCCTCTTTGCTGCCATT	60	45	209
	Rev-CAAGAACACAGACTGAATGCTG			
IFN-Y	For-GAAAATCCTGCAGAGCCAGA	60	45	183
	Rev-CATGAATGCATCCTTTTTCG			
IL-17A	For-TCTCTGATGCTGTTGCTGCT	60	45	195
	Rev-CGTGGAACGGTTGAGGTAGT			
IL-10	For-CAGGCAGAGAAGCATGGC	66	45	83
	Rev-TGCTCCACTGCCTTGCTC			
PDGFB	For-GAAGATCATCAAAGGAGCGG	62	45	120
	Rev-CCTTCCTCTCTGCTGCTACC			
PDGFRB	For-AGGACAACCGTACCTTGGGTGACT	62	45	89
	Rev-CAGTTCTGACACGTACCGGGTCTC			

Table 5 Instruments

Instrument	Cat	Supplier
Scientific balance	PG203-S	Waagendienst Winkler GmbH, Germany

pH meter	pH7110	WTW GmbH, Weilheim, Deutschland
Centrifuge	5424	Eppendorf AG, Hamburg, Germany
Centrifuge	5430 R	Eppendorf AG, Hamburg, Germany
Thermo Cycler	2720	Applied Biosystems, Thermo Scientific™
Cryotome	CRYOSTAR NX70	HISTOSERVE GmbH, Celle, Germany
SimpliNano	29-0887-91	GE Healthcare Life Sciences
ELISA Reader	MRXTC	DYNEX® Technologies GmbH, Baden-Württemberg, Germany
Fluorescence microscope	DM6 B	Leica Microsystems, Wetzlar, Germany
Fluorescence microscope	Axio Imager 2	Carl-Zeiss GmbH, Munich, Germany
Laser scanning microscope	LSM880	Carl-Zeiss GmbH, Munich, Germany
Flow cytometer	BD LSRFortessa	BD Biosciences, NJ, USA
Sorter	MoFlo Astrios AT13011	Beckman Coulter Biomedical GmbH, Munich, Germany
Thermo Cycler	StepOnePlus™ Real-Time PCR System	Life Technologies, California, USA
Imaging cytometer	ImageStreamX Mark-II	AMNIS Corporation, Seattle, WA, USA

Table 6 Software

Software	**Source**
Carl Zeiss™ AxioVision Rel. 4.8.2	Carl-Zeiss GmbH, Munich, Germany
GraphPad prism 8	GraphPad Software, California, USA
MS Office	Microsoft Corporation, Redmond, USA

IDEAS	Luminex Corporation, Texas, USA
BD FACS.D.iva v8.0	BD Biosciences, NJ, USA
FlowJo-v10	BD Biosciences, NJ, USA
ZEN Blue	Carl-Zeiss GmbH, Munich, Germany
INKSCAPE	Open source, online
Carl Zeiss™ AxioVision Rel. 4.8.2	Carl-Zeiss GmbH, Munich, Germany

5. METHODS

5.1 Government approval statement

8-12 weeks old mice of mixed gender were used in the study. All animal experiments were performed after approval from the Government of Upper Bavaria, Germany.

5.2 Anesthesia and post-surgical management

Mice were anesthetized with standard 3 combo mixture using, fentanyl (0.05 mg/kg), midazolam (5 mg/kg), and medetomidine (0.5 mg/kg) in 100µL via subcutaneously. After the surgical procedure, mice were given buprenorphine (0.05 mg/kg). After performing the perfusion measurement, anesthesia effect was antagonized with naloxone (1.2 mg/kg), flumazenil (0.5 mg/kg) and atipamezole (2.5 mg/kg). The route of administration was subcutaneous. Post-operative pain was managed with buprenorphine (0.05 mg/kg) for every 8-12 hr until day 3.

5.3 Induction of arteriogenesis

After anesthetizing mice, bepanthen was applied to the eyes to avoid desiccation. Upper thigh skin on both limbs was disinfected, and hair from the surgical site was shaved. Mice were placed on a heating pad (37°C). Mice limbs were fixed with surgical tape. The profunda femoris origin was estimated and a small skin incision was made. Skin and epithelial layers were prepared to access femoral artery by carefully separating it from femoral vein and nerve. After separating the artery, a surgical thread was placed under artery (Fig. 3) distally to the epigastric and profunda femoris branch. The thread was tied closely using a holder. The exact surgical procedure was performed on the other limb (left leg) without closing the surgical thread, which serves as intra sham control (Limbourg et al., 2009). The skin incision was closed with a surgical suture. Any arterial/venule/surrounding tissue damage during the procedure was strictly avoided.

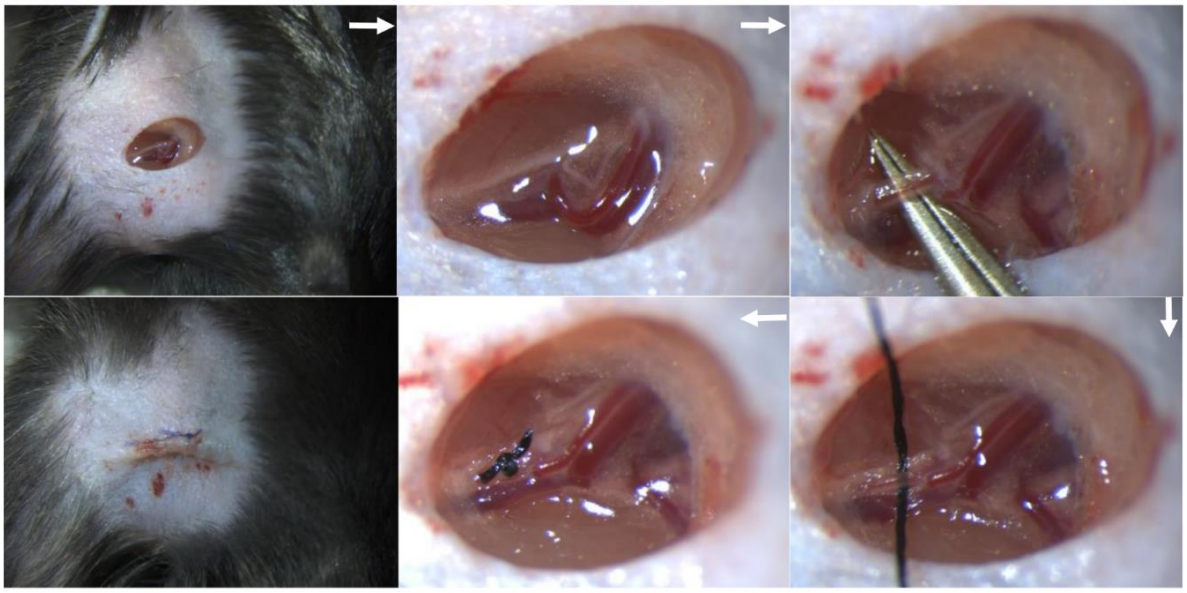

Figure 3. Surgical procedure of femoral artery ligation. A small skin incision was made and femoral artery at the branching site was carefully separated from femoral vein and nerve. Surgical thread was placed under the femoral artery and closed tightly to stop the blood flow distally. Skin incision was later closed with sutures.

5.4 Laser Doppler Imaging for perfusion measurement

Blood perfusion recovery measurement is one of the important methods to characterize arteriogenesis. This was done by a Laser Doppler. After being anesthetized, the mouse was placed in an incubator at 37 °C for 10 min. Using a low-power laser beam the instrument scan the lower hind limbs and generates a flux image. An arbitrary flux mean values were generated after drawing an ROI (Region of Interest) on each limb from ankle to toe. The relative perfusion recovery was calculated by the mean of ligated to sham-operated ratio (Fig. 4, 5). A value of < 12% immediately after surgical procedure was set as the cut-off for accurate femoral artery ligation; mice showed the value more than the cutoff was ignored for further analysis. Perfusion recovery was analyzed at different time points, i.e., baseline perfusion before the surgical procedure, immediately after surgery, day 3, and day 7 after surgery was measured.

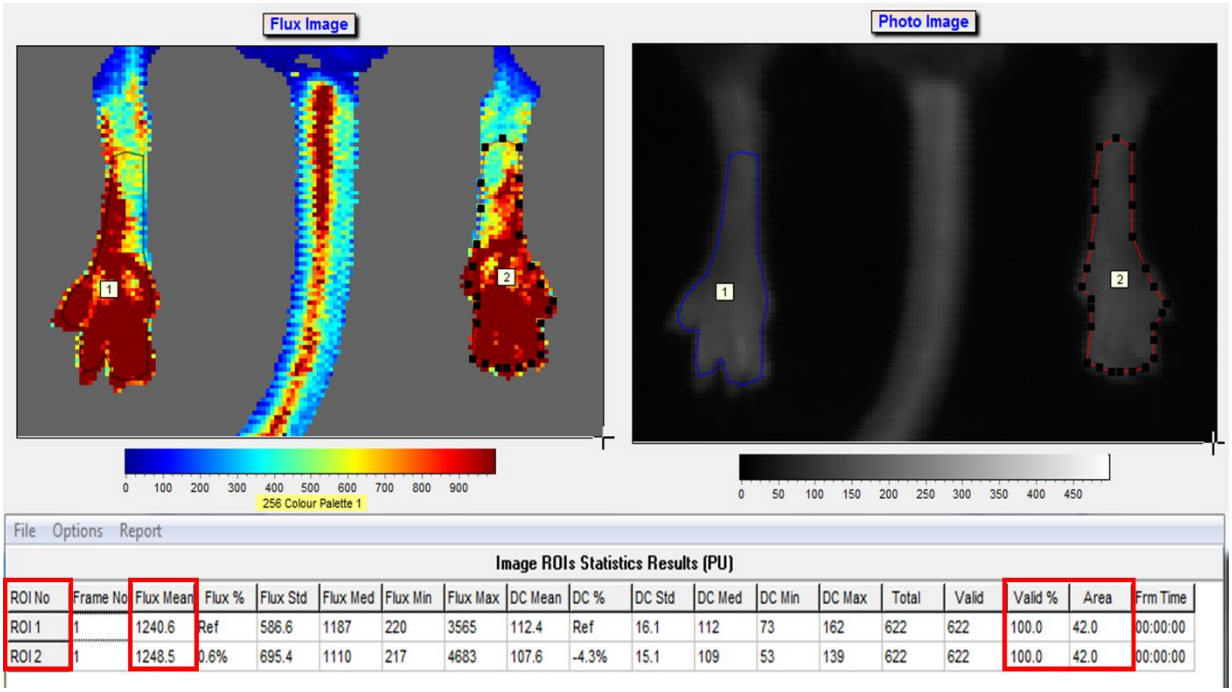

ROI No	Frame No	Flux Mean	Flux %	Flux Std	Flux Med	Flux Min	Flux Max	DC Mean	DC %	DC Std	DC Med	DC Min	DC Max	Total	Valid	Valid %	Area	Frm Time
ROI 1	1	1240.6	Ref	586.6	1187	220	3565	112.4	Ref	16.1	112	73	162	622	622	100.0	42.0	00:00:00
ROI 2	1	1248.5	0.6%	695.4	1110	217	4683	107.6	-4.3%	15.1	109	53	139	622	622	100.0	42.0	00:00:00

Figure 4. LDI output image of at baseline showing the drawing the ROI, corresponding flux mean value, validity of the ROI selection and area of the ROI.

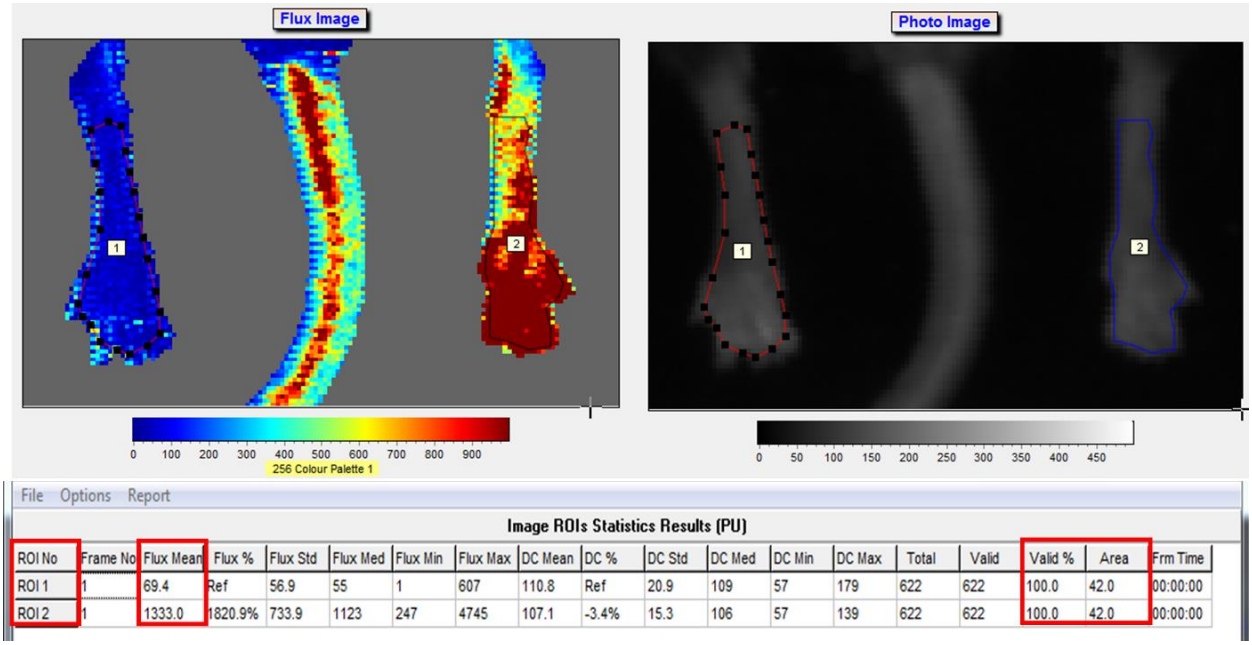

ROI No	Frame No	Flux Mean	Flux %	Flux Std	Flux Med	Flux Min	Flux Max	DC Mean	DC %	DC Std	DC Med	DC Min	DC Max	Total	Valid	Valid %	Area	Frm Time
ROI 1	1	69.4	Ref	56.9	55	1	607	110.8	Ref	20.9	109	57	179	622	622	100.0	42.0	00:00:00
ROI 2	1	1333.0	1820.9%	733.9	1123	247	4745	107.1	-3.4%	15.3	106	57	139	622	622	100.0	42.0	00:00:00

Figure 5. LDI output image of at immediately after surgery showing the drawing the ROI, corresponding flux mean value, validity of the ROI selection and area of the ROI.

5.5 In vivo treatments

5.5.1 In vivo CD20 cell depletion

For CD20 cell depletion, 200-250 µg of Ultra-LEAF™ Purified anti-mouse CD20 antibody (BioLegend) was injected intravenously (i.v.) on 7 days before the surgical procedure. This time point has been reported to completely depleted B cells in mice. The Control group was treated with the same concentration of Ultra-LEAF™ Purified Rat IgG2b, κ Isotype control antibody (Schaheen et al., 2016).

5.5.2 In vivo γδ T cell depletion

γδ T cell depletion was carried out by injecting a single dose of 200-250 µg of Ultra-LEAF™ Purified anti-mouse TCR γ/δ antibody (BioLegend) intravenously on 1 day before the surgical procedure. The Control group was treated with the same concentration of Ultra-LEAF™ Purified armenian Hamster IgG Isotype control antibody.

5.5.3 Bromodeoxyuridine (BrdU) treatment

BrdU is a structural analogue of thymidine. During the DNA replication (S phase), BrdU is incorporated in the DNA of replicating cell; thus it is used as a proliferative marker. Mice received a daily dose of 1.25 mg BrdU dissolved in 100 µl of PBS, intraperitoneally, starting from surgical procedure day until one day before the endpoint.

5.6 Perfusion and tissue harvesting

Mice were sacrificed humanly. The skin was disinfected, and the abdominal cavity was accessed by opening the abdomen. The aortic artery and vena cava were separated next to the kidneys. The sharp end of a butterfly needle was cut away in order to avoid damage during the catheterization of the aorta. A small incision was made in the aorta, and the butterfly needle was inserted, and the incision was closed with a surgical silk thread. Using a three-way

cannula fitted with a perfusion tube with 50 ml capacity syringe and a 5 ml syringe. The perfusion syringe was filled with 20 ml of freshly prepared pre-warmed (37°C) vasodilation buffer (check buffers) and allow the buffer to flow throw the aorta. To fix the dilated vessels, 10-20 ml of 3-4% of paraformaldehyde was perfused afterwards.

After the perfusion, the skin was removed from both thighs, and the muscle was excised (Kumaraswami et al., 2020). For cryopreservation, excised muscle was placed in tissue cassettes and incubated in 15% sucrose for 1 hr and then in 30% sucrose overnight. Later, the excess sucrose solution from tissue was removed by blotting on paper and later embedded in cryomolds filled with TissueTek. These cryomolds were placed on dry ice for a an hour and later stored at -80°C.

5.7 Histology Immunofluorescence

TissueTek embedded muscles were cut in two parts where the femoral artery was ligated (or sham-operated). One of the parts was placed on disc and later fixed to cryotome. 8-10 µm thick cross-sections were prepared from tissue.

5.7.1 BrdU staining

Cryosections were incubated with 2N HCL for 30 minutes at 37°C to denature the DNA, then washed three times with PBS, each time incubating 10 minutes in PBS. After that, slices were incubated in a humidified dark room overnight at 4 °C with anti-BrdU antibody (1/50). The sections were washed three times in PBS the next day. The primary labelling was detected by incubating with alexa fluor 546 conjugated secondary antibody (1/200) for 1 hour at room temperature. The sections were washed three times in PBS. Finally, for 10 minutes at ambient temperature, DAPI counter-stained (1/1000). After washing in PBS, slices were mounted with a Mowiol or mounting media and stored at 4 °C until imaging.

5.7.2 Macrophage staining

8-10 µm cryosections were stained with alexa fluor 488 conjugated anti-CD68 (1/100), anti-MRC (1/200), anti-F4/80 (1/50), alexa fluor 647 conjugated anti-CD169 (1/50), PE-conjugated anti-CD163 (1/50), anti-MARCO (1/50), PE-conjugated anti-CD40 (1/50) antibodies 4 °C for overnight. Following the next day, sections were washed as described above and incubated with corresponding secondary antibodies (for unconjugated primary antibodies) for 1 hr at ambient temperature, followed by washing and counterstaining with DAPI. All antibodies were diluted in PBS.

5.7.2 Image acquisition and analysis

Immunofluorescence images were acquired with Zeiss LSM 880 confocal laser scanning microscope with an Airyscan feature. 2-3 superficial collateral adductor muscle sections were imaged. In total 6-10 collateral arteries were analyzed by microscope. For macrophage and BrdU positive cell quantification, all images were acquired with 20x objective without area zoom. For Mean Fluorescence Intensity (MFI) analysis, the slide was overviewed (Fig. 6), multiple positions where the macrophages were accumulated around the perivascular space were selected. The focus was increased to zoom 4. Around 16 µm Z-stack with 30 slices planes were set up. Laser exposure was adjusted and fixed using the brightest position. These standard Staining and imaging conditions were strictly followed throughout the experiment to maintain integrity in MFI analysis. Finally, a polygonal ROI was drawn around the macrophage. The software generated an arbitrary mean value for each channel and was compared and analyzed. Since I did not include the area from the muscle section, background intensity subtraction was avoided.

Representative images were acquired either with 20x (plane or oil) or 40x (oil) objective with the same (above) Z-stack setup. Image format was either 1024*1024 or 2048*2048. Acquired images were analyzed with ZEN black software (Carl Zeiss AG, Germany). For MFI representation, macrophages located in close proximity to growing artery was selected and imaged with 15 zoom, 2024*2024 image formats for detailed quality.

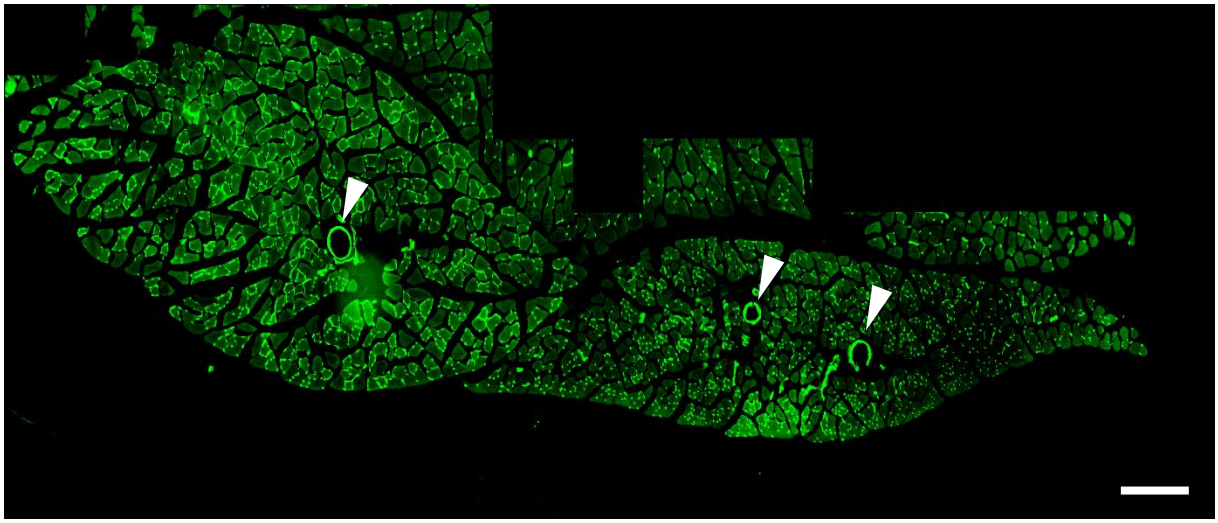

Figure 6. Representative immunofluorescence image showing location of collateral arteries (arrows) in WT mice adductor muscle collected on day 7 after surgical procedure. Muscle section was stained for CD31 marker.

5.8 Flow cytometry, imaging cytometry, sorting and gene expression

5.8.1 Flow cytometry

Mice were anesthetized and sacrificed humanly. Cardiac blood was collected in EDTA-coated collecting tubes by cardiac puncture. Organs were collected from mice and placed in a petri dish filled with cold PBS. Bone marrow was collected by flushing the tibia with cold PBS.

The cardiac blood was centrifuged at 350-420 g for 5 min at 4 °C. The cell pellet was dissolved in 10 ml of RBC lysis buffer and incubated on ice for 5 min. Later, tubes were filled with 5 ml of cold PBS and centrifuged. The supernatant was discarded, RBS lysis was repeated if the pellet was still contained Red blood cells. Finally, RBC free cell pellet was dissolved in 20 µL of FACS buffer.

For single-cell suspensions from organs, the organs were cut into small pieces with surgical scissors and placed in a tube with 1 ml of RPMI media. To digest the tissue 1 ml of enzyme cocktail, which contains collagenase IV (200U/) and DNase I (0.2 mg/) was added, and the mixture was incubated in a laboratory shaker for 1 hr at 37 °C with 120 rpm. Digested tissue mixture was filtered through a 70 µm cell strainer and filled up 50 ml with FACS buffer. Tubes were centrifuged at 350-420 g for 5 min at 4 °C. The supernatant was discarded. The cell pellet was dissolved in 4 ml of 70% Percoll. 4 ml of 37% Percoll was gently layered over 70% Percoll, followed by 30% Percoll. Tubes were centrifuged for 30 min at room temperature with 940 g speed. The acceleration was set to a minimum, and the break was removed to preserve the gradient separation. Cell layer from the interface between 70% and 37% Percoll was collected in a fresh tube and filled up to 15 ml with FACS buffer. Tubes were centrifuged at 350-420 g for 5 min at 4 °C. The supernatant was discarded, and the cell pellet was dissolved in 200 µL of FACS buffer.

Cell suspension was later transferred to 96 well V bottom plate and centrifuged at 350-420 g for 5 min at 4 °C. The supernatant was discarded carefully. The Cell pellet was dissolved in 200 µL of eFluor 450 fixable/viability dye (1/1000 dilution) and incubated in the dark at 4 °C for 30 min. Thereafter cell suspension was centrifuged, and the cell pellet was resuspended in 200 µL of FACS buffer and centrifuged. The cell pellet was resuspended in 50 µL of Fc-Block and incubated at 4 °C for 10 min. A two-fold concentration of FACS antibody cocktail was prepared in FACS buffer. 50 µL of antibody cocktail was added and incubated at 4 °C for 20 min. The cell suspension was centrifuged at 350-420 g for 5 min at 4 °C. The cell pellet was resuspended in 20 µL of FACS buffer and centrifuged. For intracellular staining, cells were fixed in 1% PFA for 15 min at room temperature and washed with 200 µL of FACS buffer by centrifugation at 350-420 g for 5min at 4 °C. The cell pellet was suspended in 0.1% TritonX for 15 min at 37 °C. Later, centrifuged at 350-420 g for 7 min at 4 °C. The cell pellet was resuspended in 100µL of antibody solution at incubated at 4 °C for 20 min in the dark. After incubation, the plate was centrifuged at 350-450 g for 7 min at 4 °C. The supernatant was discarded carefully without losing the cell pellet. Later pellet was resuspended in 200 µL of FACS buffer and centrifuged. AT final, the cell pellet was dissolved in 100 µL of FACS buffer and analyzed by a flow cytometer (Kumaraswami et al., 2020).

5.8.2 Single-cell imaging

Single-cell suspension was prepared as explained in Flow cytometry (5.8.1).

The cell pellet was resuspended 20 µL of fixable/viability dye (eFluor780) (1/1000 dilution) for 20 min at 4 °C in the dark. Centrifuged and washed with 20 µL of FACS buffer. Cell pellet then incubated with antibodies of interest mixture at 4 °C for 20 min. Next, cells were centrifuged at 350-420 g for 5 min at 4 °C. The supernatant was discarded, and the cell pellet was resuspended in 200 µL of FACS buffer and centrifuged. The cell pellet was fixed and permeabilized as explained previously (3.8.1). Next, the cell pellet was incubated with anti-CD20 antibody (for intracellular staining) for 30 min at 4 °C in dark. Then after centrifuged and washed with 200 µL of FACS buffer. At finally, the cell pellet was resuspended in 50 µL of DAPI (1/2000, PBS). Cell imaging was performed in AMNIS, and the data was analyzed by IDEAs software (Fig. 7).

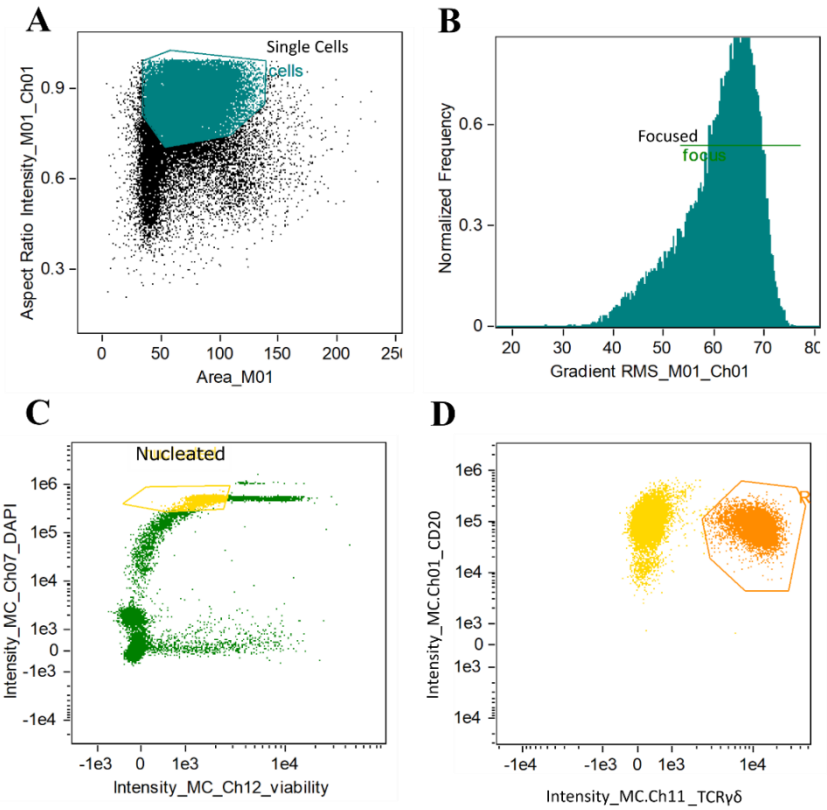

Figure 7. Gating strategy

Gating strategy showing (A) single cells were identified by gating Area vs. Aspect Ratio. (B) cells in focus were identified by gradient RMS. (C) Nucleated cells were identified high intensity for DAPI channel. (D) CD20 signal for each cell was identified by gating against the respective marker. Single cells identified by this procedure were added to the analysis area and later exported for further comparison.

5.8.3 Cell sorting

The single cell suspension was prepared as explained above. The cell pellet was incubated with antibodies of interest for 30 min at 4 °C in dark. Cells were centrifuged at 350 g for 5 min at 4 °C. The cell pellet was resuspended in 200 µL of cold PBS and centrifuged at 350 g for 5 min at 4 °C. Finally, the cell pellet was resuspended in 200 µL of cold PBS. Cytox blue was added (1/1000 dilution) right before feeding to the sorter. Sorted cells were collected in sterile tubes contained 100 µL of cold PBS. Sorting protocol using cold PBS showed improved RNA yield and quality.

5.8.4 RNA isolation, cDNA synthesis

Sorted cells were centrifuged for 5 minutes at 350g at 4 °C. The cell pellet was dissolved in cell lysis buffer. RNA isolation was carried out using a commercially available kit (Qiagen) according to the manufacturer's instructions. The supernatant was discarded after the sorted cells were pelleted. After that, the cells were lysed in cell lysis buffer. After the lysis, ethanol was added. Total volume was then transferred to RNeasy spin columns. RNA was then bound to the column. Bound RNA was eluted with elution buffer at a final volume of 30 µL of RNAse free water. RNA concentration and purity were analyzed by nanodrop. Complementary DNA (cDNA) was synthesized using maximal H minus kit (ThermoFisher) followed by manufacturer's instructions.

Reaction conditions

Reagent	**Concentration or volume**
Template RNA	50-100 pg
Primers (Forward and Reverse)	0.25 µl
10 Mm Dntp mix	1 µl
Nuclease free water	adjust to 15 µl volume

5X RT Buffer	4 µl	
Maximal H Minus Enzyme Mix	1 µl	
Final total volume	20 µl	
Reaction Program		
Incubation	10 min	25 °C
Reverse Transcription	15 min	50 °C
Termination	5 min	85 °C
Holding	-	4 °C

5.8.5 Real time PCR

PCR master mix was prepared with 5 µm forward and reverse primer, 2 µl of ddH_20 and 5 µl of Powerup SYBR Green amplification mix. 2 µl of undiluted cDNA was used as template in 8 µl of master mix (10 µl reaction mix). Real time PCR was carried out in StepOne Plus PCR machine (Cycle condition refer Table.2.7.). Data was analyzed with ΔΔCt method.

5.9 Statistics

All the results were analysed with GraphPad Prism 8 (GraphPad Software, California, USA). Data from two groups with single timepoint was analysed by student's t test. Data from multiple groups from more than one timepoint was analysed by 2-way ANOVA with Bonferroni correction. Data represented as either mean±S.D. or mean±S.E.M. The detailed description was mentioned in figure legend. A p-value <0.05 was considered statistically significant.

6. RESULTS

6.1.1 Relevance of lymphocytes in arteriogenesis

6.1.2 Arteriogenesis in the absence of B and T cells

The hindlimb ischemia mouse model is the better suited mouse model to evaluate arteriogenesis. Arteriogenesis is induced by ligating femoral artery distal to the epigastric and profunda femoris brach (Fig. 3). Due to arteriogenesis the collateral arteries in the adductor muscle grow in a characteristic corkscrew pattern (Fig. 2). Laser Doppler Imaging (LDI) allows for a highly controlled surgical ligation (Fig. 4 & 5). LDI can detect any faulty ligation after femoral artery ligation, which could help to avoid evaluation errors. To see if arteriogenesis drives in an adaptive immunological manner involving B and T lymphocytes, I utilized Rag1 KO mice, which lack B and T cells in the system. Arteriogenesis was induced in wild-type (WT) and Rag1 KO mice by surgically ligating the femoral artery distal to the epigastric and profunda femoris branches. Perfusion recovery was measured before ligation, immediately after ligation, on day 3, and on day 7 after ligation. Rag1 KO mouse had significantly worse relative perfusion recovery on days 3 and 7 after femoral ligation than WT mice (Fig. 8A-B). I then checked to see if Rag1 KO mice had any issues with vascular cell proliferation. On day 7 after femoral ligation, the adductor muscle was cut into 10µm thick sections and stained with anti-BrdU antibody (Fig. 8C). Vascular cell proliferation was measured by counting $BrdU^+$ nucleated cells on the vascular wall. Rag1 KO mice had a significantly lower number of proliferating vascular cells than WT mice (Fig. 8D). Next, I checked collateral artery growth by analyzing the luminal diameter of superficial collateral arteries in adductor muscle. Rag1 KO mice demonstrated considerably less collateral artery growth as defined by luminal diameter on day 7 after femoral ligation than WT mice (Fig. 8E). Macrophages provide growth-promoting factors during arteriogenesis. Macrophage phenotype $CD68^+MRC1^-$ considered as inflammatory, whereas $CD68^+MRC1^+$ are anti-inflammatory/regenerative macrophages. I wanted to see if the Rag1 KO mice poor arteriogenesis response was linked to perivascular macrophage accumulation. Adductor muscle sections from WT mice and Rag1 KO mice on day 7 after femoral artery ligation were stained with anti-CD68 and anti-MRC1 antibodies (Fig. 8F).

Rag1 KO mice had a considerably higher number of $CD68^{+}MRC1^{-}$ inflammatory macrophages than WT mice (Fig. 8G), whereas $CD68^{+}MRC1^{+}$ macrophage accumulation was significantly reduced (Fig. 8H).

The conclusion drawn: Lack of functional B and T cells in Rag1 KO mice significantly attenuated arteriogenesis.

Figure 8

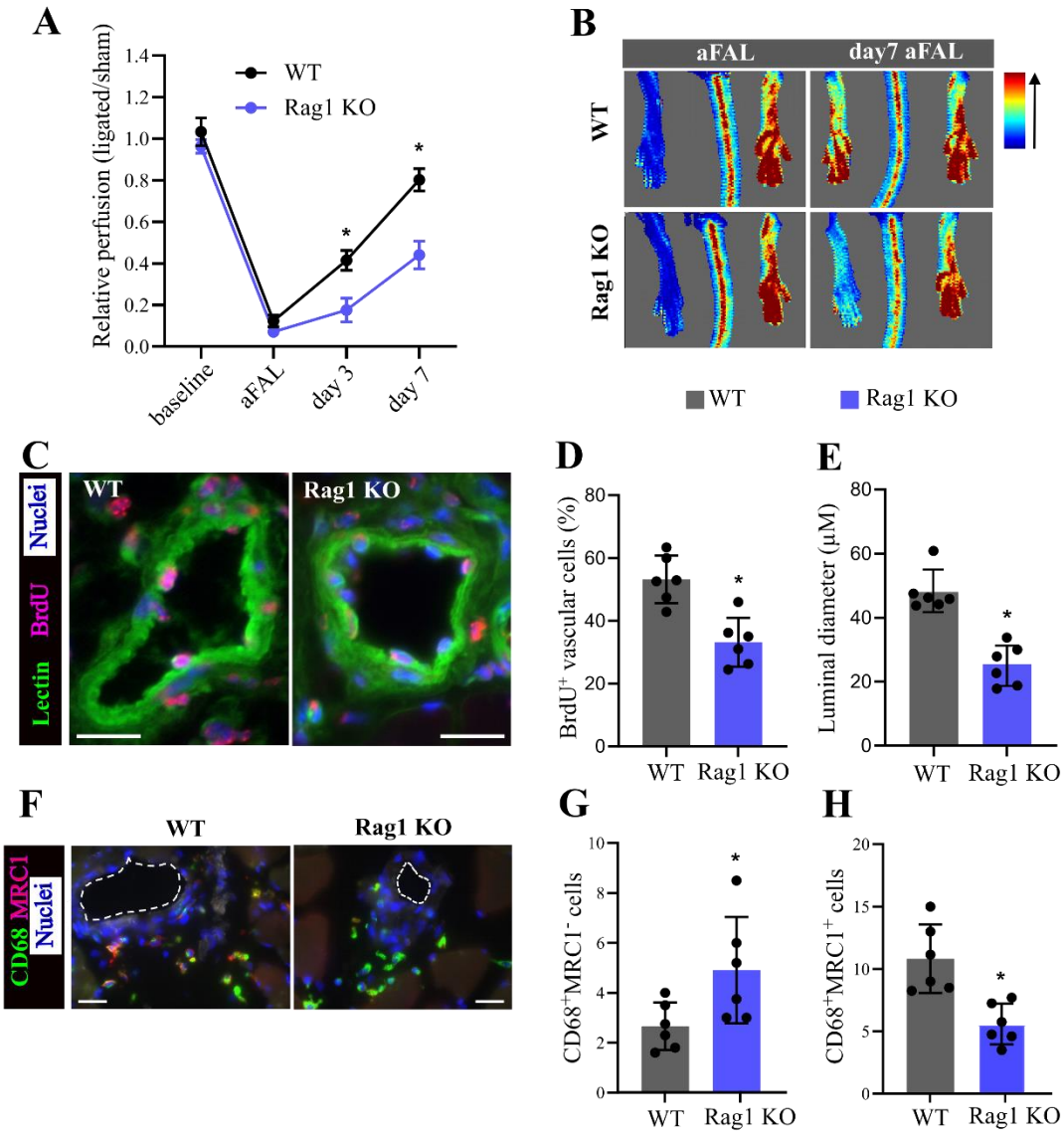

Figure 8. Impaired arteriogenesis in mice genetically lack of B and T cells

- **A.** Relative perfusion of WT and Rag1 KO mice as calculated by ligated / sham at baseline, immediately after femoral artery ligation, at day 3 and at day 7 after femoral artery ligation (aFAL). Data represent mean±S.D. *P<0.05 by two-way ANOVA multiple comparison test with Bonferroni correction, n=6 mice.
- **B.** Representative Doppler flux images of WT (upper panel) and Rag1 KO (lower panel) mice at immediately after femoral artery ligation (left) and at day 7 after femoral artery ligation (right). Flux color scale indicate low (blue) to high (red).
- **C.** Epifluorescence microscope images of WT and Rag1 KO mice adductor muscle at day 7 after femoral artery ligation, stained for BrdU (pink), lectin (green, to visualize arteries) and nuclei (blue). Proliferating vascular cells were identified as $BrdU^+$ nucleated cells residing on vascular wall. Scale bar 20μm.
- **D.** Bar graph data showing the number of $BrdU^+$ vascular cells. Each dot represents the mean data of one mouse in the group. A total of 6-10 collateral arteries were analyzed. Data mean±S.D., *P<0.05, as analyzed by t test, n=6 mice.
- **E.** Bar graph data showing the luminal diameter of collateral arteries. Each dot represents mean of 6-10 collateral arteries. Data mean±S.D., *P<0.05, as analyzed by t test, n=6 mice.
- **F.** Representative immunofluorescence images of macrophages around perivascular space of collateral artery in WT and Rag1 KO mice day 7 aFAL. Scale bar 20μm.
- **G.** Bar graph showing number of $CD68^+MRC1^-$ macrophages.
- **H.** The number of $CD68^+MRC1^+$ macrophages. **G** and **H** at day 7 after femoral artery ligation. Data mean±S.D. Each dot represents mean of 6-10 collateral arteries. * P<0.05 by t test, n=6 mice.

6.1.3 Relevance of B lymphocytes in Arteriogenesis

6.1.4 Arteriogenesis in the absence of B cells

6.1.5 CD20 mediated B cell depletion

B cells can control the inflammation due to their immune regulatory properties. The role of B cells in arteriogenesis has never been studied. B cells, I speculate that B cells might play a role in transitioning from the inflammatory to the regenerative phases by influencing the macrophage compartment, likely via IL-10. To test this hypothesis, I treated WT mice with anti-CD20 antibody, and the control group received the same dose of Isotype control antibody (Fig. 9A). After a single dose of anti-CD20 antibody treatment, B lymphocytes as determined by $CD19^+$ cells by flow cytometry were significantly decreased in bone marrow (Fig. 9B), spleen (Fig. 9C), and blood (Fig. 9D).

Figure 9

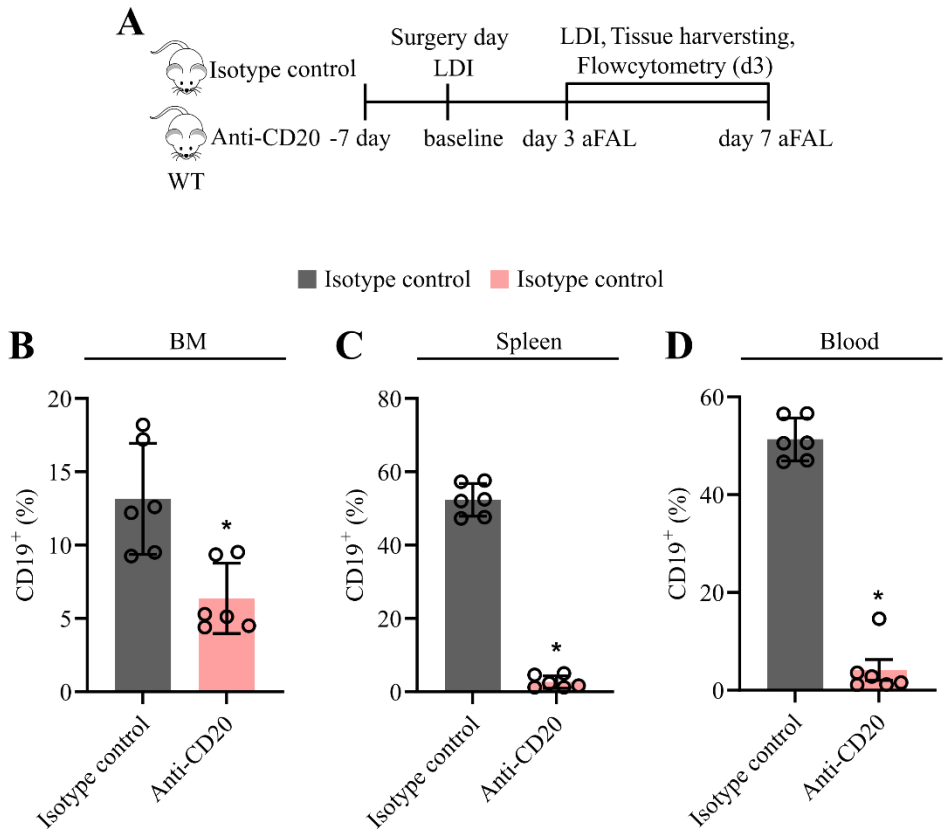

Figure 9. Anti-CD20 treatment effectively deplete B cells in BM, spleen and blood

A. Diagram showing study design. WT mice were randomly divided into two groups. One group received Isotype control antibody (200-250 µg/mice, intravenously), another group received anti-CD20 antibody (200-250 µg, intravenously) at -7 day before femoral artery ligation. Perfusion was measured at baseline, aFAL, at day 3 and day 7. Mice were humanly sacrificed at day 3 (blood and spleen were harvested for flow cytometry) and day 7. After perfusion, muscles were cryopreserved and used for histology analysis.

B. & **C, D;** Bar graphs showing B cells (% of CD45) in **(B)** BM, **(C)** spleen, and **(D)** blood. Each circle represents the value of one mouse. Data mean±S.D., **P*<0.05, as analyzed by t test, n=6 mice.

6.1.6 Effect of CD20 depletion on arteriogenesis

At day 3 and day 7 after femoral artery ligation, anti-CD20 antibody-treated mice had significantly lower perfusion recovery than WT mice treated with Isotype control antibody (Fig. 10A-B). In the anti-CD20 antibody-treated group, vascular cell proliferation (Fig. 10C) and collateral artery growth (Fig. 10D) were similarly significantly reduced. In anti-CD20 antibody-treated WT mice, the number of perivascular $CD68^{+}MRC1^{-}$ inflammatory macrophages was

unaltered (Fig. 10E), while the number of regenerative $CD68^{+}MRC1^{+}$ macrophages was drastically reduced (Fig. 10F).

The conclusion drawn: CD20 depletion impaired arteriogenesis in WT mice.

Figure 10

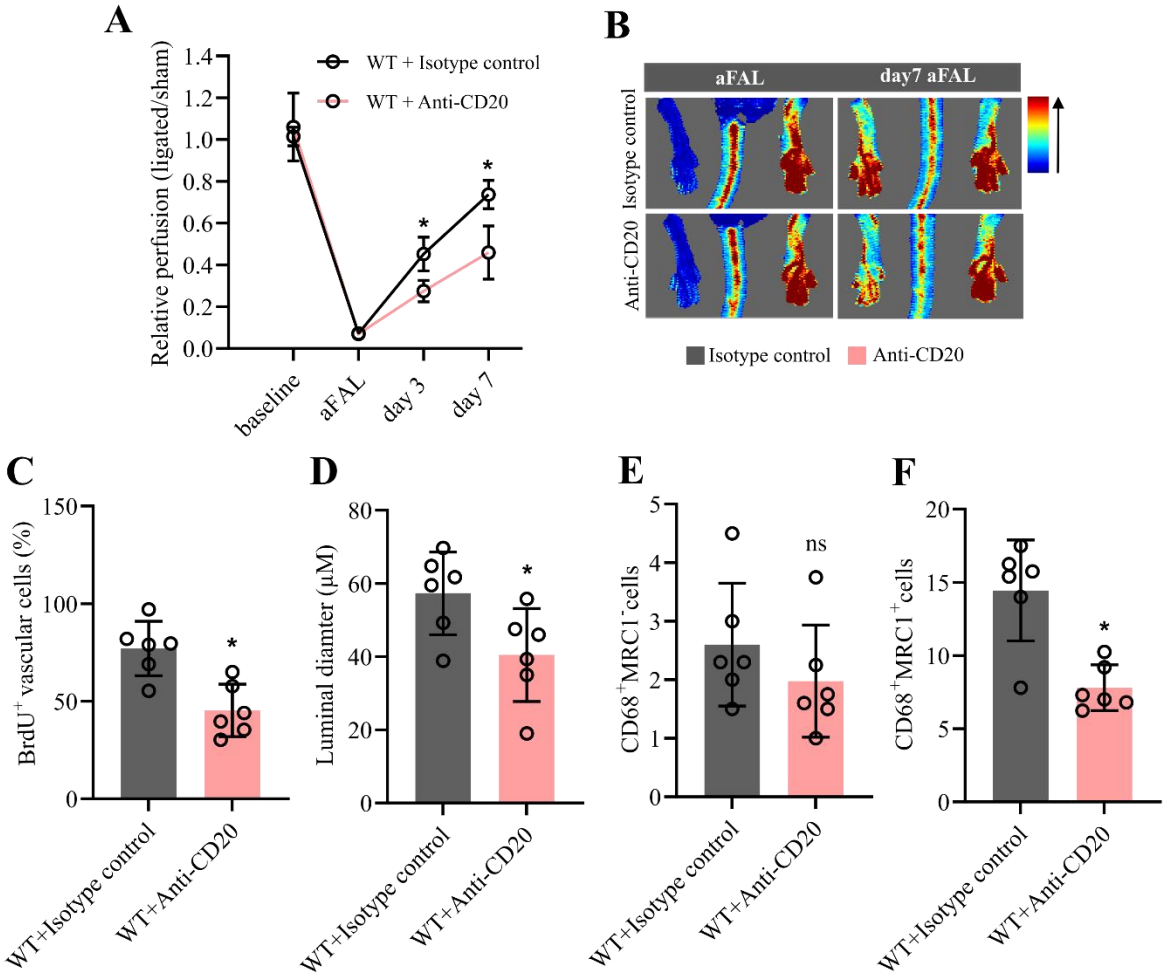

Figure 10. CD20 depletion interferes with arteriogenesis in WT mice

- **A.** Data showing relative perfusion differences between two groups (Isotype control vs Anti-CD20). Data mean±S.D., **P*<0.05 by two-way ANOVA multiple comparison test with Bonferroni correction, n=6 mice.
- **B.** Representative Doppler flux images from WT mice treated with Isotype control (upper panel) and Anti-CD20 antibody (lower panel) at aFAL, at day 7 aFAL.
- **C.** Bar graph data showing the data of $BrdU^{+}$ vascular cells.
- **D.** Luminal diameter of collateral arteries at day 7.
- **E.** & **F**. Bar graphs showing the number of $CD68^{+}MRC1^{-}$ **(E)** and $CD68^{+}MRC1^{+}$ **(F)** macrophages at day 7 aFAL.

C, D, E and **F**; Each dot represents mean of 6-10 collateral arteries. Data represent mean±S.D., ns no significance, * *P*<0.05 by t test, n=6 mice.

6.1.7 Effect of CD20 depletion on splenic T cells and eosinophils

B cells are known to have some regulatory activities, as previously stated. I would like to see how the Anti-CD20 treatment affects T cells and eosinophils (see Fig. 14 for gating strategy), since it drastically reduced B cells. There was no significant difference in the percentage of CD4 (Fig. 11A), CD8 (Fig. 11B), or eosinophils (Fig. 11D) between Isotype and Anti-CD20 treated WT mice in flow cytometry analyses. Anti-CD20-treated mice, on the other hand, showed significantly increased γδ T cells (Fig. 11C).

The conclusion drawn: CD20 depletion showed no effect on CD4, CD8, γδ T cells and eosinophils.

Figure 11

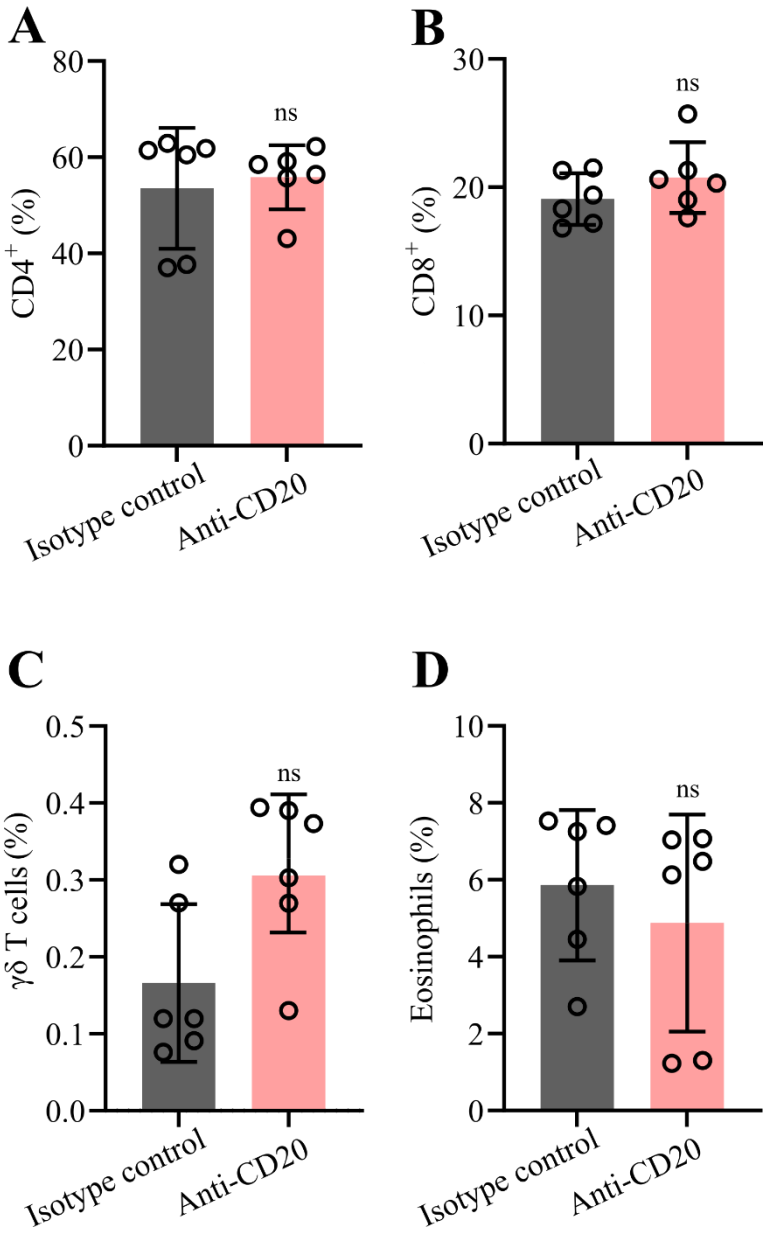

Figure 11. Effect of CD20 depletion on splenic T cells and Eosinophils

Bar graphs showing data of **(A)** CD4 (% of CD3), **(B)** CD8 (% of CD3), **(C)** γδ T cells (% of CD45) and, **(D)** eosinophils (% of CD45) in the spleen, analyzed by flow cytometry. Each circle represents the value of one mouse. Data mean±S.D., ns no significance, as analyzed by t test, n=6 mice.

6.1.8 Effect of CD20 depletion on CD20 positive T cells and eosinophils

Flow cytometry analysis revealed that fraction of T cells and eosinophils are CD20 positive (Fig. 12). Since anti-CD20 treatment targets CD20, I would like to check whether CD20 positive T cells and eosinophils were also targeted by anti-CD20 treatment. The percentage of $CD4^+CD20^+$ cells (out of $CD4^+$) in WT mice treated with anti-CD20 antibody was significantly lower than in WT mice treated with isotype control antibody (Fig. 12A). Anti-CD20 therapy had no effect on $CD8^+CD20^+$ cells (Fig. 12B). Anti-CD20 therapy, on the other hand, significantly reduced the percentage of $TCR\gamma\delta^+CD20^+$ T cells (Fig. 12C) and $Siglec\text{-}F^+CD20^+$ eosinophils (Fig. 12D).

Figure 12

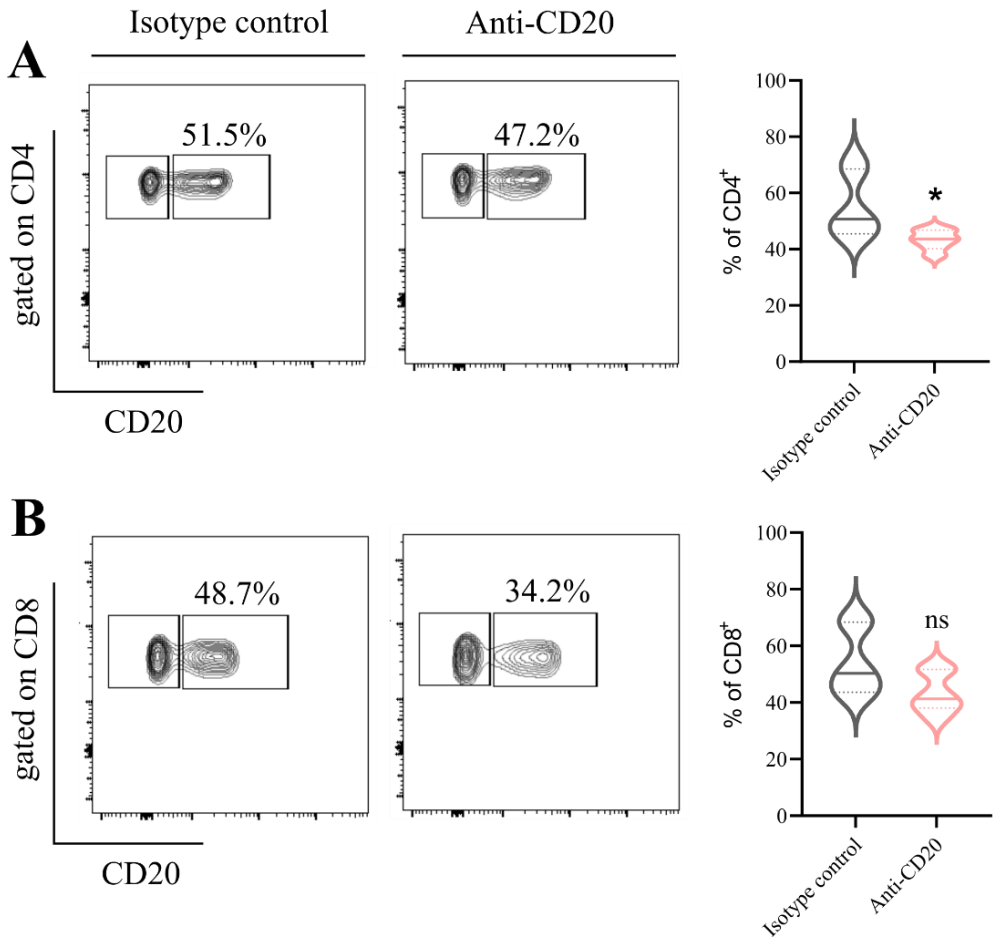

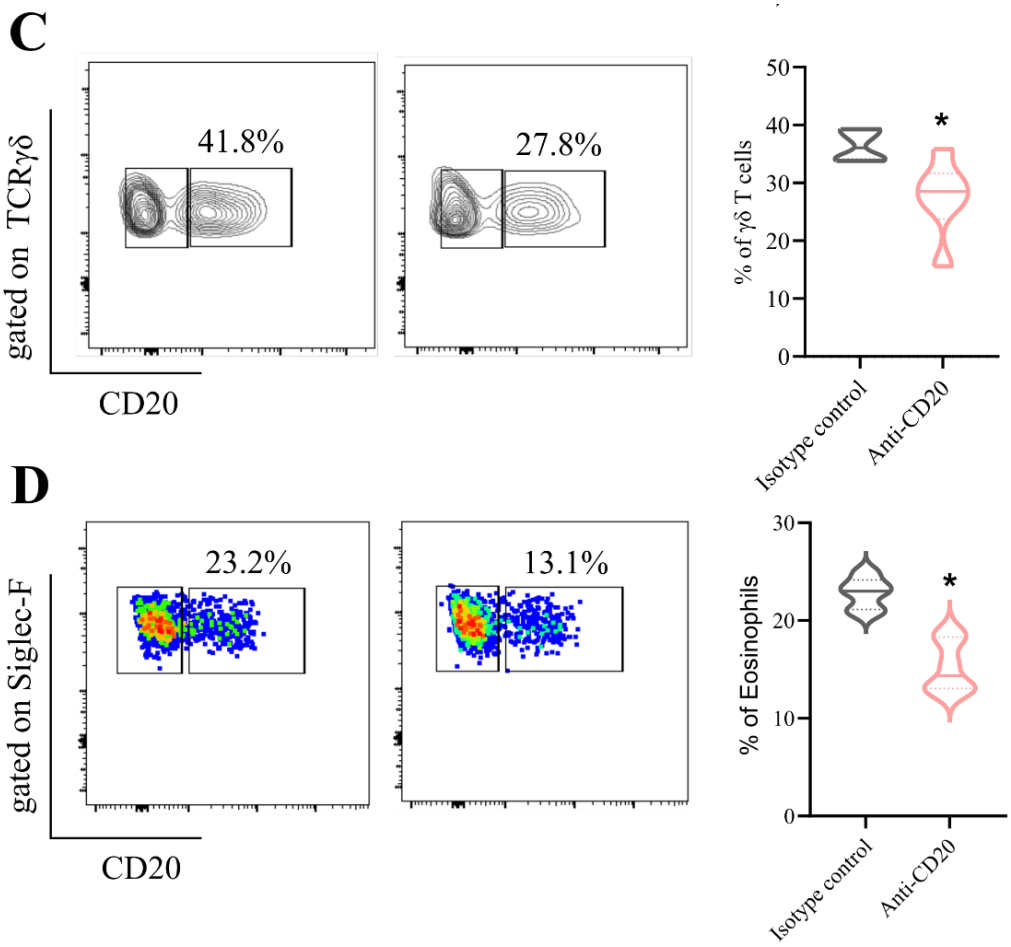

Figure 12. Effect of CD20 depletion on CD20 positive splenic CD4, CD8, γδ T cells, and eosinophils

Representative flowcytometry contour plots showing % of **(A)** $CD4^+CD20^+$ T cells, **(B)** $CD8^+CD20^+$ T cells, **(C)** $TCR\gamma\delta^+CD20^+$T cells, **(D)** Siglec-F^+CD20^+ eosinophils (pseudocolor plot), (left panel-Isotype control, right panel-Anti-CD20). Violin graphs showing data (of A, B, C, D). Data mean±S.E.M., ns no significance, **P*<0.05, as analyzed by t test, n=6 mice.

My Flowcytometry findings raise doubt on the specificity of CD20 antibodies (ref flowcytometry antibodies in material section under antibodies). To answer this question, I collected blood leukocytes from WT mice on day 3 aFAL. Staining was performed using anti-CD19, anti-TCRβ, anti-TCRγδ antibodies. I precisely used two clones of anti-CD20 antibodies from two different companies (BioLegend and invitrogen). Both clones of anti-CD20 antibodies were able to stain $CD19^+$ B cells, which served as a positive reference cell type (Fig. 13A). Anti-TCRβ, anti-TCRγδ antibodies were used to stain conventional T cells and γδ T cells respectively. Single cell imaging was performed in AMNIS. This approach (Fig. 7) clearly demonstrated that

both clones of CD20 are co-stained on conventional T cells and γδ T cell (Fig. 13B-C). CD20 expression has been observed in conventional T cells, but it has not been reported in γδ T cells to my knowledge. To confirm my findings further, I sorted B cells and γδ T cells from WT mice blood collected on day 3 after femoral artery ligation and sham operation. RNA was extracted from the sorted cell and cDNA was synthesized. Real-time PCR was used to examine CD20 gene expression. B cells ($CD19^{+}$) were used as a positive reference cell population (Fig. 13D). CD20 is expressed at measurable levels in γδ T cells (Fig. 13E). However, the difference between ligated vs sham surgery was not significant in both B and γδ T cells.

Figure 13

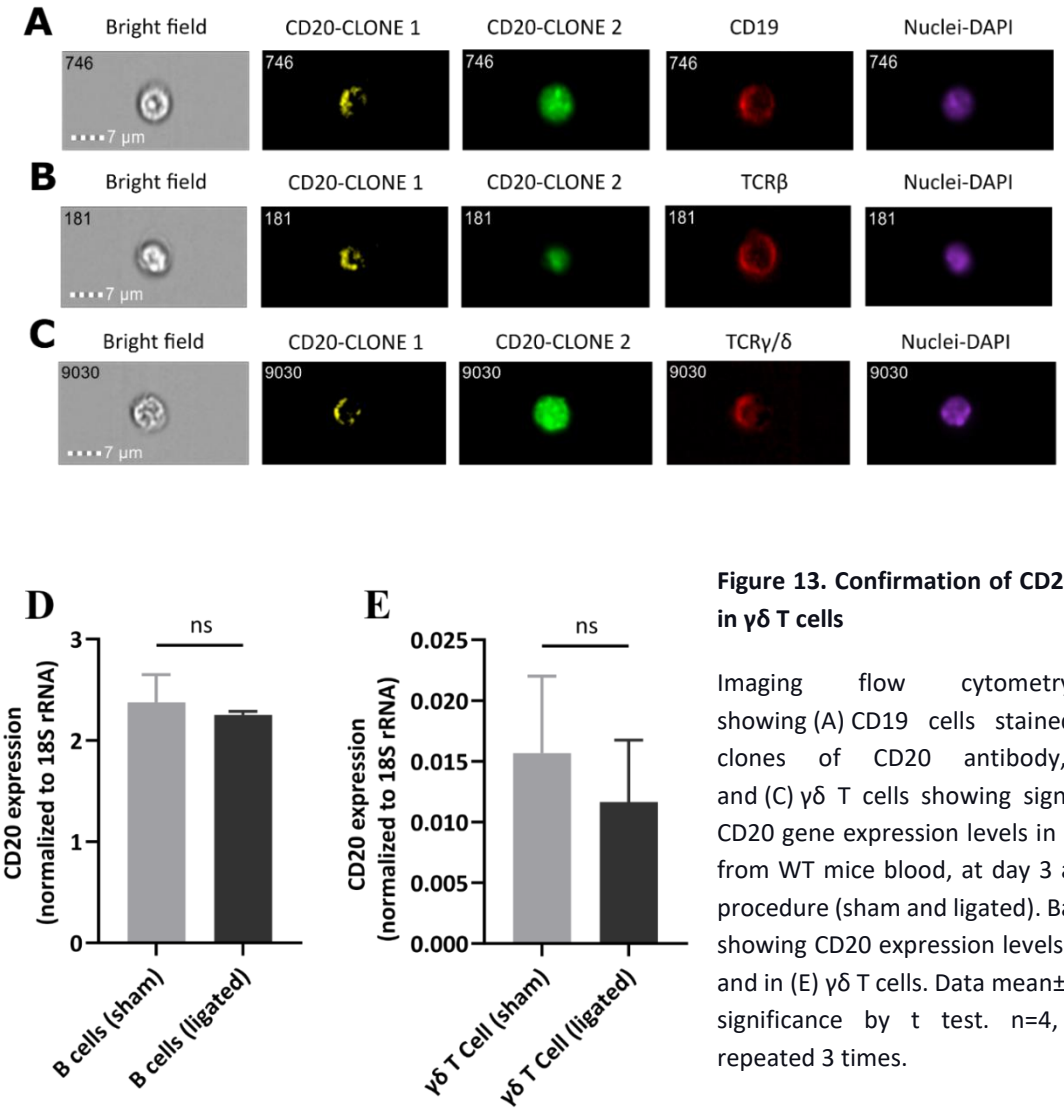

Figure 13. Confirmation of CD20 expression in γδ T cells

Imaging flow cytometry images showing (A) CD19 cells stained with two clones of CD20 antibody, (B) TCR β, and (C) γδ T cells showing signal for CD20. CD20 gene expression levels in cells isolated from WT mice blood, at day 3 after surgical procedure (sham and ligated). Bar graph data showing CD20 expression levels in (D) B cells and in (E) γδ T cells. Data mean±S.E.M., ns no significance by t test. n=4, experiment repeated 3 times.

6.1.9 Flow cytometry gating strategy for identification of different leukocytes

Figure 14

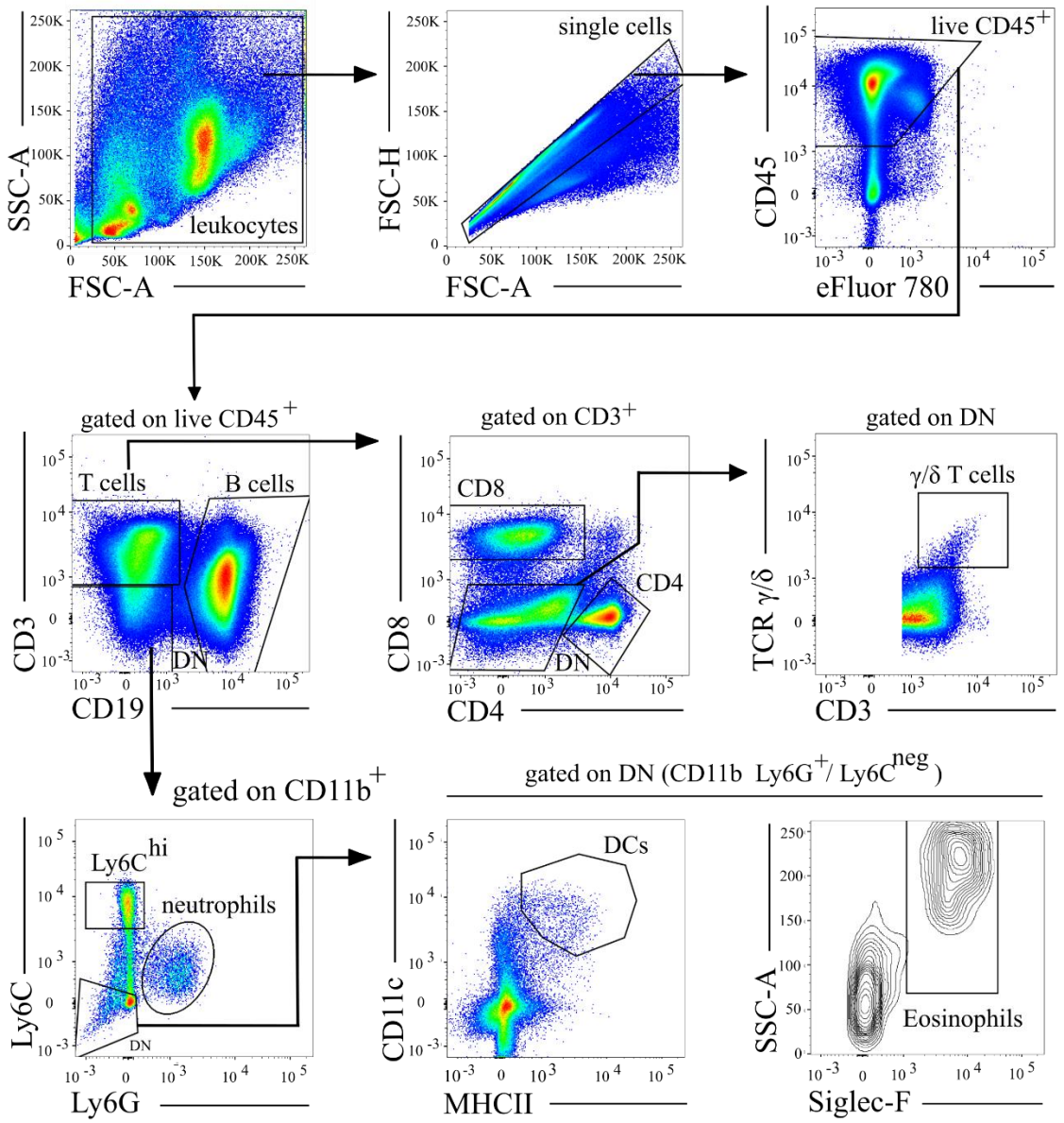

Figure 14. Flow cytometry gating strategy

Sequential flow cytometry gating strategy showing identification of different leukocytes. Top panel to identify live $CD45^+$ leukocytes. Middle panel showing $CD3^+$ T cells and $CD19^+$ B cells gated from live $CD45^+$. $CD4^+$ and $CD8^+$ cell populations were gated from $CD3^+$. γδ T cells were identified from $CD3^+$DN (double negative) cells. Lower panel showing inflammatory monocytes (Ly6Chi) and neutrophils identified from DN ($CD3^-CD19^-CD11b^+$). Dendritic cells (DCs) and eosinophils were identified from DN ($Ly6C^-Ly6G^-$) cell population.

6.2 Arteriogenesis in B cell-deficient (JHT KO) mice

Anti-CD20-mediated B cell depletion has been reported as a promising treatment option for B cell malignancies. One of the mechanisms hypothesized for the successful depletion of B cells by anti-CD20 antibody therapy was macrophage activation. As a result of CD20-mediated B cell depletion, the splenic and circulatory macrophage compartments maybe affected, and could be potentially interfering with macrophage accumulation during arteriogenesis. Second, my flow cytometry investigation revealed that fraction of T cells and eosinophils are CD20 positive. My data from CD20 depletion, taken collectively, is insufficient to define the role of B cells in arteriogenesis. As a result, a better model approach is required to determine the role of B cells. To answer this question, I planned to replicate my findings (from Figure.10) using B cell-deficient (JHT KO) mouse, which have the *Jh* region of the heavy chain knocked out and cannot produce B cells in the system under any circumstances. To induce arteriogenesis, both WT and JHT KO mice had their femoral arteries ligated. Laser Doppler imaging analysis on days 3 and 7 revealed a significant reduction in perfusion recovery in B cell-deficient mice (Fig. 15A-B), which was consistent with the perfusion findings from CD20 depleted mice. In B cell-deficient mice, vascular cell proliferation (Fig. 15C-D) and collateral artery growth (Fig. 15E) were similarly considerably reduced. Surprisingly, perivascular macrophage analysis (Fig. 15F) showed that the number of inflammatory ($CD68^{+}MRC1^{-}$) (Fig. 15G) and regenerative ($CD68^{+}MRC1^{+}$) macrophages (Fig. 15H) did not differ significantly.

The conclusion drawn: B cell deficiency results in reduced arteriogenesis without any impact on perivascular macrophage accumulation.

Figure 15

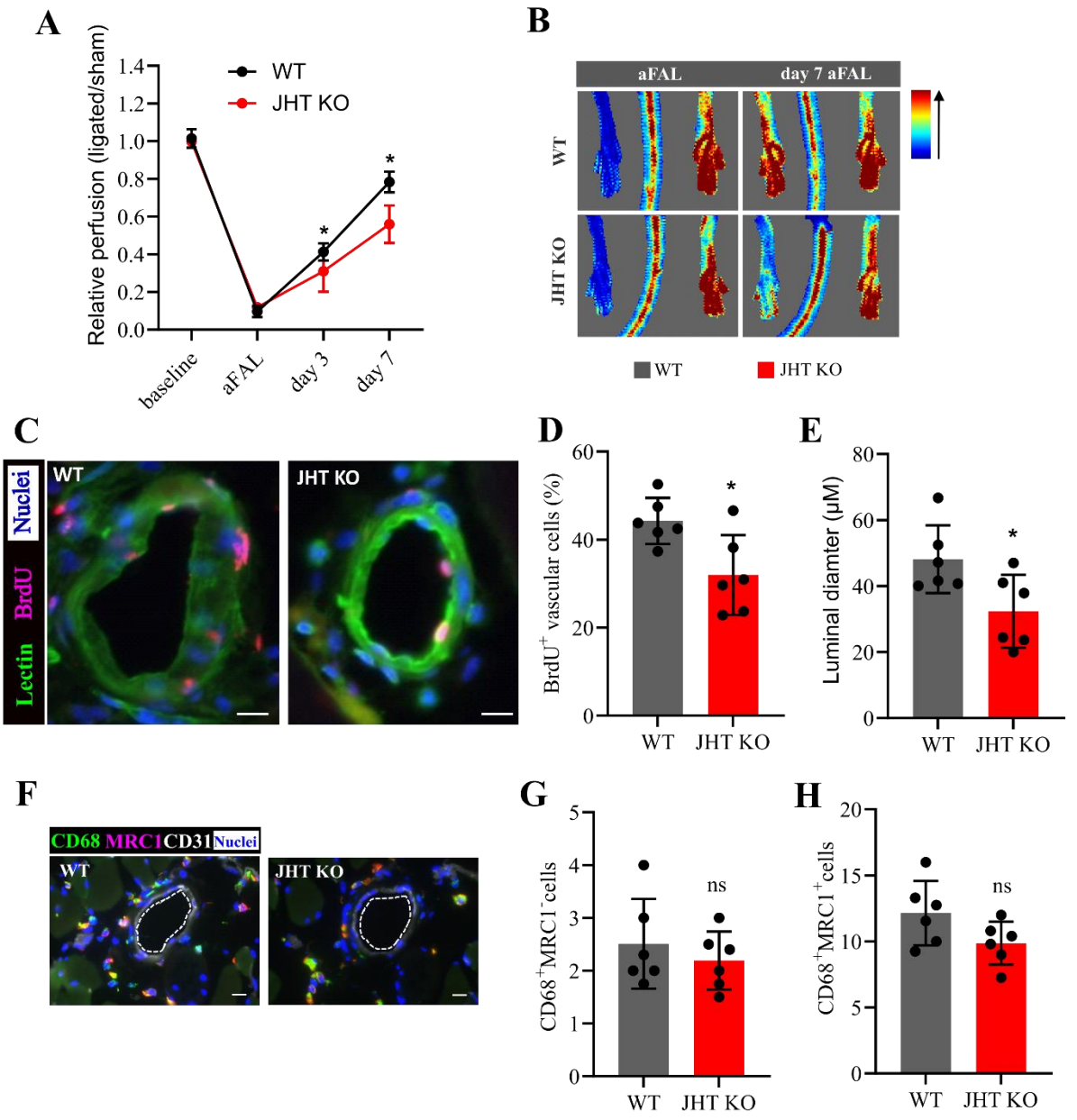

Figure 15. Reduced arteriogenesis in B cell-deficient mice

- **A.** Laser Doppler perfusion measurements of WT and JHT KO mice at baseline, immediately after femoral artery ligation (aFAL), at day 3, and at day 7. Data represent mean±S.D., **P*<0.05 by two-way ANOVA multiple comparison test with Bonferroni correction. n=8 mice.
- **B.** Doppler flux images of WT (upper panel) and JHT KO (lower panel) mice at aFAL and at day 7.
- **C.** Epifluorescence images showing $BrdU^+$ cells in WT and JHT KO mice at day 7 aFAL.
- **D.** & **E**; Bar graphs data showing **(C)** % of BrdU+ vascular cells, **(D)** Inner luminal diameter of collateral arteries at day 7. Data represent mean±S.D., **P*<0.05 by t test. n=6 mice.
- **F.** Representative immunofluorescence images of macrophages around perivascular space of collateral artery in WT and JHT KO mice day 7 aFAL. Scale bar 20μm.
- **G.** & **H**; Number of perivascular **(G)** $CD68^+MRC1^-$, **(H)** $CD68^+MRC1^+$ macrophages. Data represent mean±S.D., ns no significance by t test. n=6 mice.

6.2.1 Effect of CD20 depletion in B cell-deficient mice

Arteriogenesis was impaired in B cell-deficient animals without affecting perivascular macrophage accumulation. I stained B cell-deficient mice adductor muscle to see whether there was a conceivable cause. Surprisingly, $CD20^+$ cells were detected in the vicinity of developing collateral arteries in B-cell deficient mouse (Fig. 16A). Despite the fact that CD20 is a well-known B cell marker in mice and humans, my flow cytometry analysis found that CD20 is also present in T cells and eosinophils. In B cell-deficient mice, I expected that $CD20^+$ cell population would be recruited to the perivascular area of collateral arteries. Because B cell-deficient mice had a similar amount of regenerative macrophages at day 7 after surgery, I wondered if these $CD20^+$ cells were the cause of the observed phenomenon in B cell-deficient mice. I used anti-CD20 antibody to investigate the relevance of $CD20^+$ cells in B cell-deficient mice, while the control group got Isotype control antibody. Surprisingly, mice lacking B cells responded to CD20 depletion. Anti-CD20 treated mice had significantly lower perfusion recovery than B cell-deficient mice treated with Isotype control antibody (Fig. 16B). This was associated with significantly reduced vascular cell proliferation (Fig. 16C) and collateral artery growth (Fig. 16D). In B cell-deficient mice with anti-CD20 antibody, the number of inflammatory ($CD68^+MRC1^-$) macrophages (Fig. 16F) was significantly increased, whereas the number of regenerative ($CD68^+MRC1^+$) macrophages (Fig. 16G) was significantly reduced.

The conclusion drawn: CD20 expressing cells were relevant to arteriogenesis and macrophage accumulation in B cell-deficient mice.

Figure 16

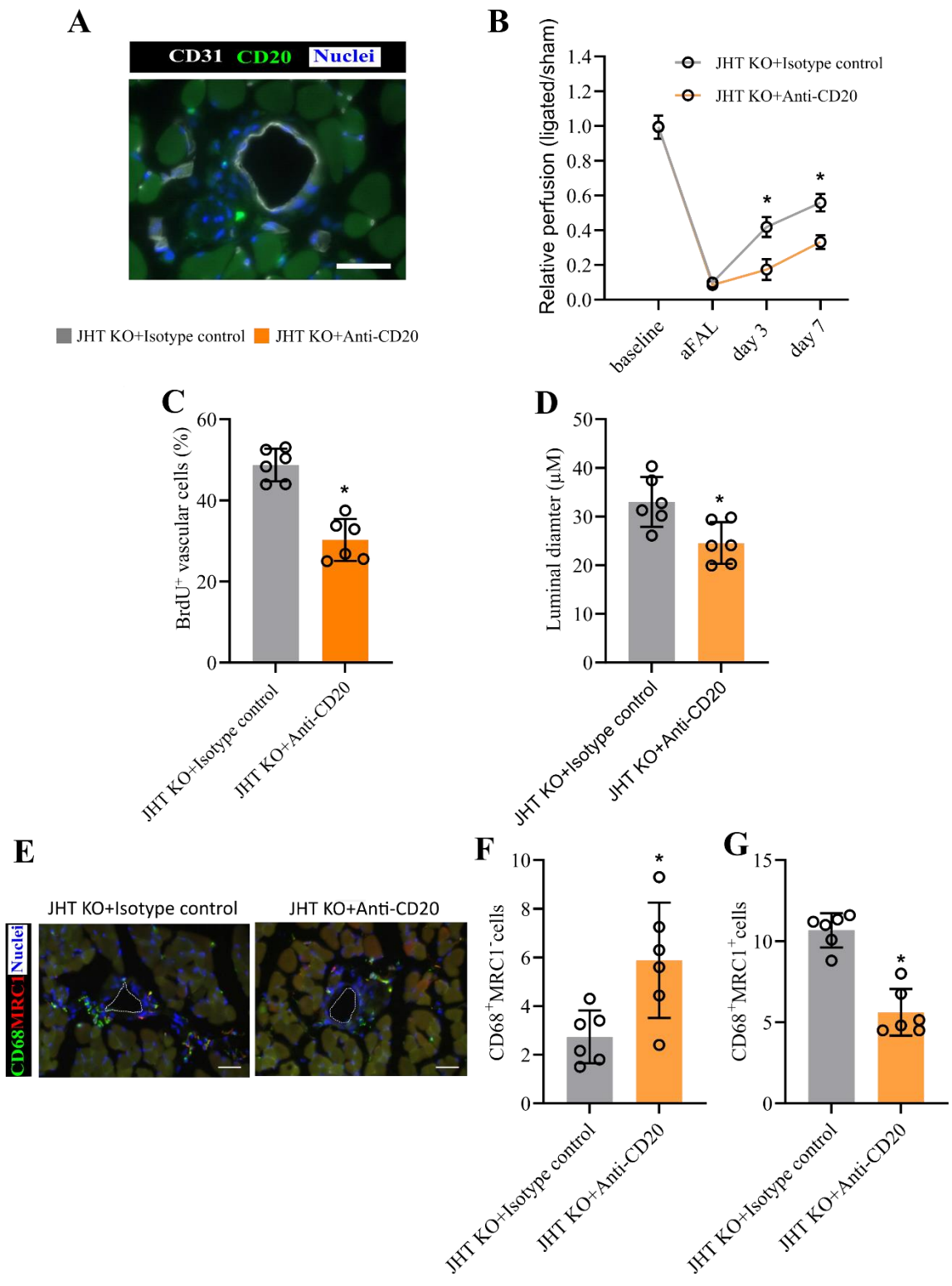
A
CD31 CD20 Nuclei
JHT KO+Isotype control
JHT KO+Anti-CD20
B
Relative perfusion (ligated/sham)
JHT KO+Isotype control
JHT KO+Anti-CD20
baseline
aFAL
day 3
day 7
C
BrdU+ vascular cells (%)
JHT KO+Isotype control
JHT KO+Anti-CD20
D
Luminal diamter (μM)
JHT KO+Isotype control
JHT KO+Anti-CD20
E
JHT KO+Isotype control
JHT KO+Anti-CD20
CD68MRC1Nuclei
F
CD68+MRC1- cells
JHT KO+Isotype control
JHT KO+Anti-CD20
G
CD68+MRC1+ cells
JHT KO+Isotype control
JHT KO+Anti-CD20

Figure 16. Impact of CD20 depletion on arteriogenesis in B cell-deficient mice

- **A.** Immunofluorescence image showing the presence of CD20 expressing cells in B cell-deficient (JHT KO) mice at 7 aFAL. Scale bar 20 µm.
- **B.** Relative perfusion recovery of B cell-deficient (JHT KO) mice treated with Isotype control and anti-CD20 antibody as analyzed ligated/sham at baseline, aFAL, at day 3 and at day 7. Data represent mean±S.D., **P*<0.05 by two-way ANOVA multiple comparison test with Bonferroni correction. n=6 mice.
- **C. & D**; Bar graph showing the data of **(C)** $BrdU^+$ vascular cells**, (D)** luminal diameter.
- **E.** Epifluorescence images showing macrophages in perivascular space at day 7. Scale bar 20µm:
- **F. & G**; Number of **(F)** $CD68^+MRC1^-$ and **(G)** $CD68^+MRC1^+$ macrophages at day 7 aFAL.
  C, D, F, G; Each circle represents mean of 6-10 collateral arteries. Data represent mean±S.D., * *P*<0.05 by t-test, n=6 mice.

6.3 Arteriogenesis in the absence of T cells

6.3.1 Arteriogenesis in absences of conventional T cells

TCRα KO mice lack the alpha and beta TCR population, which accounts for the majority of T cells. To investigate the role of T cells in arteriogenesis, WT and TCRα KO mice underwent femoral arteries ligation. In TCRα KO mice, the loss of T cells had no influence on perfusion recovery (Fig. 17A-B). WT and TCRα KO mice had similar vascular cell proliferation (Fig. 17C-D) and collateral artery growth (Fig. 17E). Perivascular macrophage analysis (Fig. 18A) showed that TCRα KO mice had no difference in the number of proinflammatory ($CD68^+MRC1^-$) macrophages. Moreover, surprisingly, TCRα KO mice had considerably more regenerative ($CD68^+MRC1^+$) macrophages (Fig. 18C).

The conclusion drawn: T cell deficiency does not affect arteriogenesis and instead favors macrophage accumulation in TCRα KO mice.

Figure 17

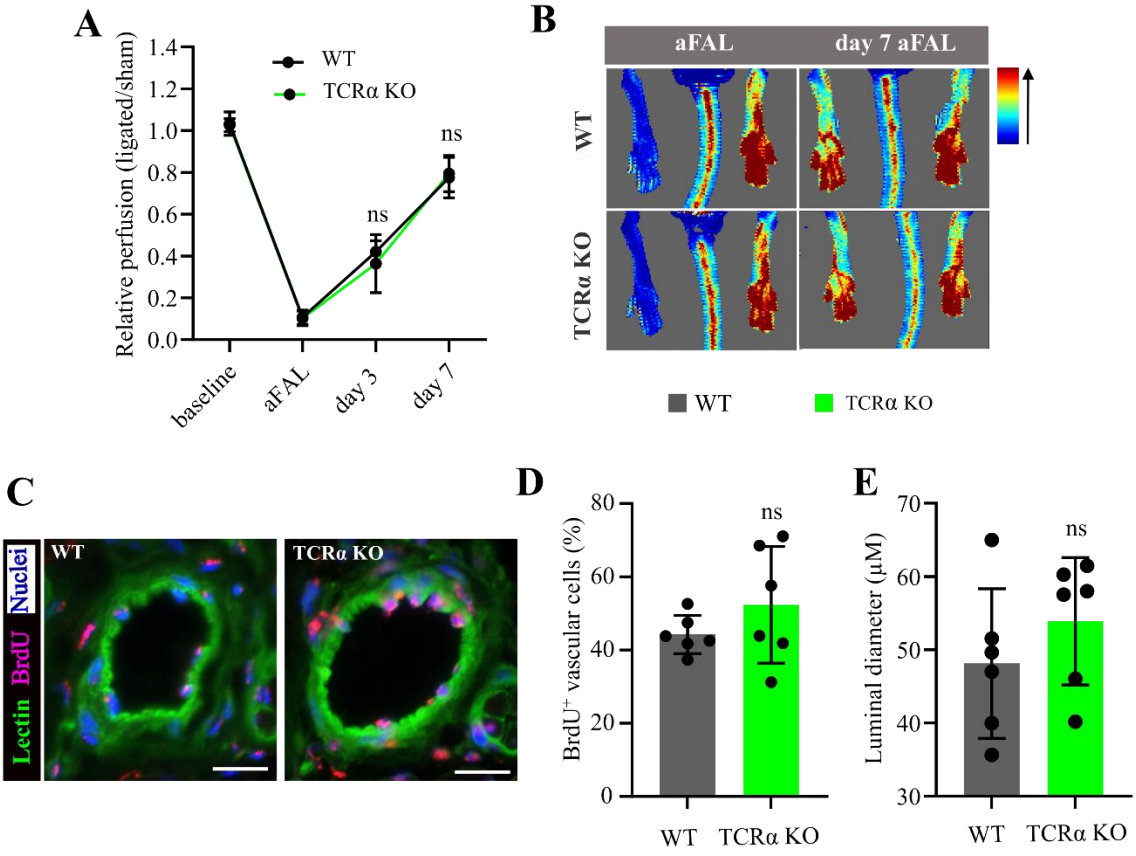

Figure 17. Conventional T cell deficiency does not interfere with arteriogenesis in TCRα KO mice

- **A.** Laser Doppler perfusion analysis of WT and TCRα KO mice at baseline, immediately after femoral artery ligation (aFAL), at day 3 and at day 7. n=6 mice. Data represent mean±S.D., ns no significance by two-way ANOVA multiple comparison test.
- **B.** Representative Doppler flux images of WT (upper) and TCRα KO (lower) mice at immediately aFAL and at day 7.
- **C.** Epifluorescence images showing $BrdU^+$ cells in WT and TCRα KO mice. Scale bar 20 µm.
- **D.** Bar graphs showing the percentage of $BrdU^+$ vascular cells.
- **E.** Data showing luminal diameter of collateral arteries.

  D, E; timepoint at day 7, each dot represents mean of 6-10 collateral arteries. Data represent mean±S.D., ns no significance by t-test. n=6 mice.

Figure 18

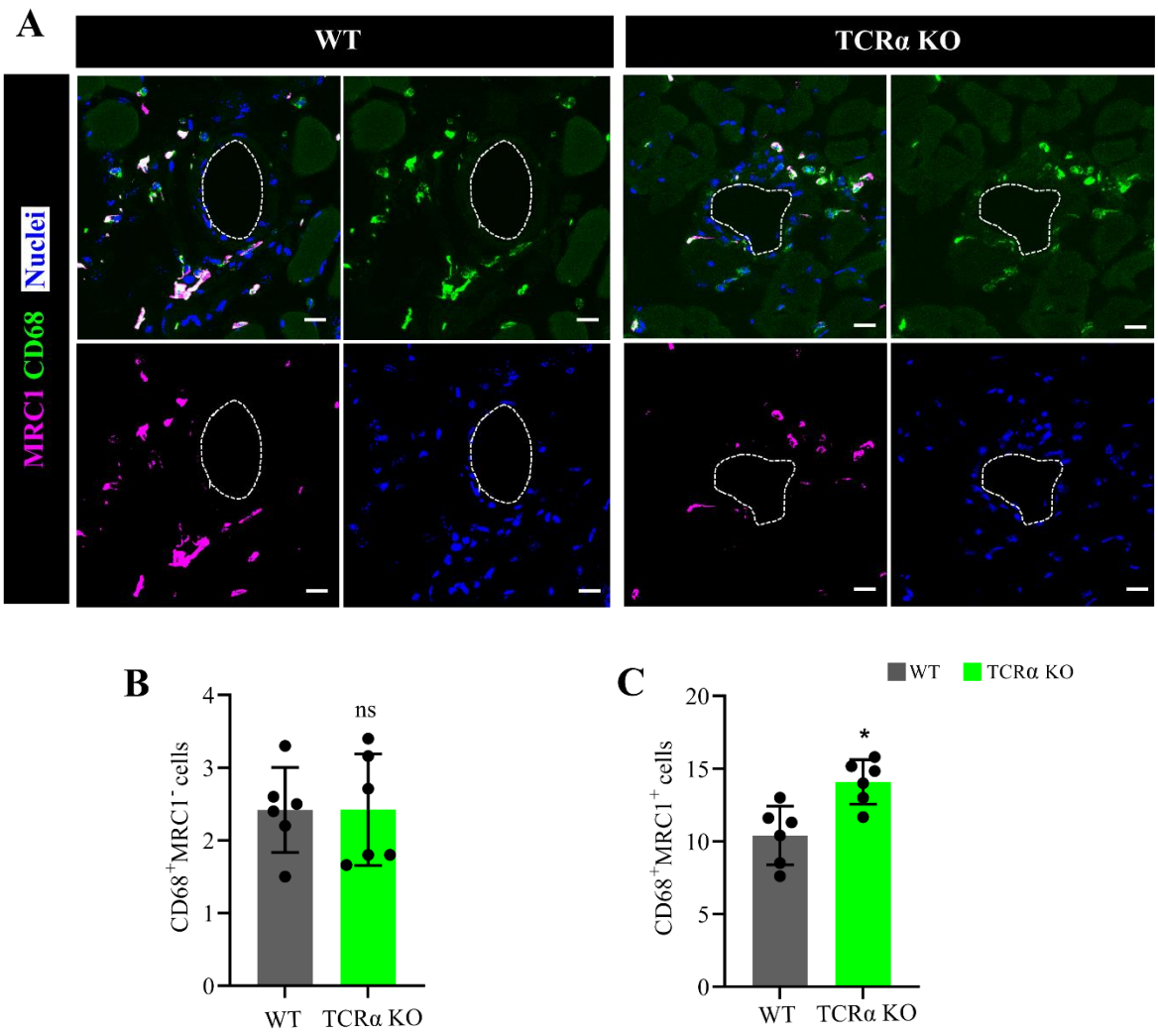

Figure 18. TCRα KO showed increased regenerative macrophage accumulation in perivascular space

A. Representative confocal immunofluorescence images of adductor muscle stained for CD68 and MRC1, DAPI for nuclei at day 7; left panel data from WT and right panel from TCRα KO mice. Scale bar 20 µm.

B. & **C;** Bar graphs data showing the number of (B) $CD68^{+}MRC1^{-}$, (C) $CD68^{+}MRC1^{+}$ macrophages of growing collaterals in adductor muscle. The time timepoint of the analyzed data was day 7. Each dot represents a mean of 6-10 collaterals. Data mean±S.D., ns no significance, * $P<0.05$, by t-test, n=6 mice.

6.3.2 γδT cell depletion interfered with arteriogenesis in TCRα KO mice

Although TCR alpha/beta (TCR TCRαβ) chain is found in the majority of T cells, a small percentage of T cells are TCR gamma/delta (TCR TCRγδ) chain positive which are referred to as γδ T cells. γδ T cells can exist in TCRα KO mice. The absence of conventional T cells in TCRα KO mice had no effect on arteriogenesis, implying that γδ T cells might play a role. To support my hypothesis, my immunofluorescence staining showed the presence of γδ T cells in the adductor muscle of TCRα KO mice on day 7 after femoral artery ligation (Fig. 19A). The localization of γδ T cells are in close proximity to the growing collateral artery (artery lumen was indicated with dashed line). Secondly, Anti-CD20 depletion is showed impaired arteriogenesis and decreased number of $CD20^+$ γδ T cells. So I sought to check the relevance of γδ T cells to arteriogenesis in TCRα KO mice. γδ T cells were depleted in TCRα KO mice mice with Anti-TCR γδ antibody and control group received isotype control antibody (Fig. 19B). Both groups underwent femoral artery ligation surgery and were kept under observation for 7 days. This treatment approach significantly effectively depleted γδ T cells in blood (Fig. 19C) and spleen (Fig. 19D). Perfusion recovery was assessed on day 3 and also day 7 (endpoint) (Figure. 20A). Compared to the Isotype control antibody-treated group, the perfusion recovery was reduced in TCRα KO treated with anti-TCRγδ antibody. However, the difference was significant only on day 7 (Fig. 20A). A clear visible reduction in collateral arteries growth (arrows) is seen in adductor muscle of anti-TCRγδ treated TCRα KO mice (Fig. 20B). Vascular cell proliferation (Fig. 20C, corresponding quantification Fig. 20D) and collateral artery growth (Fig. 20E) were significantly reduced with anti-TCRγδ antibody treatment. On day 7 following femoral artery ligation, perivascular macrophage (Fig. 20F) analysis revealed that the number of proinflammatory ($CD68^+MRC1^-$) macrophages was significantly increased (Fig. 20G), whereas the number of regenerative ($CD68^+MRC1^+$) macrophages was significantly reduced (Fig. 20H) in TCRα KO mice treated with anti-TCRγδ antibody.

The conclusion drawn: γδ T cells contributed to arteriogenesis in TCRα KO mice.

Figure 19

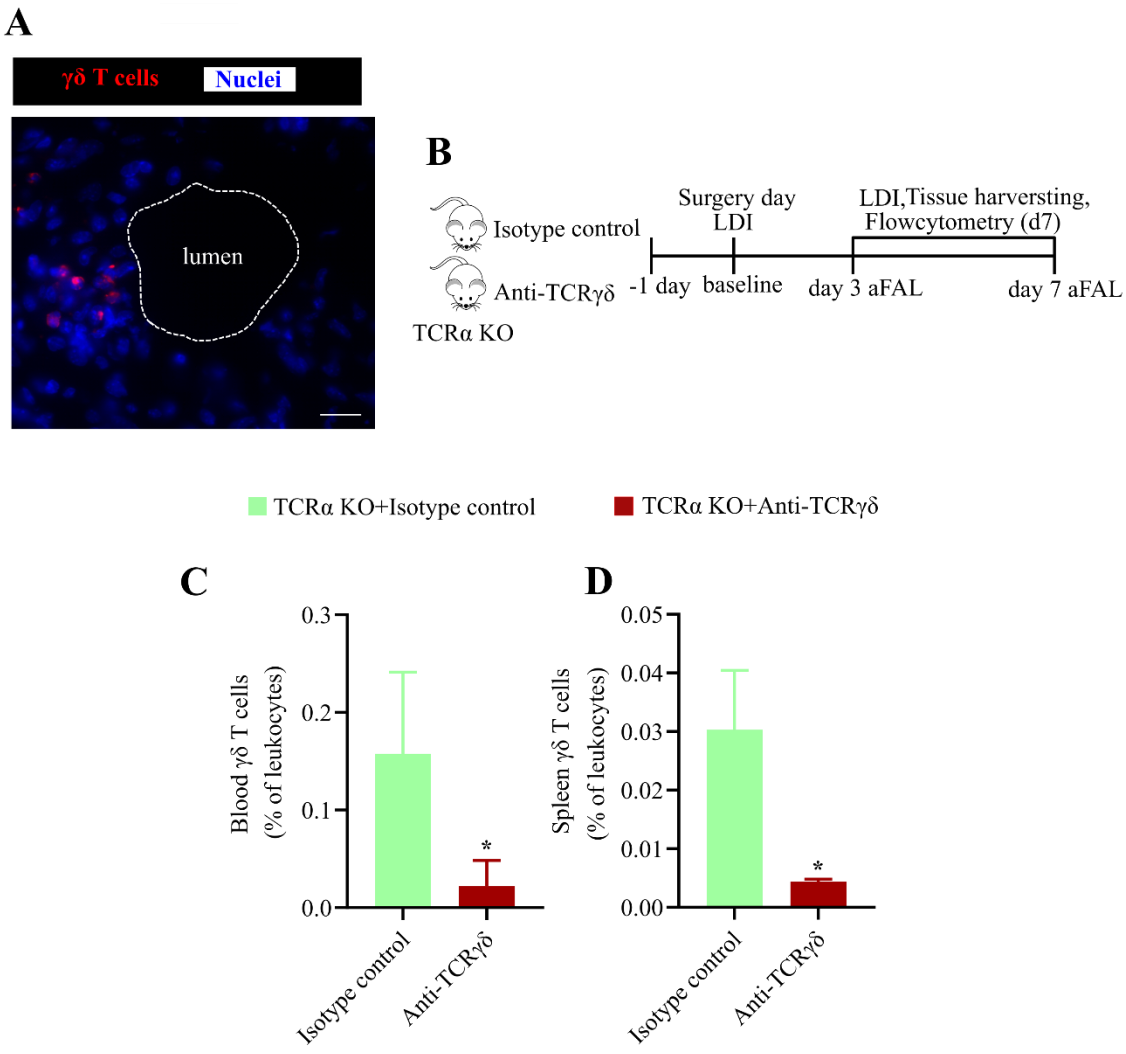

Figure 19. γδ T cell depletion by Anti-TCR γδ in TCRα KO mice

A. Immunofluorescence image showing the presence of γδ T cells in the adductor muscle of TCRα KO mice at day 7 after surgery. Dashed line indicate arterial lumen. Scale bar 20 µm.

B. Schema of experiment design showing TCRα KO mice were randomly divided into two groups. One group was treated with an Isotype control antibody, and another group with Anti-TCR γδ antibody on one day prior to the surgical procedure (-1day) via intravenously. Perfusion was measured at baseline, immediately after surgery, at day 3, and at day 7 after surgery. Mice were humanly sacrificed at day 3 and day 7 time points. Blood and spleen (on day 7) were harvested and processed for flow cytometry. Muscles were harvested (on day 3 and on day 7) and cryopreserved for histology analysis.

C. Bar graph data showing flow cytometry analysis of γδ T in the blood (%) at day 7. Data mean±S.E.M., * P<0.05, by t test, n=3-4 mice.

D. Data showing flow cytometry analysis of γδ T in the spleen (%) at day 7. Data mean±S.E.M., * P<0.05, by t test, n=3-4 mice.

Figure 20

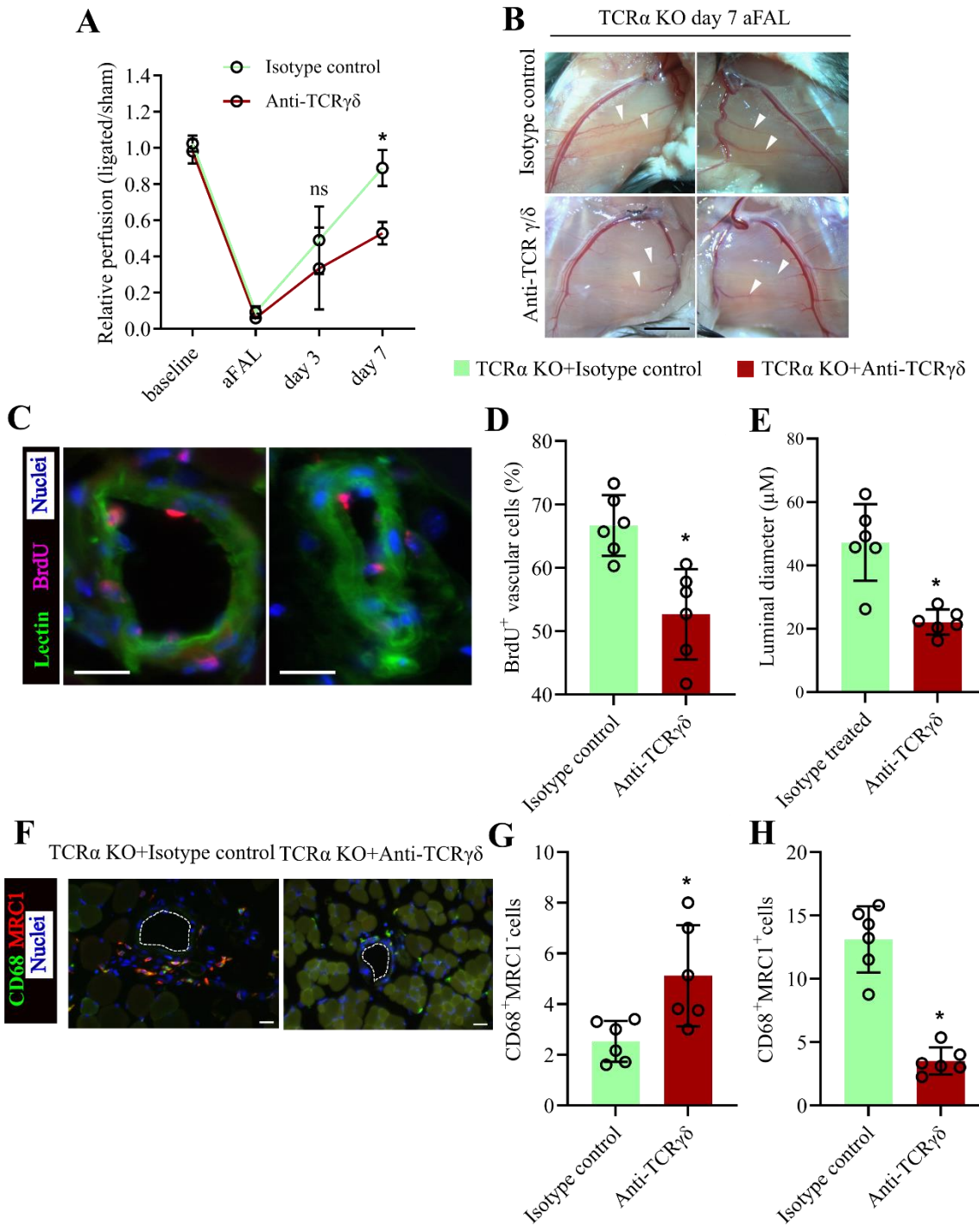

Figure 20. γδ T cell depletion impaired arteriogenesis in TCRα KO mice

A. Relative perfusion analysis of TCRα KO mice treated with Isotype control and anti-TCR γδ antibody, at baseline, immediately after surgery, at day 3 and at day 7. Data represent mean±S.D., ns no significance, **P*<0.05 by two-way ANOVA multiple comparison test with Bonferroni correction. n=6 mice.

B. Representative microscopic adductor muscle image showing blood-filled collaterals (arrows) in TCRα KO mice treated with Isotype control (top), anti-TCR γδ (lower) at day 7.

C. Epifluorescence images showing $BrdU^+$ cells. Scale bar 20 μm.

D. & **E**; Bar graphs showing percentage **(D)** (%) of BrdU+ vascular cells, **(E)** luminal diameter of collateral arteries at day 7.

E. Confocal microscope images showing macrophages around perivascular space. Scale abr20 μm.

F. & **H**; Number of $CD68^{+}MRC1^{-}$ (left) and $CD68^{+}MRC1^{+}$ (right) macrophages at day 7.

D, E, G & H; Each circle represents a mean of 6-10 collateral arteries. Data mean±S.D., ns no significance, **P*<0.05 by t-test. n=5-6 mice.

6.3.3 Relevance of γδ T cells to arteriogenesis in WT mice

Anti-TCR antibody-mediated depletion of γδ T cells in TCRα KO mice confirmed the importance of γδ T cells in arteriogenesis. Following that, I wanted to see if γδ T cells have a role in arteriogenesis also in WT mice. I tested the effect of γδ T cell depletion on arteriogenesis in WT mice. WT mice treated with anti-TCRγδ antibody showed significantly impaired perfusion recovery on day 3 and day 7 after femoral artery ligation (Fig. 21A), and reduced collateral artery growth (Fig. 21B), similar to prior experimental data from TCRα KO mice (Fig. 21A-B). Anti-TCRγδ antibody-treated WT mice had considerably lower vascular cell proliferation (Fig. 21C) and luminal diameter (Fig. 21D) than Isotype control antibody-treated WT mice.

The conclusion drawn: γδ T cells contribute to arteriogenesis in WT mice.

Figure 21

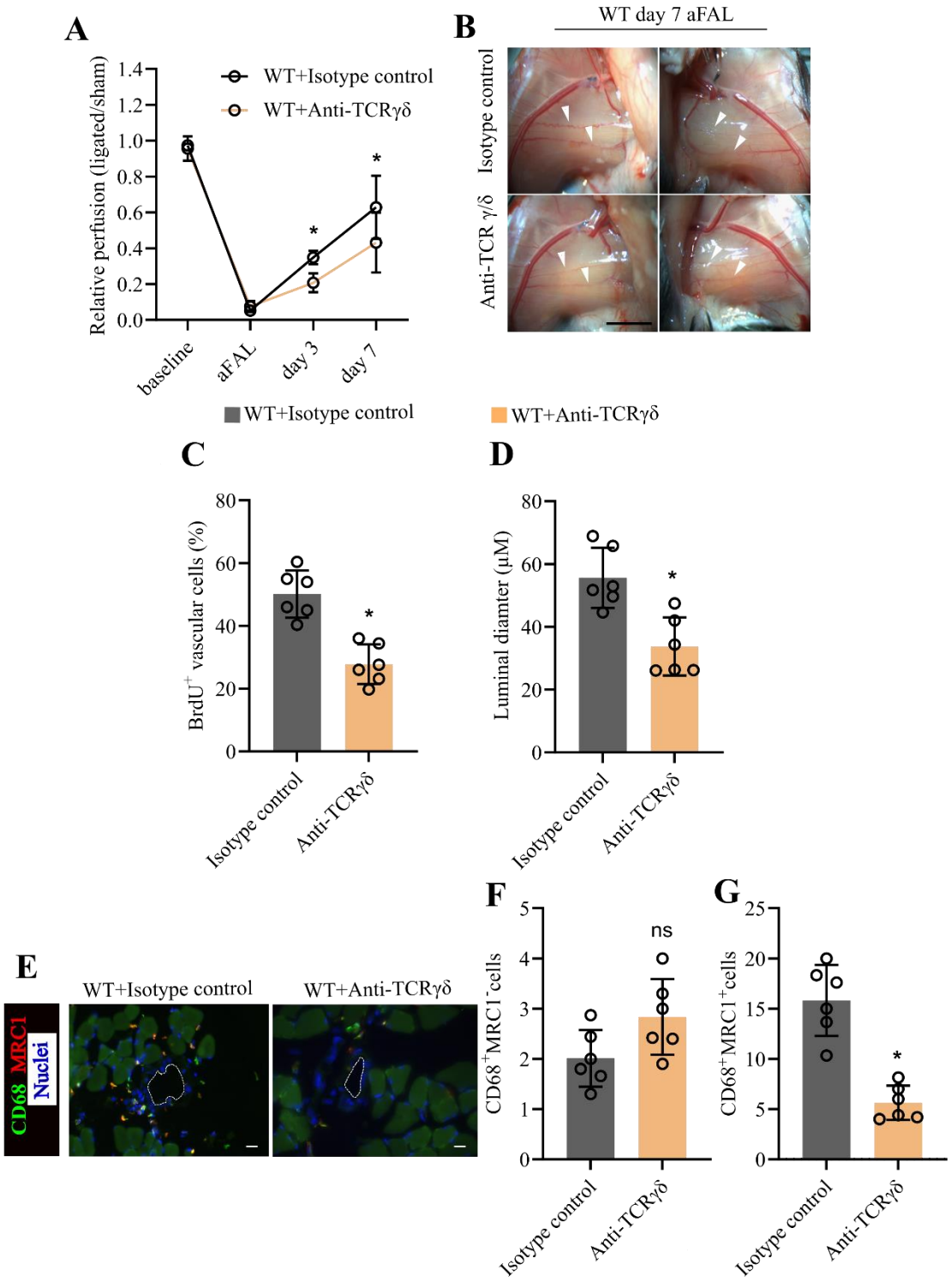

Figure 21. Relevance of γδ T cells to arteriogenesis in WT mice

A. Perfusion analysis of WT mice treated with Isotype control and anti-TCRγδ antibody. Data represent mean±S.D., **P*<0.05 by two-way ANOVA multiple comparison test with Bonferroni correction. n=6 mice.

B. Representative microscopic blood-filled collaterals in adductor muscle of TCRα KO mice treated with Isotype control (top), anti-TCR γδ (lower) at day 7, arrows showing superficial collaterals.

C. & D; Bar graphs showing percentage **(C)** % of $BrdU^+$ vascular cells, **(D)** luminal diameter of collateral arteries at day7.

E. Epifluorescence images showing macrophages in perivascular space. scale bar 20 µm.

F. & G; Number of **(F)** $CD68^+MRC1^-$ and **(G)** $CD68^+MRC1^+$ macrophages at day 7.

C, D, E & F; Each circle represents mean of 6-10 collateral arteries. Data mean±S.D., ns no significance, *P<0.05 by t test. n=6 mice.

6.3.4 Functional relevance of γδ T cells in arteriogenesis

γδ T cells possibly express IL-17A or IFN-γ under inflammatory conditions, as reported previously. Since femoral artery ligation results in chronic sterile inflammation, I hypothesized that either IL-17A or IFN-γ from γδ T cells was relevant to their positive effect in arteriogenesis in mice. To investigate this, I sorted γδ T cells from WT mice blood on day 3 after femoral artery ligation and sham operation. RNA was isolated, and cDNA was synthesized. Gene expression analysis by real-time PCR showed no detected level of IL-17A (data not shown), whereas IFN-γ expression was significantly increased in cells sorted from ligated mice blood (Fig. 22).

The conclusion drawn: γδ T cells are IFN- γ expressing cells in arteriogenesis.

Figure 22

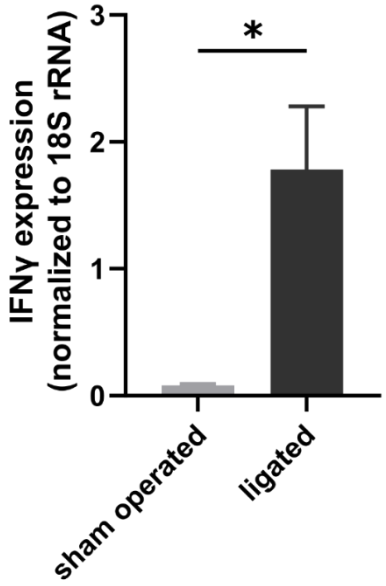

Figure 22. Functional relevance of γδ T cells in arteriogenesis

Bar graph data showing expression levels of IFN- γ in γδ T cells sorted from sham-operated and ligated WT mice on day 3 post-surgery. Data represent mean±S.E.M., *P<0.05 by t test. RNA isolated from pooled cells, n=4 mice.

6.3.5 Macrophage activation status in arteriogenesis

γδ T cells are relevant to arteriogenesis and macrophage accumulation in TCRα KO and WT mice. And γδ T cells are IFN-γ expressing cells. IFN-γ was reported to induce macrophage polarization towards pro-inflammatory phenotypes in In vitro assays. However, this phenomenon cannot be applied to the tissue microenvironment. By using MRC1 and CD169 macrophage markers, I would like to explore the activation status of perivascular macrophages in relevance to γδ T cells. Cryosections from adductor muscles collected on day 3 after femoral artery ligation from WT and TCRα KO mice treated with anti-TCRγδ antibody and Isotype control antibody were stained with CD68, MRC1, and CD169 antibodies. Mean fluorescence intensity (MFI) analysis revealed that anti-TCRγδ treated WT (Fig. 23A) and TCRα KO mice (Fig. 23B) showed no significant difference in MRC1 expression whereas CD169 expression was significantly decreased with anti-TCRγδ treatment. Moreover, CD169 perivascular macrophages also expressing lymphotoxin beta receptor (LTBR) (Fig. 23C).

Figure 23

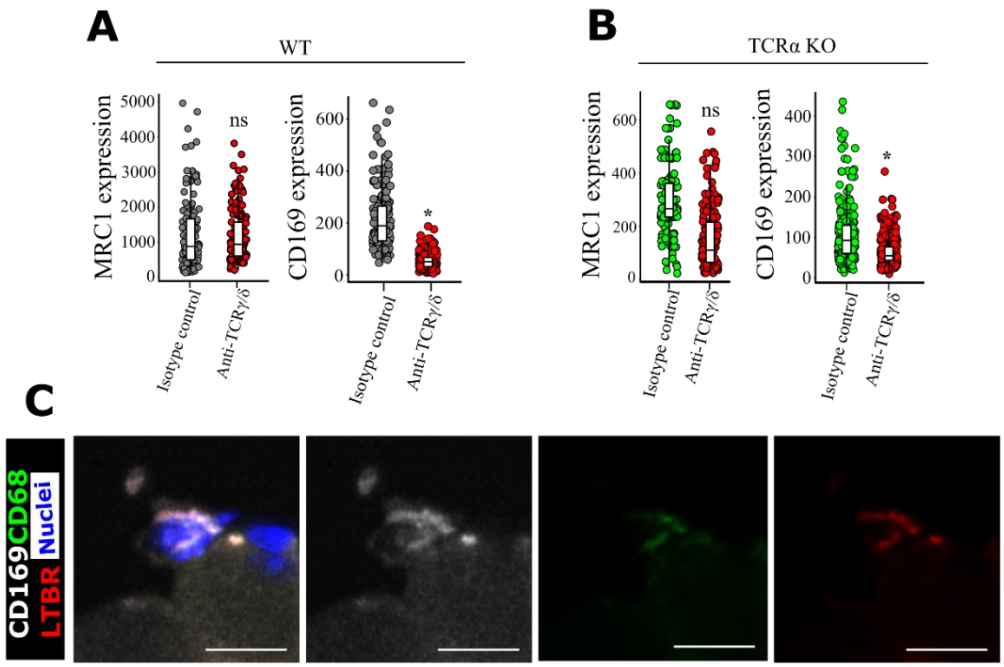

Figure 23. Macrophage activation status in arteriogenesis ggplot data showing expression of MRC1 (left) and CD169 (right) in WT mice. (A) and TCRα KO mice (B) treated with Isotype control and Anti-TCR γδ antibody. Each dot represents MFI value of one macrophage. Data mean±S.D., * P<0.05, by t-test, n=6 mice. (C) Confocal microscope image showing CD169 macrophage express LTBR. Scale bar 10 µm.

6.3.6 Perivascular macrophages express IL-10 and PDGF-β in arteriogenesis

Perivascularly accumulated macrophages express vascular growth factors, which ultimately promote vascular (endothelial and smooth muscle) cell proliferation. IFN-γ from γδ T cells induces classically activated macrophages. γδ T cell depletion, on the other hand, drastically reduced CD169 expression on macrophages in the current experimental setting. As a result, I would like to look at the expression of cytokines in $CD169^{+}$ macrophages that promote vascular development. $F4/80^{+}CD169^{+}$ macrophages from spleen, blood, and muscle were sorted at day 3 after femoral artery ligation. RNA was isolated, and cDNA was synthesized. Gene expression analysis by real-time PCR revealed that macrophages isolated from spleen, blood and muscle showed the expression of IL-10 (Fig. 24A), platelet-derived growth factor-β (PDGF-β) (Fig. 24B). RNA isolated from collateral showed expression of platelet-derived growth factor receptor-β (PDGFR-β) (Fig. 24C) on day 3 after femoral artery ligation. However, the difference between sham and ligated was very minimal. Immunofluorescence staining showed that PDGFRB expression on smooth muscle cell layer of collateral artery day 7 after surgical procedure (Fig. 24D).

Figure 24

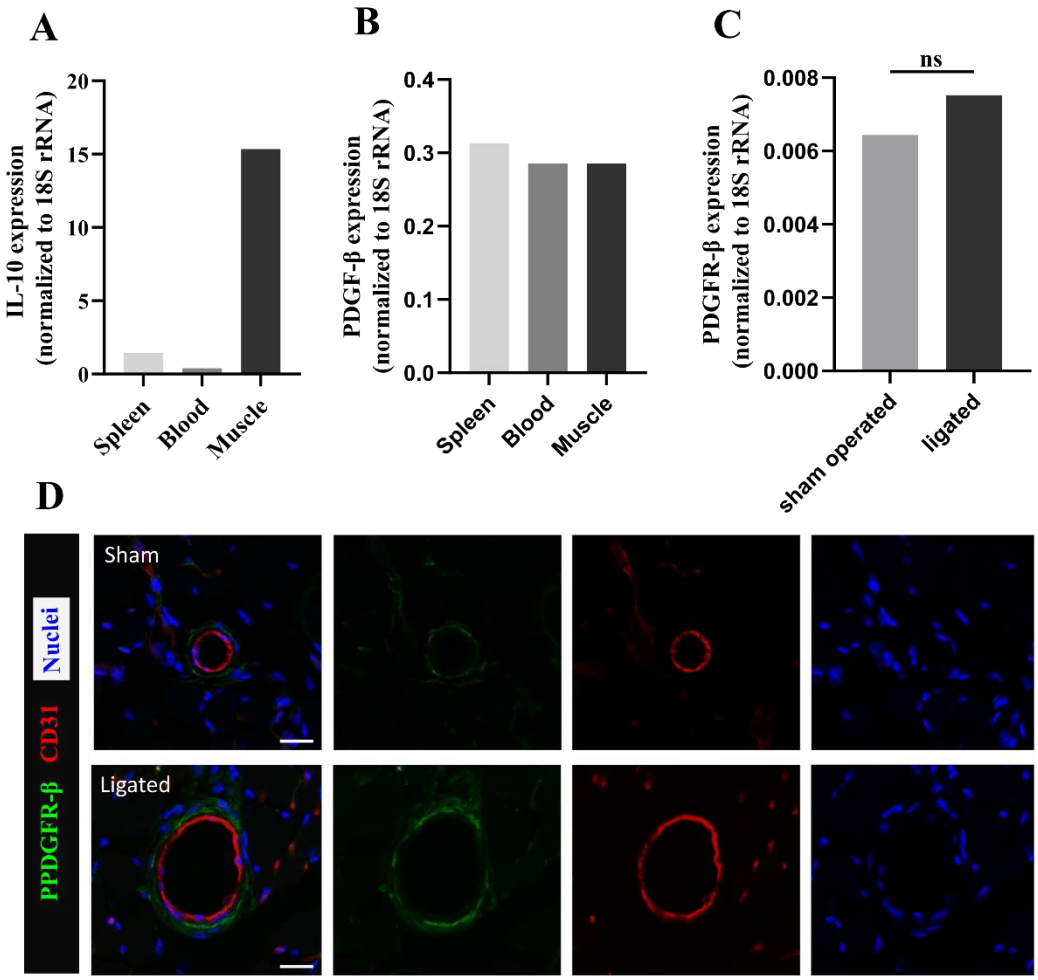

Figure 24. IL-10 and PDGFR-β expression in arteriogenesis

Bar graph data showing expression levels of (A) IL-10 and (B) PDGFR-β in splenic, blood, and muscle macrophages. Macrophages were polled from 4 WT mice, data from two independent experiments. (C) Bar graph data showing PDGFR-β expression in RNA extracted from WT mice collateral arteries on day 3 post-surgery. (D) Confocal microscope image showing PDGFR-β expression on collateral arteries in sham-operated (top) and femoral ligated (lower) WT mice at day 7 after ligation. Scale bar 20 µm.

7. DISCUSSION

7.1 Role of adaptive immunity in arteriogenesis

Since the adaptive immune response needs a longer time to rise after exposure to the antigens, the innate immune response provides rapid and non-specific defense reactions (Kuby Immunology, 7th edition). Therefore, the cells of the innate immune (Fig. 1) system typically act minutes after exposure to the danger signal. This action is majorly a coordinate job between neutrophils and mast cells by increased phagocytosis and cytokine release. These cellular events are collectively referred to as Inflammation (Kuby Immunology, 7th edition). Increased fluid shear stress in the vasculature is one of the crucial physiological forces for arteriogenesis. Once the endothelium experiences fluid shear stress, mechanosensing molecules activate many molecular and cellular events, which causes inflammatory leukocyte recruitment and cytokine release (Lasch et al., 2019), since this process happens in the absence of infectious agents, hence called ***sterile inflammation*** (Beneke et al., 2017). Over the past years, a substantial knowledge from our group and other groups has already explained the crucial involvement of the innate immune system in arteriogenesis.

Shear stress experienced endothelium attracts myeloid cells. Locally recruited neutrophils disappear 1 day after surgical ligation of the femoral artery. At a similar time interval, mast cell activation also reduced, and the macrophage accumulation slowly rose and reach peak level on a week after the surgery (Chillo et al., 2016), (Lasch et al., 2019). Macrophage and lymphocyte crosstalk have been established in chronic inflammatory mouse models (Mosser & Edwards, 2008). This data clearly shows that adaptive immunity might be important to control the sterile inflammation by influencing the macrophage compartment and facilitating collateral artery growth in arteriogenesis (La Sala et al., 2012). The main aim of my study is to

identify the role of adaptive immunity in arteriogenesis by using a mouse model of hindlimb ischemia, a preclinical animal model to study arteriogenesis (collateral artery growth). Few studies attempted to find the role of T cell involvement in arteriogenesis. However, the outcome was contradictory due to the different mouse strains sued and treatments applied (Van Weel et al., 2007). These findings made me speculate that the role of adaptive immunity in arteriogenesis is minimal. However, the role of B cells in arteriogenesis has never been reported. To fill this gap, I wanted to study arteriogenesis by using a better mouse model that lacks both B and T cells in system. Rag1 KO mice lacks functional B and T cells and provides the potential opportunity to study the role of adaptive immunity (Mombaerts et al., 1992).

Arteriogenesis was evaluated in Rag1 KO mice through perfusion recovery, vascular cell proliferation, and luminal diameter of collateral arteries. Having no functional B and T cells in Rag1 KO mice showed impaired arteriogenesis, which was associated with the increased number of inflammatory ($CD68^{+}MRC1^{-)}$ macrophages accumulation in the perivascular space of growing collateral arteries (Fig. 8).

The reduced arteriogenesis in Rag1 KO mice could be viewed in two ways; first, since the myeloid system and lymphoid system crosstalk is crucial for the survival of cells of the immune system (Innate and adoptive). Lack of lymphocytes in Rag1 KO mice could affect myelopoiesis. Arteriogenesis is majorly dependent on monocyte/macrophages (Deindl & Schaper, 2005). If the mouse has altered myelopoiesis, this can result in reduced arteriogenesis. However, Rag1 KO mice showed normal myelopoiesis (Aiello et al., 2007). Hence, the impaired arteriogenesis in Rag1 KO mice was not due to altered myelopoiesis but due to the lack of B and T cells. Secondly, earlier studies in arteriogenesis focused on locally accumulated leukocytes but lacked knowledge about secondary lymphoid organs involvement. In atherosclerosis mouse

models, B cell and T cell activation analysis showed that lymphocytes were exposed to antigens more rapidly (Paulsson et al., 2000), indicating that primary and secondary lymphoid compartments might be necessary in chronic inflammatory models (Hansson et al., 2006). Rag1 KO mice resulted in reduced arteriogenesis support my hypothesis that the adaptive immune compartment might play a role in arteriogenesis by resolving the inflammation to enable the growth of collateral arteries through regenerative ($CD68^{+}MRC1^{+}$) macrophages. However, since Rag1 KO mice lack both B and T cells, the reduced arteriogenesis in Rag1 KO mice could be the result of a collective lack of B cells and T cells.

To solve the aforesaid question, arteriogenesis was studied independently in B cell and T cell-deficient mouse models.

7.2 Role of B lymphocytes in arteriogenesis

The Role of B cells in arteriogenesis was never reported yet. However, data from similar chronic inflammation mouse models have shown a positive and negative role of B cells. To start with, in atherosclerosis models, deposition of oxidative lipids and phospholipids were proposed as the pathological initiators (Binder et al., 2002). The progress of atherosclerotic lesion development linked with natural IgM and IgG antibodies to oxidized low-density lipoproteins (Shaw et al., 2000). These antibodies accumulate in lesions and interfere with the macrophage-mediated clearance of lipids (Shaw et al., 2000). However, it is also reported that activated B1 cells possess an atheroprotective role via IgM type anti-oxidized low-density lipoproteins (anti-oxLDL) (Srikakulapu et al., 2017) via CXCR4 expression (Döring et al., 2020). Above findings has indicated the involvement of B cell through their natural antibodies. It is noteworthy that B cells also possess a regulatory function by inhibiting the BCR activation

signaling and negatively regulate the inflammation. The anti-inflammatory regulatory nature of the B cells were defined by their capacity to release anti-inflammatory cytokine IL-10, hence regulatory B cells named as B-10 b cells (Iwata et al., 2011), (Tedder, 2015), (Radomir et al., 2021). By using B cell depletion through anti-CD20 antibody treatment was found to reduce the atherosclerosis development in mice (Ait-Oufella et al., 2010). The same study identified two significant phenomenons which explained the pro-atherogenic role of B cells, and hence the depletion reduced atherosclerosis. Firstly, CD20 depletion restored the IgG type anti-oxLDL antibody levels, whereas IgM type anti-oxLDL levels were significantly decreased. Secondly, they found B cells drive CD3 T cells infiltration is the reason for the inflammation and probably the cause of lesion progression. Since CD20 depletion reduced the B cells, subsequently dendritic cells and CD3 T cells activation was reduced (Cochain & Zernecke, 2016), (Zernecke, 2015), (Bobryshev, 2010). In addition, CD20 depletion markedly also reduced macrophage accumulation (Ait-Oufella et al., 2010). However, some macrophage phenotypes are anti-atherogenic (Chinetti-Gbaguidi et al., 2015), (Willemsen & de Winther, 2020). In an interesting study showed B cell depletion through anti-CD20 antibody treatment protected the mice from abdominal aortic aneurysm (Schaheen et al., 2016). Similar to Ait-Oufella et al., Schaheen et al., also found that CD20 depletion did not affect IgG levels, whereas IgM levels were lowered. Interestingly, Schaheen et al., found $B220^{+}$ (murine B cells marker) plasmacytoid dendritic cells in CD20 depleted mice aorta that were not targeted by anti-CD20 antibodies. A similar experimental setting in my study showed the opposite outcome. B cell depletion was carried out with a single dose of anti-CD20 antibody. Similar to others (Ait-Oufella et al., 2010), (Schaheen et al., 2016), this treatment approach (Fig. 9A) significantly depleted B cells from BM (Fig. 9B), spleen (Fig. 9C), and blood (Fig. 9D). Anti-CD20 antibody

treatment resulted in reduced arteriogenesis in WT mice (Fig. 10), as analyzed by perfusion recovery (Fig. 10A), vascular cell proliferation (Fig. 10C), and luminal diameter (Fig. 10D). The anti-arteriogenic effect of CD20 depletion was associated with reduced regenerative macrophage accumulation (Fig. 10F), whereas inflammatory macrophages (Fig. 10E) were not affected. Numerous studies conducted in human multiple sclerosis patients (treated with Rituximab) reported that some T cells were also depleted by anti-CD20 treatment (Palanichamy et al., 2014), (Sabatino et al., 2019). This knowledge led me to check whether a similar effect could also be possible in my experimental settings. T cell (CD4, CD8, γδ T) and eosinophil number were not affected with CD20 depletion (Fig. 11A, B, C, D). Surprisingly my flow cytometry analysis showed CD20 expression on CD4, CD8, γδ T cells, and eosinophil. Anti-CD20 treatment significantly reduced $CD20^{+}CD4^{+}$ T cells (Fig. 12A), $CD20^{+}TCR\gamma\delta^{+}$ T cells (Fig. 12C), and $CD20^{+}$Siglec-F^{+} eosinophils (Fig. 12D) but not $CD20^{+}CD8^{+}$ T cells (Fig. 12B). A limited data already suggesting that T cells can express CD20 marker (Palanichamy et al., 2014), but according to my knowledge, my study for the first time showing that CD20 expression on γδ T cells and on eosinophils. Next, I used two clones of CD20 antibodies to confirm my finding of CD20 expression by using Imaging flow cytometry (AMINS). Imaging cytometry data clearly showed CD20 expression in TCR^{+} β (used to identify $CD4^{+}$ $CD8^{+}$) cells (Fig. 13B), and $TCR\gamma\delta^{+}$ T cells (Fig. 13C). $CD19^{+}$ cells serve as a reference cell population (Fig. 13D). Furthermore, using $CD19^{+}$ B cell (Fig. 13D) as reference cell population, I confirm CD20 expression in $TCR\gamma\delta^{+}$ T cells sorted from WT mice blood collected on day 3 after surgical procedure. However, no difference was found in cells sorted from femoral ligated compared to sham-operated mice (Fig. 13E). The above observation is a paradigm shift in what we know about CD20 expression.

Data from the CD20 depletion experiment could not draw any conclusions to my understanding because CD20 depletion not only depleted B cells but showed some effect on multiple cell compartments.

Due to this reason, a better experimental setting is needed to understand the role of B cells in arteriogenesis. At this stage, I used B cell-deficient (JHT KO) mice. B cell-deficient mice showed impaired arteriogenesis (Fig. 15A), associated with reduced vascular cell proliferation (Fig. 15D), collateral artery growth (Fig. 15E). However, both inflammatory and regenerative macrophages were unchanged (Fig. 15G, H) speculate the idea, maybe B cells could involve in arteriogenesis progress independently without working through macrophage compartment, or locally accumulated macrophages acquire different activation status in the absence of B cells (Srikakulapu & Mcnamara, 2020). B cell-deficient mice showed $CD20^+$ cells in adductor muscle (Fig. 16A). Since I found CD20 expression not only limited to B cells, I speculate the idea that $CD20^+$ cells might be relevant for observed arteriogenesis and macrophages accumulation in B cell-deficient mice. To rule out the relevance of these $CD20^+$ cells to arteriogenesis in B cell-deficient mice, I repeated CD20 depletion in B cell-deficient mice. Surprisingly B cells deficient having no B cells in the system still responded to the CD20 depletion treatment. CD20 depletion has a strong negative effect on arteriogenesis (Fig. 16B-D). This was associated with increased inflammatory macrophages (Fig. 16F) and decreased regenerative macrophage accumulation (Fig. 16G). This data supports my previous finding of CD20 expression on different cell compartments.

7.3 Role of T lymphocytes in arteriogenesis

T cells reported to module macrophage differentiation in inflammatory models (Weirather et al., 2014). Since B cell-deficient mice showed no difference in macrophage phenotype. I

speculate that macrophage accumulation in arteriogenesis is T cell-dependent. Stabile et al. reported that IL-16 expressing $CD8^+$ cells contribute to hindlimb blood flow recovery (Stabile et al., 2006). Van Weel et al. showed an essential role of $CD4^+$ T cells in arteriogenesis. Subsequently, similar data was reproduced in MHC-II deficient mice, which lack mature $CD4^+$ T helper cells. The same study also found the critical role of $NK1.1^+$ cells (Van Weel et al., 2007). However, this study lacks mechanistic insights to bias the cell-cell-dependent regulatory function. Another study reports the role of T cell costimulatory signaling molecule along with the role of regulatory T (Treg) cells in post-ischemic neovascularization. They observed reduced Treg cell number either in CD28 deficient mice or anti-CD25 treatment enhanced postischemic neovascularization (Zouggari et al., 2009). In contrast, Hellingman et al., reported the limited role of Treg cells in neovascularization. Using the anti-CD25 antibody and DEREG Foxp3 approach, they achieved Treg depletion and found that under both conditions, the difference was minimal (Hellingman et al., 2012). However, the data ambiguity in all the studies above made no clear conclusions and lacked the observed effect mechanism. In addition, there was a difference in surgical procedures, and methodological evaluations could have some impact on results which may not simply apply to the model I used in my study.

Considering all the factors, I wanted to test whether conventional (TCRα based) T cells play a role in arteriogenesis. By using TCRα KO mice (lacks $CD4^+$ and CD8+ cells), I found arteriogenesis was not affected in the absence of conventional T cells (Fig. 17A-E). Inflammatory macrophage number was comparable in TCRα KO mice (Fig. 18B). Interestingly lack of conventional T cells favoured an increased number of regenerative macrophage accumulation (Fig. 18C). I asked a question about how these mice compensated for the loss of major T cell population. TCR γδ T cells protected TCRα/β KO mice against malaria parasite

infection (Tsuji et al., 1994). This finding led me to speculate the idea that TCRα KO mice might get benefitted from the presence of γδ T cells since TCRα KO do not show any difference in arteriogenesis and, in fact showed significantly increased regenerative macrophage. My immunofluorescence images showing the infiltration of γδ T cells in adductor muscle (Fig. 19A). To rule out the relevance of γδ T cells in TCRα KO mice, I depleted γδ T cells using anti-TCRγδ antibody. Clone UC7-13D5 for the depletion of γδ T cells was debatable (Koenecke et al., 2009), (Wu et al., 2007). However, in my current experimental setting (Fig. 19B), I found anti-TCRγδ (Clone UC7-13D5) antibody significantly depleted γδT cells in the blood (Fig. 19C) and spleen (Fig. 19D), as analyzed by flow cytometry. TCRα KO mice treated with anti-TCRγδ antibody showed impaired arteriogenesis response (Fig. 20A-E) associated with an increased number of inflammatory macrophage accumulation (Fig. 20G), whereas regenerative macrophage accumulation was significantly decreased (Fig. 20H). A similar effect was also observed in WT mice with anti-TCRγδ treatment (Fig. 21A-E). The number of inflammatory macrophages in WT mice treated with anti-TCRγδ also showed an increased trend, however, the difference was not significant (Fig. 21G). In line with previous data (Fig. 20H), WT mice treated with anti-TCRγδ showed significantly decreased regenerative macrophage accumulation (Fig. 20H). This observation backs up my prior findings that γδ T cells are engaged in arteriogenesis not just in TCRα KO mice, but also in WT mice. IL-17A γδ T cells and IFN-γ γδ T cells were reported to be involved in inflammatory models (Kohlgruber et al., 2018). Next, I would like to check the signatory cytokine that γδ T cells express in arteriogenesis. γδ T cells were sorted from WT mice on day 3 after surgical procedure, and gene expression was analyzed by real-time PCR. IL-17A cytokine expression was undetectable under present the experimental setting. I found significantly increased IFN-γ expression in γδ T cells from ligated

WT mice than sham operated WT mice (Fig. 22). Hence, γδ T cell are IFN-γ expressing cells in arteriogenesis. IFN-γ cytokine was reported as a pro-inflammatory cytokine in many experimental settings (Schroecksnadel et al., 2006), (Lee et al., 2017), (Kopitar-Jerala, 2017). It's been reported from in-vitro studies that IFN-γ polarizes macrophages towards inflammatory subtypes. However, the tissue microenvironment is the strong determinant during macrophage polarization by providing a signal in a time-dependent manner. For example, inflammatory macrophages (M1) dominates in the initial phase of arteriogenesis, whereas regenerative or anti-inflammatory macrophages (M2) in the later phase (Troidl et al., 2013). Interestingly macrophages stimulated by IFN-γ can negatively regulate neutrophil infiltration (Hoeksema et al., 2015) could resolve the inflammation. I want to check the function of IFN-γ in arteriogenesis by identifying the macrophage activation status. Our group's data has shown that exogenous IFN-γ treatment can rescue mice from γδ T cell depletion (unpublished data). This somehow indicates that IFN-γ is a pro-arteriogenic cytokine. However, further confirmation has to be done in the future. Since I found γδ T cells were IFN-γ expressing cells and were relevant to arteriogenesis in TCRα KO mice and also in WT mice, however, $CD8^+$ T cells can express a high amount of IFN-γ in cell-mediated immunity, which leads to diverse responses (Pandiyan et al., 2007). Based on that, I would like to explore macrophage activation status in arteriogenesis. Perivascular macrophages activation status was analyzed at day 3 after femoral artery ligation by using MRC1 and CD169 (Siglec-1) markers (by means of mean fluorescence intensity). WT and TCRα KO mice treated with anti-TCRγδ treatment showed reduced CD169 expression on macrophages, but not MRC1 (Fig. 23A, B). γδ T cells were IFN-γ expressing in arteriogenesis. CD169 expression on macrophages induced by IFNs (Bourgoin et al., 2020), (Martinez-Pomares & Gordon, 2012). CD169, also

known as siglec-1 or sialoadhesin is expressed on a subset of macrophages. CD169 major work involving cell-cell adhesion. CD169 macrophages reported activating B cells, iNKT T cells, and CD8 T cells (Jian HR et al., 2006). Circulating neutrophils showed high levels of ligands for CD169. Mice model of renal ischemia-reperfusion experiments showed that depletion of CD169 macrophages facilitated increased endothelial ICAM-1 expression, excessive neutrophil infiltration, and caused irreversible renal damage (Karasawa K et al., 2015). However, no reports were available about CD169 macrophages in cardiovascular disease mouse models. T cells showed reduced proliferation capacity in sialodhesin KO mice (Jiang HR et al., 2006). Moreover, CD169 macrophages can activate T cells to secrete IFN-γ. However, in my observation, γδ T cells are essential T lymphocytes for arteriogenesis and are expressing IFN-γ. Depletion of γδ T cells resulted in reduced CD169 expression on perivascular macrophages. T cells from sialoadhesin KO mice showed lower levels of IFN-γ secretion (Jiang HR et al., 2006) indicating CD169 macrophage cross-talk with T cells. I speculate the idea that depletion of γδ T cells might interfere with the availability of IFN-γ in arteriogenesis. Hence perivascular macrophages from anti-TCRγδ treated mice showed reduced CD169 expression. Perivascular CD169 macrophages co-express LTβR (Fig. 22C), indicating possible T and B lymphocyte cross-talk (Perez et al., 2017). This finding led me to speculate the idea that CD169 macrophages were might be crucial macrophage subtype in arteriogenesis. To answer this, $F4/80^{+}CD169^{+}$ macrophages were sorted from spleen, blood, and muscle on day 3 after femoral artery ligation. Gene expression analysis by real-time PCR from sorted macrophages showed expression of IL-10 and PDGFβ (Fig. 24). However, high expression levels of IL-10 were observed in macrophages isolated from muscle (Fig. 24A), whereas no difference in PDGFβ expression levels was observed among splenic, blood, and muscle macrophages (Fig. 24B).

Convincingly collateral arteries were expressing a receptor for PDGFβ (Fig. 24C, D). However, the expression levels were not significant between ligated and sham-operated (Fig. 24C). This data indicates CD169 macrophages could promote collateral artery growth via PDGFβ.

8. GRAPHICAL ABSTRACT

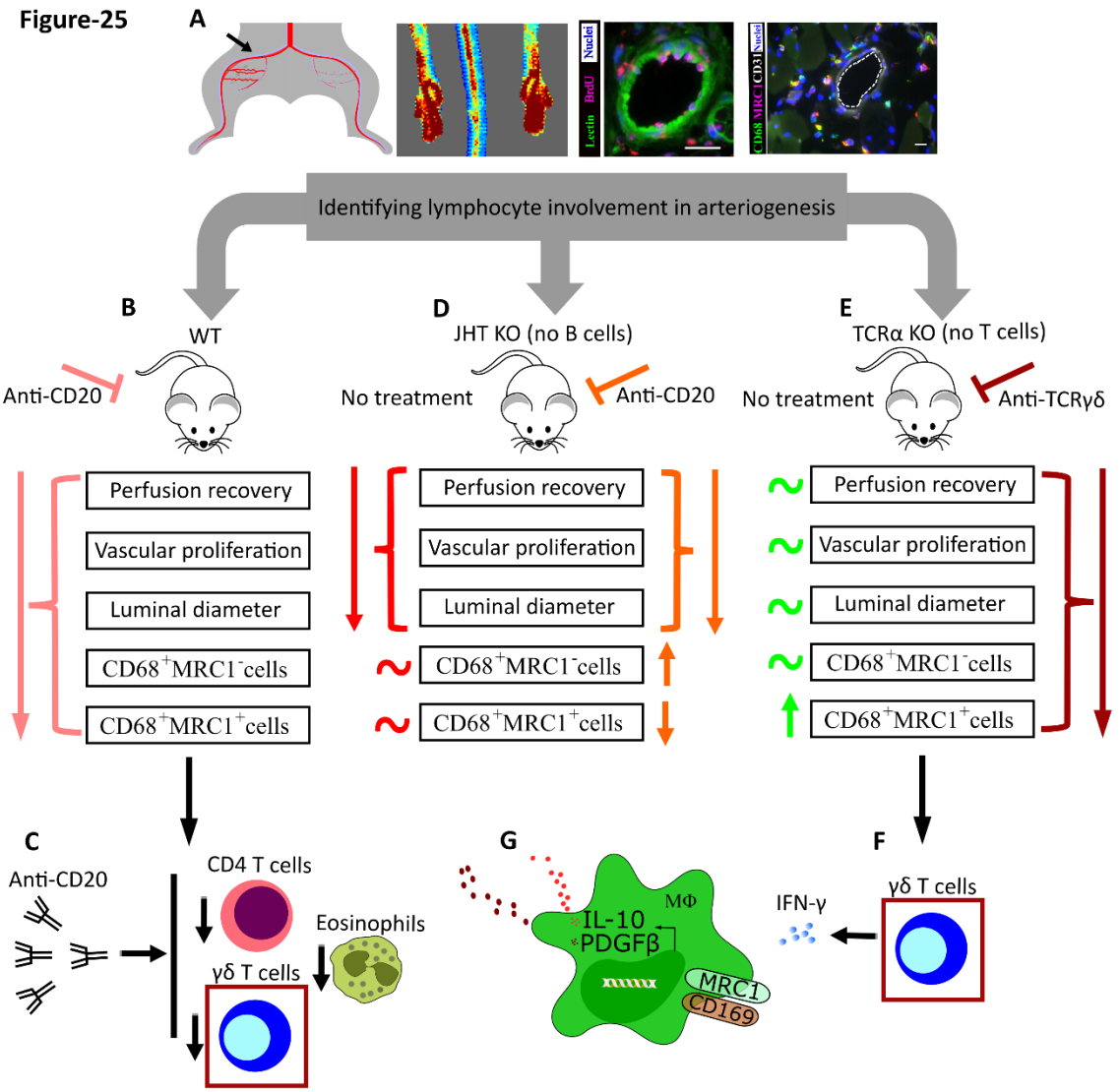

Figure 25. Model illustrating lymphocyte involvement in arteriogenesis

A. Model approach. Arteriogenesis was induced by ligating right femoral artery and left femoral was sham operated. As a result of arteriogenesis fully grown collateral arteries were seen in right adductor muscle (arrow). Arteriogenesis was characterized by analysis of perfusion recovery by LDI, vascular cell proliferation, analysis of luminal diameter and perivascular macrophages by Immunofluorescence. B. CD20 targeted B cell depletion resulted in decreased arteriogenesis in WT mice. C. Anti-CD20 treatment targeted not only B cells but $CD20^+$ CD4 T cells, γδ T cells and eosinophils. (B & C observation was WT+Isotype control vs WT+anti-CD20). D. B cell deficient (JHT KO) mice showed decreased arteriogenesis without effecting perivascular macrophages (observation was WT vs JHT KO). Anti-CD20 treatment showed negative effect in JHT KO mice with decreased regenerative ($CD68^+MRC1^+$) macrophages, whereas inflammatory ($CD68^+MRC^-$) macrophages were increased (Observation was JHT KO+Isotype control vs JHT KO+anti-CD20). E. Lack of conventional T cells showed no effect in Arteriogenesis and more over favored $CD68^+MRC1^+$ macrophage recruitment (observation was WT vs TCRα KO). However, depletion of γδ T cells with anti- TCRγδ showed decreased arteriogenesis and decreased macrophage recruitment (observation was TCRα KO+Isotype control vs TCRα KO+anti-TCRγδ). F. γδ T cells are IFN-γ expressing cells in arteriogenesis. G. CD169 macrophages can express IL-10 and PDGFβ and may promote vascular growth.

9. OUTLOOK

Promoting arteriogenesis could be a better alternative for invasive management of cardiovascular diseases. However, due to its complexity, extensive research has to be done. Any knowledge to understand and to add to molecular mechanism in arteriogenesis is greatly useful for therapeutics development. My present study provides convincing evidence of B and T lymphocyte involvement in arteriogenesis. For the first time, my study shows the evidence that IFN-γ expressing γδ T cell are pro-arteriogenic in nature. Furthermore, my study also found that CD169 expression on macrophages is reduced in γδ T cell depleted mice.

10. STUDY LIMITATIONS

My study has fewer limitations. To begin with, my experimental approaches provided convincing evidence about the role of lymphocytes in arteriogenesis; however, they did not provide mechanistic insights at this stage. Secondly, My study did not explore the subtypes of γδ T (Vγ1+ γδ T cells, Vγ4+ γδ T cells) and B cells (B1-B cells, B2-B cells) and needs to elucidate in the future. Finally, IFN-γ signaling concerning CD169 macrophage vascular growth promoting feature remains to be elucidated.

11. REFERENCES

- Aiello, F. B., Keller, J. R., Klarmann, K. D., Dranoff, G., Mazzucchelli, R., & Durum, S. K. (2007). IL-7 Induces Myelopoiesis and Erythropoiesis. *The Journal of Immunology*, *178*(3). https://doi.org/10.4049/jimmunol.178.3.1553
- Ait-Oufella, H., Herbin, O., Bouaziz, J. D., Binder, C. J., Uyttenhove, C., Laurans, L., Taleb, S., Van Vré, E., Esposito, B., Vilar, J., Sirvent, J., Van Snick, J., Tedgui, A., Tedder, T. F., & Mallat, Z. (2010). B cell depletion reduces the development of atherosclerosis in mice. *Journal of Experimental Medicine*, *207*(8). https://doi.org/10.1084/jem.20100155
- Ait-Oufella, H., Salomon, B. L., Potteaux, S., Robertson, A. K. L., Gourdy, P., Zoll, J., Merval, R., Esposito, B., Cohen, J. L., Fisson, S., Flavell, R. A., Hansson, G. K., Klatzmann, D., Tedgui, A., & Mallat, Z. (2006). Natural regulatory T cells control the development of atherosclerosis in mice. *Nature Medicine*, *12*(2). https://doi.org/10.1038/nm1343
- Beneke, A., Guentsch, A., Hillemann, A., Zieseniss, A., Swain, L., & Katschinski, D. M. (2017). Loss of PHD3 in myeloid cells dampens the inflammatory response and fibrosis after hind-limb ischemia. *Cell Death & Disease*, *8*(8). https://doi.org/10.1038/cddis.2017.375
- Beutler B. Innate immunity: an overview. Mol Immunol. 2004 Feb;40(12):845-59. doi: 10.1016/j.molimm.2003.10.005. PMID: 14698223.
- Binder, C. J., Chang, M. K., Shaw, P. X., Miller, Y. I., Hartvigsen, K., Dewan, A., &

Witztum, J. L. (2002). Innate and acquired immunity in atherogenesis. In *Nature Medicine* (Vol. 8, Issue 11). https://doi.org/10.1038/nm1102-1218

- Bobryshev, Y. V. (2010). Dendritic cells and their role in atherogenesis. In *Laboratory Investigation* (Vol. 90, Issue 7). https://doi.org/10.1038/labinvest.2010.94
- Bourgoin, P., Biéchelé, G., Ait Belkacem, I., Morange, P. E., & Malergue, F. (2020). Role of the interferons in CD64 and CD169 expressions in whole blood: Relevance in the balance between viral- or bacterial-oriented immune responses. *Immunity, Inflammation and Disease*, *8*(1). https://doi.org/10.1002/iid3.289
- Buschmann, I. R., Hoefer, I. E., van Royen, N., Katzer, E., Braun-Dulleaus, R., Heil, M., Kostin, S., Bode, C., & Schaper, W. (2001). GM-CSF: a strong arteriogenic factor acting by amplification of monocyte function. Atherosclerosis, 159(2), 343–356. https://doi.org/10.1016/s0021-9150(01)00637-2
- Carmeliet, P. (2000). Mechanisms of angiogenesis and arteriogenesis. In *Nature Medicine* (Vol. 6, Issue 4). https://doi.org/10.1038/74651
- Hansson, G., Hermansson, A. The immune system in atherosclerosis. Nat Immunol 12, 204–212 (2011). https://doi.org/10.1038/ni.2001
- Chillo, O., Kleinert, E. C., Lautz, T., Lasch, M., Pagel, J. I., Heun, Y., Troidl, K., Fischer, S., Caballero-Martinez, A., Mauer, A., Kurz, A. R. M., Assmann, G., Rehberg, M., Kanse, S. M., Nieswandt, B., Walzog, B., Reichel, C. A., Mannell, H., Preissner, K. T., & Deindl, E. (2016). Perivascular Mast Cells Govern Shear Stress-

Induced Arteriogenesis by Orchestrating Leukocyte Function. *Cell Reports*, *16*(8). https://doi.org/10.1016/j.celrep.2016.07.040

- Chinetti-Gbaguidi, G., Colin, S., & Staels, B. (2015). Macrophage subsets in atherosclerosis. In *Nature Reviews Cardiology* (Vol. 12, Issue 1). https://doi.org/10.1038/nrcardio.2014.173
- Cochain, C., & Zernecke, A. (2016). Protective and pathogenic roles of CD8+ T cells in atherosclerosis. In *Basic Research in Cardiology* (Vol. 111, Issue 6). https://doi.org/10.1007/s00395-016-0589-7
- Danilova N. The evolution of adaptive immunity. Adv Exp Med Biol. 2012;738:218-35. doi: 10.1007/978-1-4614-1680-7_13. PMID: 22399382.
- Deindl, E., & Schaper, W. (2005). The art of arteriogenesis. *Cell Biochemistry and Biophysics*, *43*(1). https://doi.org/10.1385/cbb:43:1:001
- Döring, Y., Jansen, Y., Cimen, I., Aslani, M., Gencer, S., Peters, L. J. F., Duchene, J., Weber, C., & van der Vorst, E. P. C. (2020). B-cell-specific CXCR4 protects against atherosclerosis development and increases plasma IgM levels. In *Circulation Research*. https://doi.org/10.1161/CIRCRESAHA.119.316142
- Duchosal MA. B-cell development and differentiation. Semin Hematol. 1997 Jan;34(1 Suppl 1):2-12. PMID: 9122742.
- Franken, L., Schiwon, M., & Kurts, C. (2016). Macrophages: Sentinels and regulators of the immune system. *Cellular Microbiology*, *18*(4). https://doi.org/10.1111/cmi.12580
- Gordon, S. (2003). Alternative activation of macrophages. In *Nature Reviews*

Immunology (Vol. 3, Issue 1). https://doi.org/10.1038/nri978

- Hansson, G. K., Robertson, A. K. L., & Söderberg-Nauclér, C. (2006). Inflammation and atherosclerosis. In *Annual Review of Pathology* (Vol. 1). https://doi.org/10.1146/annurev.pathol.1.110304.100100
- Hellingman, A. A., van der Vlugt, L. E. P. M., Lijkwan, M. A., Bastiaansen, A. J. N. M., Sparwasser, T., Smits, H. H., Hamming, J. F., & Quax, P. H. A. (2012). A limited role for regulatory T cells in post-ischemic neovascularization. *Journal of Cellular and Molecular Medicine*, *16*(2). https://doi.org/10.1111/j.1582-4934.2011.01300.x
- Hoeksema, M. A., Scicluna, B. P., Boshuizen, M. C. S., van der Velden, S., Neele, A. E., Van den Bossche, J., Matlung, H. L., van den Berg, T. K., Goossens, P., & de Winther, M. P. J. (2015). IFN-γ Priming of Macrophages Represses a Part of the Inflammatory Program and Attenuates Neutrophil Recruitment. *The Journal of Immunology*, *194*(8). https://doi.org/10.4049/jimmunol.1402077
- Iwata, Y., Matsushita, T., Horikawa, M., DiLillo, D. J., Yanaba, K., Venturi, G. M., Szabolcs, P. M., Bernstein, S. H., Magro, C. M., Williams, A. D., Hall, R. P., St Clair, E. W., & Tedder, T. F. (2011). Characterization of a rare IL-10-competent B-cell subset in humans that parallels mouse regulatory B10 cells. *Blood*, *117*(2). https://doi.org/10.1182/blood-2010-07-294249
- Jiang, H. R., Hwenda, L., Makinen, K., Oetke, C., Crocker, P. R., & Forrester, J. V. (2006). Sialoadhesin promotes the inflammatory response in experimental autoimmune uveoretinitis. Journal of immunology (Baltimore, Md. : 1950),

177(4), 2258–2264. https://doi.org/10.4049/jimmunol.177.4.2258

- Judith A Owen; Jenni Punt; Sharon A Stranford; Patricia P Jones; Janis Kuby. Immunology. New York : W.H. Freeman, 2013
- Kazunori Karasawa, Kenichi Asano, Shigetaka Moriyama, Mikiko Ushiki, Misa Monya, Mayumi Iida, Erika Kuboki, Hideo Yagita, Keiko Uchida, Kosaku Nitta, Masato Tanaka
- JASN Apr 2015, 26 (4) 896-906; DOI: 10.1681/ASN.2014020195
- Koelwyn, G. J., Corr, E. M., Erbay, E., & Moore, K. J. (2018). Regulation of macrophage immunometabolism in atherosclerosis. In *Nature Immunology* (Vol. 19, Issue 6). https://doi.org/10.1038/s41590-018-0113-3
- Koenecke, C., Chennupati, V., Schmitz, S., Malissen, B., Föster, R., & Prins, I. (2009). In vivo application of mAb directed against the γδ TCR does not deplete but generated "invisible" γδ T cells. *European Journal of Immunology*, *39*(2). https://doi.org/10.1002/eji.200838741
- Kohlgruber, A. C., Gal-Oz, S. T., Lamarche, N. M., Shimazaki, M., Duquette, D., Nguyen, H. N., Mina, A. I., Paras, T., Tavakkoli, A., Von Andrian, U., Banks, A. S., Shay, T., Brenner, M. B., & Lynch, L. (2018). γδ T cells producing interleukin-17A regulate adipose regulatory T cell homeostasis and thermogenesis /631/250/256 /631/250/2504 article. *Nature Immunology*, *19*(5). https://doi.org/10.1038/s41590-018-0094-2
- Kopitar-Jerala, N. (2017). The role of interferons in inflammation and inflammasome activation. In *Frontiers in Immunology* (Vol. 8, Issue JUL).

https://doi.org/10.3389/fimmu.2017.00873

- Kumaraswami, K., Salei, N., Beck, S., Rambichler, S., Kluever, A. K., Lasch, M., Richter, L., Schraml, B. U., & Deindl, E. (2020). A simple and effective flow cytometry-based method for identification and quantification of tissue infiltrated leukocyte subpopulations in a mouse model of peripheral arterial disease. *International Journal of Molecular Sciences*, *21*(10). https://doi.org/10.3390/ijms21103593
- Kumar BV, Connors TJ, Farber DL. Human T Cell Development, Localization, and Function throughout Life. Immunity. 2018 Feb 20;48(2):202-213. doi: 10.1016/j.immuni.2018.01.007. PMID: 29466753; PMCID: PMC5826622.
- Kyaw, T., Winship, A., Tay, C., Kanellakis, P., Hosseini, H., Cao, A., Li, P., Tipping, P., Bobik, A., & Toh, B. H. (2013). Cytotoxic and proinflammatory CD8+ T lymphocytes promote development of vulnerable atherosclerotic plaques in ApoE-deficient mice. *Circulation*, *127*(9). https://doi.org/10.1161/CIRCULATIONAHA.112.001347
- Land WG. The Role of Damage-Associated Molecular Patterns in Human Diseases: Part I - Promoting inflammation and immunity. Sultan Qaboos Univ Med J. 2015 Feb;15(1):e9-e21. Epub 2015 Jan 21. PMID: 25685392; PMCID: PMC4318613.
- La Sala, A., Pontecorvo, L., Agresta, A., Rosano, G., & Stabile, E. (2012). Regulation of collateral blood vessel development by the innate and adaptive immune system. In *Trends in Molecular Medicine* (Vol. 18, Issue 8).

https://doi.org/10.1016/j.molmed.2012.06.007

- Lasch, M., Kleinert, E. C., Meister, S., Kumaraswami, K., Buchheim, J. I., Grantzow, T., Lautz, T., Salpisti, S., Fischer, S., Troidl, K., Fleming, I., Randi, A. M., Sperandio, M., Preissner, K. T., & Deindl, E. (2019). Extracellular RNA released due to shear stress controls natural bypass growth by mediating mechanotransduction in mice. *Blood*, *134*(17). https://doi.org/10.1182/blood.2019001392
- Lee, S. H., Kwon, J. Y., Kim, S. Y., Jung, K. A., & Cho, M. La. (2017). Interferon-gamma regulates inflammatory cell death by targeting necroptosis in experimental autoimmune arthritis. *Scientific Reports*, *7*(1). https://doi.org/10.1038/s41598-017-09767-0
- Limbourg, A., Korff, T., Napp, L. C., Schaper, W., Drexler, H., & Limbourg, F. P. (2009). Evaluation of postnatal arteriogenesis and angiogenesis in a mouse model of hind-limb ischemia. *Nature Protocols*, *4*(12). https://doi.org/10.1038/nprot.2009.185
- Liuzzo, G., Goronzy, J. J., Yang, H., Kopecky, S. L., Holmes, D. R., Frye, R. L., & Weyand, C. M. (2000). Monoclonal T-cell proliferation and plaque instability in acute coronary syndromes. *Circulation*, *101*(25). https://doi.org/10.1161/01.CIR.101.25.2883
- Luckheeram RV, Zhou R, Verma AD, Xia B. $CD4^+$T cells: differentiation and functions. Clin Dev Immunol. 2012;2012:925135. doi: 10.1155/2012/925135. Epub 2012 Mar 14. PMID: 22474485; PMCID: PMC3312336.

- Martinez-Pomares, L., & Gordon, S. (2012). CD169 + macrophages at the crossroads of antigen presentation. In *Trends in Immunology* (Vol. 33, Issue 2). https://doi.org/10.1016/j.it.2011.11.001
- Möbius-Winkler, S., Uhlemann, M., Adams, V., Sandri, M., Erbs, S., Lenk, K., Mangner, N., Mueller, U., Adam, J., Grunze, M., Brunner, S., Hilberg, T., Mende, M., Linke, A. P., & Schuler, G. (2016). Coronary Collateral Growth Induced by Physical Exercise: Results of the Impact of Intensive Exercise Training on Coronary Collateral Circulation in Patients With Stable Coronary Artery Disease (EXCITE) Trial. *Circulation*, *133*(15), 1438–1448. https://doi.org/10.1161/CIRCULATIONAHA.115.016442
- Mombaerts, P., Iacomini, J., Johnson, R. S., Herrup, K., Tonegawa, S., & Papaioannou, V. E. (1992). RAG-1-deficient mice have no mature B and T lymphocytes. *Cell*, *68*(5). https://doi.org/10.1016/0092-8674(92)90030-G
- Mosser, D. M., & Edwards, J. P. (2008). Exploring the full spectrum of macrophage activation. In *Nature Reviews Immunology* (Vol. 8, Issue 12). https://doi.org/10.1038/nri2448
- Murray, P. J., Allen, J. E., Biswas, S. K., Fisher, E. A., Gilroy, D. W., Goerdt, S., Gordon, S., Hamilton, J. A., Ivashkiv, L. B., Lawrence, T., Locati, M., Mantovani, A., Martinez, F. O., Mege, J. L., Mosser, D. M., Natoli, G., Saeij, J. P., Schultze, J. L., Shirey, K. A., … Wynn, T. A. (2014). Macrophage Activation and Polarization: Nomenclature and Experimental Guidelines. In *Immunity* (Vol. 41, Issue 1).

https://doi.org/10.1016/j.immuni.2014.06.008

- Niessner, A., Sato, K., Chaikof, E. L., Colmegna, I., Goronzy, J. J., & Weyand, C. M. (2006). Pathogen-sensing plasmacytoid dendritic cells stimulate cytotoxic T-cell function in the atherosclerotic plaque through interferon-α. *Circulation*, *114*(23). https://doi.org/10.1161/CIRCULATIONAHA.106.642801
- Niessner, A., & Weyand, C. M. (2010). Dendritic cells in atherosclerotic disease. In *Clinical Immunology* (Vol. 134, Issue 1). https://doi.org/10.1016/j.clim.2009.05.006
- Palanichamy, A., Jahn, S., Nickles, D., Derstine, M., Abounasr, A., Hauser, S. L., Baranzini, S. E., Leppert, D., & von Büdingen, H.-C. (2014). Rituximab Efficiently Depletes Increased CD20-Expressing T Cells in Multiple Sclerosis Patients. *The Journal of Immunology*, *193*(2). https://doi.org/10.4049/jimmunol.1400118
- Pandiyan, P., Hegel, J. K. E., Krueger, M., Quandt, D., & Brunner-Weinzierl, M. C. (2007). High IFN-γ Production of Individual CD8 T Lymphocytes Is Controlled by CD152 (CTLA-4). *The Journal of Immunology*, *178*(4). https://doi.org/10.4049/jimmunol.178.4.2132
- Paulsson, G., Zhou, X., Törnquist, E., & Hansson, G. K. (2000). Oligoclonal T cell expansions in atherosclerotic lesions of apolipoprotein E-deficient mice. *Arteriosclerosis, Thrombosis, and Vascular Biology*, *20*(1). https://doi.org/10.1161/01.ATV.20.1.10
- Perez, O. A., Yeung, S. T., Vera-Licona, P., Romagnoli, P. A., Samji, T., Ural, B. B., Maher, L., Tanaka, M., & Khanna, K. M. (2017). CD169+ macrophages

orchestrate innate immune responses by regulating bacterial localization in the spleen. *Science Immunology*, *2*(16). https://doi.org/10.1126/sciimmunol.aah5520

- Radomir, L., Kramer, M. P., Perpinial, M., Schottlender, N., Rabani, S., David, K., Wiener, A., Lewinsky, H., Becker-Herman, S., Aharoni, R., Milo, R., Mauri, C., & Shachar, I. (2021). The survival and function of IL-10-producing regulatory B cells are negatively controlled by SLAMF5. *Nature Communications*, *12*(1). https://doi.org/10.1038/s41467-021-22230-z
- Rus H, Cudrici C, Niculescu F. The role of the complement system in innate immunity. Immunol Res. 2005;33(2):103-12. doi: 10.1385/IR:33:2:103. PMID: 16234578.
- Sabatino, J. J., Wilson, M. R., Calabresi, P. A., Hauser, S. L., Schneck, J. P., & Zamvil, S. S. (2019). Anti-CD20 therapy depletes activated myelin-specific CD8+ T cells in multiple sclerosis. *Proceedings of the National Academy of Sciences of the United States of America*, *116*(51). https://doi.org/10.1073/pnas.1915309116
- Saigusa, R., Winkels, H., & Ley, K. (2020). T cell subsets and functions in atherosclerosis. In *Nature Reviews Cardiology* (Vol. 17, Issue 7). https://doi.org/10.1038/s41569-020-0352-5
- Schaheen, B., Downs, E. A., Serbulea, V., Almenara, C. C. P., Spinosa, M., Su, G., Zhao, Y., Srikakulapu, P., Butts, C., McNamara, C. A., Leitinger, N., Upchurch, G. R., Meher, A. K., & Ailawadi, G. (2016). B-Cell Depletion Promotes Aortic

Infiltration of Immunosuppressive Cells and Is Protective of Experimental Aortic Aneurysm. *Arteriosclerosis, Thrombosis, and Vascular Biology*, *36*(11). https://doi.org/10.1161/ATVBAHA.116.307559

- Scholz, D., Ito, W., Fleming, I., Deindl, E., Sauer, A., Wiesnet, M., Busse, R., Schaper, J., & Schaper, W. (2000). Ultrastructure and molecular histology of rabbit hind-limb collateral artery growth (arteriogenesis). *Virchows Archiv*, *436*(3). https://doi.org/10.1007/s004280050039
- Schroecksnadel, K., Frick, B., Winkler, C., & Fuchs, D. (2006). Crucial Role of Interferon-γ and Stimulated Macrophages in Cardiovascular Disease. *Current Vascular Pharmacology*, *4*(3). https://doi.org/10.2174/157016106777698379
- Seijkens, T. T. P., Poels, K., Meiler, S., Van Tiel, C. M., Kusters, P. J. H., Reiche, M., Atzler, D., Winkels, H., Tjwa, M., Poelman, H., Slütter, B., Kuiper, J., Gijbels, M., Kuivenhoven, J. A., Matic, L. P., Paulsson-Berne, G., Hedin, U., Hansson, G. K., Nicolaes, G. A. F., … Lutgens, E. (2019). Deficiency of the T cell regulator Casitas B-cell lymphoma-B aggravates atherosclerosis by inducing CD8 + T cell-mediated macrophage death. *European Heart Journal*, *40*(4). https://doi.org/10.1093/eurheartj/ehy714
- Shaw, P. X., Hörkkö, S., Chang, M. K., Curtiss, L. K., Palinski, W., Silverman, G. J., & Witztum, J. L. (2000). Natural antibodies with the T15 idiotype may act in atherosclerosis, apoptotic clearance, and protective immunity. *Journal of Clinical Investigation*, *105*(12). https://doi.org/10.1172/JCI8472

- Smith, J. D., Trogan, E., Ginsberg, M., Grigaux, C., Tian, J., & Miyata, M. (1995). Decreased atherosclerosis in mice deficient in both macrophage colony-stimulating factor (op) and apolipoprotein E. *Proceedings of the National Academy of Sciences of the United States of America*, *92*(18). https://doi.org/10.1073/pnas.92.18.8264
- Srikakulapu, P., & Mcnamara, C. A. (2020). B Lymphocytes and Adipose Tissue Inflammation. In *Arteriosclerosis, Thrombosis, and Vascular Biology*. https://doi.org/10.1161/ATVBAHA.119.312467
- Srikakulapu, P., Upadhye, A., Rosenfeld, S. M., Marshall, M. A., McSkimming, C., Hickman, A. W., Mauldin, I. S., Ailawadi, G., Lopes, M. B. S., Taylor, A. M., & McNamara, C. A. (2017). Perivascular adipose tissue harbors atheroprotective IgM-producing B cells. *Frontiers in Physiology*, *8*(SEP). https://doi.org/10.3389/fphys.2017.00719
- Stabile, E., Kinnaird, T., La Sala, A., Hanson, S. K., Watkins, C., Campia, U., Shou, M., Zbinden, S., Fuchs, S., Kornfeld, H., Epstein, S. E., & Burnett, M. S. (2006). CD8+ T lymphocytes regulate the arteriogenic response to ischemia by infiltrating the site of collateral vessel development and recruiting CD4+ mononuclear cells through the expression of interleukin-16. *Circulation*, *113*(1). https://doi.org/10.1161/CIRCULATIONAHA.105.576702
- Stabile, E., Susan Burnett, M., Watkins, C., Kinnaird, T., Bachis, A., La Sala, A., Miller, J. M., Shou, M., Epstein, S. E., & Fuchs, S. (2003). Impaired arteriogenic response to acute hindlimb ischemia in CD4-knockout mice. *Circulation*, *108*(2).

https://doi.org/10.1161/01.CIR.0000079225.50817.71

- Tedder, T. F. (2015). B10 Cells: A Functionally Defined Regulatory B Cell Subset. *The Journal of Immunology*, *194*(4). https://doi.org/10.4049/jimmunol.1401329
- Tedgui, A., & Mallat, Z. (2006). Cytokines in atherosclerosis: Pathogenic and regulatory pathways. In *Physiological Reviews* (Vol. 86, Issue 2). https://doi.org/10.1152/physrev.00024.2005
- Troidl, C., Jung, G., Troidl, K., Hoffmann, J., Mollmann, H., Nef, H., Schaper, W., Hamm, C. W., & Schmitz-Rixen, T. (2013). The Temporal and Spatial Distribution of Macrophage Subpopulations During Arteriogenesis. *Current Vascular Pharmacology*, *11*(1). https://doi.org/10.2174/1570161111309010005
- Tsuji, M., Mombaerts, P., Lefrancois, L., Nussenzweig, R. S., Zavala, F., & Tonegawa, S. (1994). γδ T cells contribute to immunity against the liver stages of malaria in αβ T-cell-deficient mice. *Proceedings of the National Academy of Sciences of the United States of America*, *91*(1). https://doi.org/10.1073/pnas.91.1.345
- Van Royen, N., Piek, J. J., Buschmann, I., Hoefer, I., Voskuil, M., & Schaper, W. (2001). Stimulation of arteriogenesis; a new concept for the treatment of arterial occlusive disease. In *Cardiovascular Research* (Vol. 49, Issue 3). https://doi.org/10.1016/S0008-6363(00)00206-6
- van Royen, N., Schirmer, S. H., Atasever, B., Behrens, C. Y., Ubbink, D., Buschmann, E. E., Voskuil, M., Bot, P., Hoefer, I., Schlingemann, R. O., Biemond, B. J., Tijssen, J. G., Bode, C., Schaper, W., Oskam, J., Legemate, D. A., Piek, J. J.,

& Buschmann, I. (2005). START Trial: a pilot study on STimulation of ARTeriogenesis using subcutaneous application of granulocyte-macrophage colony-stimulating factor as a new treatment for peripheral vascular disease. Circulation, 112(7), 1040–1046. https://doi.org/10.1161/CIRCULATIONAHA.104.529552

- van Royen, N., Piek, J. J., Schaper, W., & Fulton, W. F. (2009). A critical review of clinical arteriogenesis research. Journal of the American College of Cardiology, 55(1), 17–25. https://doi.org/10.1016/j.jacc.2009.06.058
- Van Weel, V., Toes, R. E. M., Seghers, L., Deckers, M. M. L., De Vries, M. R., Eilers, P. H., Sipkens, J., Schepers, A., Eefting, D., Van Hinsbergh, V. W. M., Van Bockel, J. H., & Quax, P. H. A. (2007). Natural killer cells and CD4+ T-cells modulate collateral artery development. *Arteriosclerosis, Thrombosis, and Vascular Biology*, *27*(11). https://doi.org/10.1161/ATVBAHA.107.151407
- Weirather, J., Hofmann, U. D. W., Beyersdorf, N., Ramos, G. C., Vogel, B., Frey, A., Ertl, G., Kerkau, T., & Frantz, S. (2014). Foxp3+ CD4+ T cells improve healing after myocardial infarction by modulating monocyte/macrophage differentiation. *Circulation Research*, *115*(1). https://doi.org/10.1161/CIRCRESAHA.115.303895
- Willemsen, L., & de Winther, M. P. J. (2020). Macrophage subsets in atherosclerosis as defined by single-cell technologies. In *Journal of Pathology* (Vol. 250, Issue 5). https://doi.org/10.1002/path.5392
- Wu, H., Wang, Y. M., Wang, Y., Hu, M., Zhang, G. Y., Knight, J. F., Harris, D. C. H.,

& Alexander, S. I. (2007). Depletion of γδ T cells exacerbates murine adriamycin nephropathy. *Journal of the American Society of Nephrology*, *18*(4). https://doi.org/10.1681/ASN.2006060622

- Wynn, T. A., & Vannella, K. M. (2016). Macrophages in Tissue Repair, Regeneration, and Fibrosis. In *Immunity* (Vol. 44, Issue 3). https://doi.org/10.1016/j.immuni.2016.02.015
- Zernecke, A. (2015). Dendritic Cells in Atherosclerosis. *Arteriosclerosis, Thrombosis, and Vascular Biology*, *35*(4). https://doi.org/10.1161/atvbaha.114.303566
- Zhou, X., Nicoletti, A., Elhage, R., & Hansson, G. K. (2000). Transfer of CD4+ T cells aggravates atherosclerosis in immunodeficient apolipoprotein E knockout mice. *Circulation*, *102*(24). https://doi.org/10.1161/01.CIR.102.24.2919
- Zouggari, Y., Ait-Oufella, H., Waeckel, L., Vilar, J., Loinard, C., Cochain, C., Récalde, A., Duriez, M., Levy, B. I., Lutgens, E., Mallat, Z., & Silvestre, J. S. (2009). Regulatory T cells modulate postischemic neovascularization. *Circulation*, *120*(14). https://doi.org/10.1161/CIRCULATIONAHA.109.875583

12. ACKNOWLEDGEMENTS

I am grateful to Ludwig-Maximilians-Universität München, Germany, for this great opportunity.

I would like to express my heartful gratitude to my supervisor Prof. Elisabeth Deindl for allowing me to train in the fascinating research area. I am thankful for her critical supervision, outstanding motivation, and support during my thesis. Without her help, I could not finish my thesis.

My sincere thanks to Prof. Markus Sperandio and Prof. Daphne Merkus for supporting me in finishing my thesis.

I am thankful to Christine Eder and Siegfried for their love and support.

I am thankful to Prof. Dr. Klaus Rajewsky, Prof. Dr. Ludger Klein, PD Dr. rer. nat. Reinhard Obst for kindly providing me mouse strains for my work.

I thank Dr. Manuel Lasch for training me to the mouse model. Thanks to Anna Braumandl for being the best teammate and thanks to Sebastian Beck for the friendly and cooperative atmosphere in the lab. I want to extend my thanks to Dr. Thomas Lautz for conducting preliminary experiments for my project. And thanks to Dr. Rim Sabrina for her insights into the project. Finally, I appreciate the support from our teammates, Matthias Einstein Küebler, Philipp Götz-Mr. White, Christoph Arnholdt, Franziska Sciuk, Simon Rutkowski and Dr. Marc Praetner (late).

I would like to thank Dr. Hellen Ishikawa-Ankerhold, Dominic van den Heuvel, and Dr. Kerstin Troidl for their support with microscopy.

I am grateful to Dr. Lisa Richter and Pardis Khosravani for their support with flow cytometry experiments.

I would like to convey my special thanks to Michael Lorenz and Anna Titova for their crucial support.

I am thankful to Dr. Mehdi Shakarami, Dr. Bastian Popper, and the team for their support with animal maintenance.

I am thankful to Prof. Vijaykumar Kutala and Dr. Noor Ahmed Shaik for their continuous guidance and motivation.

I appreciate my friends Shivaprasad Panjala, Dr. Shivakrishna Katkam, Bheemanna Maram, Mallesh Pagidi, Naresh Koneru, Dr. Sudhakar Reddy Kalluri, Dr. Rupasree, Dr. Madhavi latha Manolla, Dr. Sireesha Vaidya, and Manga Motrapu for their support and encouragement.

Thanks to Gone Satish Rao, Dr. Ramesh and Dr. Devaiah for their encouragement and support.

Last but not least, I thank my family for their love and support.

List of Publications:

1. Arnholdt C, **Kumaraswami K**, Götz P, Kübler M, Lasch M, Deindl E. Depletion of γδ T Cells Leads to Reduced Angiogenesis and Increased Infiltration of Inflammatory M1-like Macrophages in Ischemic Muscle Tissue. Cells. 2022 Apr 29;11(9):1490. doi: 10.3390/cells11091490.
2. Götz, P., Braumandl, A., Kübler, M., **Kumaraswami, K**., Ishikawa-Ankerhold, H., Lasch, M., & Deindl, E. (2021). C3 Deficiency Leads to Increased Angiogenesis and Elevated Pro-Angiogenic Leukocyte Recruitment in Ischemic Muscle Tissue. *International journal of molecular sciences*, *22*(11), 5800. https://doi.org/10.3390/ijms22115800
3. Kübler, M., Beck, S., Fischer, S., Götz, P., **Kumaraswami, K**., Ishikawa-Ankerhold, H., Lasch, M., & Deindl, E. (2021). Absence of Cold-Inducible RNA-Binding Protein (CIRP) Promotes Angiogenesis and Regeneration of Ischemic Tissue by Inducing M2-Like MacrophagePolarization. *Biomedicines*, *9*(4),395. https://doi.org/10.3390/biomedicines9040395
4. **Kumaraswami K**, Salei N, Beck S, et al. A Simple and Effective Flow Cytometry-Based Method for Identification and Quantification of Tissue Infiltrated Leukocyte Subpopulations in a Mouse Model of Peripheral Arterial Disease. *Int J Mol Sci*. 2020;21(10):3593. Published 2020 May 19. https://doi:10.3390/ijms21103593
5. Lasch, M., **Kumaraswami, K**., Nasiscionyte, S., Kircher, S., van den Heuvel, D., Meister, S., Ishikawa-Ankerhold, H., & Deindl, E. (2020). RNase A Treatment Interferes with Leukocyte Recruitment, Neutrophil Extracellular Trap Formation, and Angiogenesis in Ischemic Muscle Tissue. *Frontiers in physiology*, *11*, 576736. https://doi.org/10.3389/fphys.2020.576736

6. Lasch, M., Caballero Martinez, A., **Kumaraswami, K**., Ishikawa-Ankerhold, H., Meister, S., & Deindl, E. (2020). Contribution of the Potassium Channels $K_V1.3$ and $K_{Ca}3.1$ to Smooth Muscle Cell Proliferation in Growing Collateral Arteries. *Cells*, *9*(4), 913. https://doi.org/10.3390/cells9040913
7. Ryll, M., Bucher, J., Drefs, M., Bösch, F., **Kumaraswami, K**., Schiergens, T., Niess, H., Schoenberg, M., Jacob, S., Rentsch, M., Guba, M., Werner, J., Andrassy, J., & Thomas, M. N. (2019). Murine Cervical Aortic Transplantation Model using a Modified Non-Suture Cuff Technique. *Journal of visualized experiments: JoVE*, (153), 10.3791/59983. https://doi.org/10.3791/59983
8. Lasch, M., Kleinert, E. C., Meister, S., **Kumaraswami, K.**, Buchheim, J. I., Grantzow, T., Lautz, T., Salpisti, S., Fischer, S., Troidl, K., Fleming, I., Randi, A. M., Sperandio, M., Preissner, K. T., & Deindl, E. (2019). Extracellular RNA released due to shear stress controls natural bypass growth by mediating mechanotransduction in mice. *Blood*, *134*(17), 1469–1479. https://doi.org/10.1182/blood.2019001392